Supplementary Materials to:

Fentanyl family at the mu-opioid receptor: uniform assessment of binding and computational analysis.

by

Piotr F. J. Lipiński,* Piotr Kosson, Joanna Matalińska, Piotr Roszkowski, Zbigniew Czarnocki, Małgorzata Jarończyk, Aleksandra Misicka, Jan Cz. Dobrowolski, Joanna Sadlej*

Corresponding authors: Piotr F. J. Lipiński: plipinski@imdik.pan.pl; Joanna Sadlej: j.sadlej@uksw.edu.pl

Table of contents

SM-RMS: RMSD measures

Figure SM-RMS-1. Root mean square deviation of receptor protein backbone over time.
Table SM-RMS-1. Root mean square fluctuations of receptor protein backbone
Figure SM-RMS-2. Root mean square deviation of TM1 helix backbone over time.
Table SM-RMS-2. Root mean square fluctuations of TM1 helix backbone.
Figure SM-RMS-3. Root mean square deviation of TM2 helix backbone over time.
Table SM-RMS-3. Root mean square fluctuations of TM2 helix backbone.
Figure SM-RMS-4. Root mean square deviation of TM3 helix backbone over time.
Table SM-RMS-4. Root mean square fluctuations of TM3 helix backbone.
Figure SM-RMS-5. Root mean square deviation of TM4 helix backbone over time.
Table SM-RMS-5. Root mean square fluctuations of TM4 helix backbone.
Figure SM-RMS-6. Root mean square deviation of TM5 helix backbone over time.
Table SM-RMS-6. Root mean square fluctuations of TM5 helix backbone.
Figure SM-RMS-7. Root mean square deviation of TM6 helix backbone over time.
Table SM-RMS-7. Root mean square fluctuations of TM6 helix backbone.
Figure SM-RMS-8. Root mean square deviation of TM7 helix backbone over time.
Table SM-RMS-8. Root mean square fluctuations of TM7 helix backbone.
Figure SM-RMS-9. RMSF mean values.

SM-DIH: dihedral angles

Table SM-DIH-1. Summary of monitored dihedral angles.
Figure SM-DIH-1. Distributions of X1 dihedral angle values of D147.
Figure SM-DIH-2. Time evolution of X1 dihedral angle of D147.
Figure SM-DIH-3. Distributions of X2 dihedral angle values of D147.
Figure SM-DIH-4. Time evolution of X2 dihedral angle of D147.
Figure SM-DIH-5. Distributions of X1 dihedral angle values of Y148.
Figure SM-DIH-6. Time evolution of X1 dihedral angle of Y148.
Figure SM-DIH-7. Distributions of X2 dihedral angle values of Y148.
Figure SM-DIH-8. Time evolution of X2 dihedral angle of Y148.
Figure SM-DIH-9. Distributions of X1 dihedral angle values of W318.
Figure SM-DIH-10. Time evolution of X1 dihedral angle of W318.
Figure SM-DIH-11. Distributions of X2 dihedral angle values of W318.
Figure SM-DIH-12. Time evolution of X2 dihedral angle of W318.
Figure SM-DIH-13. Distributions of X1 dihedral angle values of H319.
Figure SM-DIH-14. Time evolution of X1 dihedral angle of H319.
Figure SM-DIH-15. Distributions of X2 dihedral angle values of H319.
Figure SM-DIH-16. Time evolution of X2 dihedral angle of H319.
Figure SM-DIH-17. Distributions of X1 dihedral angle values of M151.
Figure SM-DIH-18. Time evolution of X1 dihedral angle of M151.
Figure SM-DIH-19. Distributions of X2 dihedral angle values of M151.
Figure SM-DIH-20. Time evolution of X2 dihedral angle of M151.
Figure SM-DIH-21. Distributions of X1 dihedral angle values of W293.
Figure SM-DIH-22. Time evolution of X1 dihedral angle of W293.
Figure SM-DIH-23. Distributions of X2 dihedral angle values of W293.
Figure SM-DIH-24. Time evolution of X2 dihedral angle of W293.
Figure SM-DIH-25. Distributions of X1 dihedral angle values of H297.
Figure SM-DIH-26. Time evolution of X1 dihedral angle of H297.
Figure SM-DIH-27. Distributions of X2 dihedral angle values of H297.
Figure SM-DIH-28. Time evolution of X2 dihedral angle of H297.
Figure SM-DIH-29. Distributions of X1 dihedral angle values of Y326.
Figure SM-DIH-30. Time evolution of X1 dihedral angle of Y326.
Figure SM-DIH-31. Distributions of X2 dihedral angle values of Y326.
Figure SM-DIH-32. Time evolution of X2 dihedral angle of Y326.
Figure SM-DIH-33. Distributions of X1 dihedral angle values of W133.
Figure SM-DIH-34. Time evolution of X1 dihedral angle of W133.
Figure SM-DIH-35. Distributions of X2 dihedral angle values of W133.
Figure SM-DIH-36. Time evolution of X2 dihedral angle of W133.
Figure SM-DIH-37. Distributions of X1 dihedral angle values of Y336.
Figure SM-DIH-38. Time evolution of X1 dihedral angle of Y336.
Figure SM-DIH-39. Distributions of X2 dihedral angle values of Y336.
Figure SM-DIH-40. Time evolution of X2 dihedral angle of Y336.

SM-WAT: hydration

Figure SM-WAT-1. Distributions of the number of water molecules within 5.0 angstroms from Y336
Table SM-WAT-1. Mean number of water molecules within 5.0 angstroms from D114.
Figure SM-WAT-2. Number of waters in proximity (5.0 angstroms) of D114 over time.
Figure SM-WAT-3. Distributions of the number of water molecules within 5.0 angstroms from Y336
Table SM-WAT-2. Mean number of water molecules within 5.0 angstroms from Y336.
Figure SM-WAT-4. Number of waters in proximity (5.0 angstroms) of Y336 over time.

SM-SCO: scoring

SM-SEQ: sequence alignment

Procedure SM-SYN-1. Cyclopropylfentanyl, Cyclopropanecarboxylic acid (1-phenethyl-4-piperidinyl)phenyl amide (F09)

The compound **F25** was prepared according to literature.[1]

To a stirred at 23-24 ºC solution of **F25** (0.280g, 0.998 mmol, 1 equiv) and triethylamine (0.180 mL, 1.297 mmol, 1.3 equiv) in anhydrous toluene (10 mL) solution of cyclopropanecarbonyl chloride (0.0907 mL, 0.998 mmol, 1 equiv) in toluene (1 mL) was added and the resulting solution was stirred for additional 30 min. After this time toluene (20 mL) and water (8 mL) were added, mixture was shaken and phases were separated. The organic extract was dried over $MgSO_4$, filtered and the solvent was removed in vacuo. The product **F09** was isolated by column chromatography on silica gel ($CHCl_3$) as white solid (0.320 g, 92%). mp = 122-123 ºC (lit.[2] mp = 119.5-120.4 ºC).

^{1}H NMR (300 MHz, CDCl3) δ 7.38 (m, 3H), 7.25 (m, 3H), 7.16 (m, 5H), 4.67 (tt, *J* = 11.7, 3.9 Hz, 1H), 3.00 (m, 2H), 2.73 (m, 2H), 2.53 (m, 2H), 2.15 (dt, *J* = 12.0, 2.4 Hz, 2H), 1.81 (m, 2H), 1.47 (dq, *J* = 12.3, 3.9 Hz, 2H), 1.09 (m, 1H), 0.97 (m, 2H), 0.54 (m, 2H). ^{13}C NMR (75 MHz, CDCl3) δ 173.2, 140.3, 138.9, 130. 8, 129.2, 128.6, 128.4, 128.1, 126.0, 60.5, 53.2, 52.5, 33.9, 30.6, 13.2, 8.4. LR-MS (ESI +): 349.2 $(M + H)^+$.

Procedure SM-SYN-2. N-(1-phenethyl-4-piperidinyl)-(4-trifluoromethylphenyl)amine (F26)[1]

A solution of 1-phenethyl-piperidin-4-one **F22** (0.50 g, 2.46 mmol, 1 equiv), 4-trifluoromethylaniline (0.225 mL, 2.46 mmol, 1 equiv) and acetic acid (2 drops) in toluene (20 mL) was heated under reflux with a Dean-Stark apparatus for 24 h. The toluene was removed in vacuo and the residue was used for the next step without further purification.

The crude imine **F24** was dissolved in methanol (10 mL) and $NaBH_4$ (0.186 g, 4.92 mmol, 2 equiv) was added gradually at 23 ºC to the stirred solution during 10 min. Obtained solution was stirred for 1.5 h at 60 ºC. After evaporation of the solvent water (5 mL) was added and the mixture was extracted with chloroform (3x15 mL). The organic extract was dried over $MgSO_4$, filtered and the solvent was removed in vacuo. The product **F26** was isolated by column chromatography on silica gel ($CHCl_3$:MeOH, 0-1% MeOH) as colourless oil (0.51 g, 74%).

^{1}H NMR (300 MHz, CDCl3) δ 7.38 (d, *J* = 8.4 Hz, 2H), 7.29 (m, 2H), 7.20 (m, 3H), 6.57 (d, *J* = 8.4 Hz, 2H), 3.88 (d, *J* = 7.8 Hz, 1H), 3.34 (m, 1H), 2.96 (m, 2H), 2.61 (m, 2H), 2.21 (m, 2H), 2.05 (m, 2H), 1.52 (m, 2H). ^{13}C NMR (75 MHz, CDCl3) δ 149.5, 140.3, 128.9, 128.4, 126.6 (q, *J* = 3.0 Hz), 126.0, 125.0 (q, *J* = 268.5 Hz), 118.4 (q, *J* = 32.2 Hz), 112.1, 60.5, 52.3, 49.6, 33.9, 32.3. LR-MS (ESI +): 349.3 $(M + H)^{+}$.

Procedure SM-SYN-3. *para*-Trifluoromethylfentanyl, N-(1-phenethyl-4-piperidinyl)-N-(4-trifluoromethylphenyl)-propionamide (F13)

To a stirred at 23-24 ºC solution of **F26** (0.270g, 0.775 mmol, 1 equiv) and triethylamine (0.140 mL, 1.007 mmol, 1.3 equiv) in anhydrous toluene (10 mL) solution of propanoic acid chloride (0.0677 mL, 0.775 mmol, 1 equiv) in anhydrous toluene (1 mL) was added and the resulting solution was stirred at 70 ºC for 3 h. After this time toluene (20 mL) and water (8 mL) were added, mixture was shaken and phases were separated. The organic extract was dried over $MgSO_4$, filtered and the solvent was removed in vacuo. The product **F13** was isolated by column chromatography on silica gel ($CHCl_3$) as white solid (0.197 g, 63%). mp = 121-122 ºC (lit.[3] mp = 237.0 ºC for HCl salt).

^{1}H NMR (300 MHz, CDCl3) δ 7.88 (d, *J* = 8.4 Hz, 2H), 7.21 (m, 7H), 4.71 (t, *J* = 11.7 Hz, 1H), 3.00 (d, *J* = 11.7 Hz, 2H), 2.72 (m, 2H), 2.53 (m, 2H), 2.16 (dt, *J* = 12.0, 2.1 Hz, 2H), 1.92 (q, *J* = 7.2 Hz, 2H), 1.82 (m, 2H), 1.38 (dq, *J* = 12.0, 3.9 Hz, 2H), 1.04 (t, *J* = 7.5 Hz, 2H). ^{13}C NMR (75 MHz, CDCl3) δ 172.90, 142.25, 140.14, 131.02, 130.62 (q, *J* = 33.0 Hz), 128.59, 128.37, 126.47 (q, *J* = 3.7 Hz), 126.03, 123.67 (q, *J* = 270.0 Hz), 60.40, 52.98, 52.29, 33.83, 30.64, 28.72, 9.49. LR-MS (ESI +): 427.2 $(M + Na)^{+}$.

Procedure SM-SYN-4. N-(3-bromopropyl)-N-phenyl propionamide (F28)

The compound **F27** was prepared according to literature.[4]

To a stirred at 23-24 ºC solution of **F27** (0.250g, 1.177 mmol, 1 equiv) and triethylamine (0.140 mL, 1.007 mmol, 1.05 equiv) in CH_2Cl_2 (10 mL) solution of propanoic acid chloride (0.102 mL, 1.17 mmol, 1 equiv) in CH_2Cl_2 (1 mL) was added and the resulting solution was stirred additionally for 30 min. After this time CH_2Cl_2 (10 mL) and water (10 mL) were added, mixture was shaken and phases were separated. The organic extract was dried over $MgSO_4$, filtered and the solvent was removed in vacuo. The product **F28** was isolated by column chromatography on silica gel (CH_2Cl_2) as colourless oil (0.280 g, 88%).

^{1}H NMR (300 MHz, CDCl3) δ 7.40 (m, 3H), 7.15 (m, 2H), 3.82 (t, *J* = 7.2 Hz, 2H), 3.40 (t, *J* = 6.9 Hz, 2H), 2.12 (qv, *J* = 7.5 Hz, 2H), 2.05 (q, *J* = 7.5 Hz, 2H), 1.04 (t, *J* = 7.5 Hz, 2H). ^{13}C NMR (75 MHz, CDCl3) δ 173.9, 142.5, 129.8, 128.1, 128.0, 48.2, 31.2, 30.5, 27.8, 9.5. LR-MS (ESI +): 270.2, 272.2 $(M + H)^{+}$.

Procedure SM-SYN-5. N-[3-(methyl-phenethylamino)propyl]-N-phenyl propionamide (F02)

The solution of N-(3-bromopropyl)-N-phenyl propionamide (0.28g, 1.04 mmol, 1 equiv) and N-methyl-phenethylamine (0.301 mL, 2.08 mmol, 2 equiv) in acetonitrile (16 mL) was stirred at 60 ºC for 2 h. After this time water (15 mL) was added and the resulting mixture was extracted with diethyl ether (1x40 mL and 2x20 mL). The organic extract was dried over $MgSO_4$, filtered and the solvent was removed in vacuo. The product **F02** was isolated by column chromatography on silica gel (hexane:diethyl ether, 0-100% Et_2O) as colorless oil (0.150 g, 44%). (lit.[5] mp = 99.0-101.0 ºC for HCl salt).

^{1}H NMR (300 MHz, CDCl3) δ 7.37 (m, 3H), 7.26 (m, 2H), 7.16 (m, 5H), 3.72 (t, *J* = 7.5 Hz, 2H), 2.71 (m, 2H), 2.54 (m, 2H), 2.40 (t, *J* = 7.5 Hz, 2H), 2.24 (s, 3H), 2.02 (q, *J* = 7.5 Hz, 2H), 1.71 (qv, *J* = 7.5 Hz, 2H), 1.04 (t, *J* = 7.5 Hz, 2H). ^{13}C NMR (75 MHz, CDCl3) δ 173.5, 142.7, 140.4, 129.6, 128.6, 128.2, 128.2, 127.7, 125.8, 59.5, 54.9, 47.5, 42.0, 33.8, 27.8, 25.8, 9.6. LR-MS (ESI +): 325.4 $(M + H)^{+}$.

Listing SM-SYN-1. References for synthetic part in Supplementary Materials.

1. Vardanyan, R.; Vijay, G.; Nichol, G. S.; Liu, L.; Kumarasinghe, I.; Davis, P.; Vanderah, T.; Porreca, F.; Lai, J.; Hruby, V. J. Synthesis and investigations of double-pharmacophore ligands for treatment of chronic and neuropathic pain *Bioorg. Med. Chem.* **2009**,*17*, 5044–5053.

2. Patent FR 1517671, 1961, N.V. Research Laboratorium Dr. C. Janssen.

3. Casy, A.F.; Huckstep, M.R. Structure-Activity Studies of Fentanyl *J. Pharm. Pharmacol.* **1988**, 40:605-608.

4. Thansandote, P; Raemy, M.; Rudolph, A.; Lautens, M. Synthesis of Benzannulated N-Heterocycles by a Palladium-Catalyzed C-C/C-N Coupling of Bromoalkylamines *Org. Lett.* **2007**, *9*, 25, 5255-5258.

5. Wright, Jr., W.B.; Brabander, H.J.; Hardy, Jr., R.A. Synthetic Analgesics. III. Basic Anilides and Carbanilates Containing the Phenalkyl Moiety *J. Org. Chem.* **1961**, *26*, 485-490.

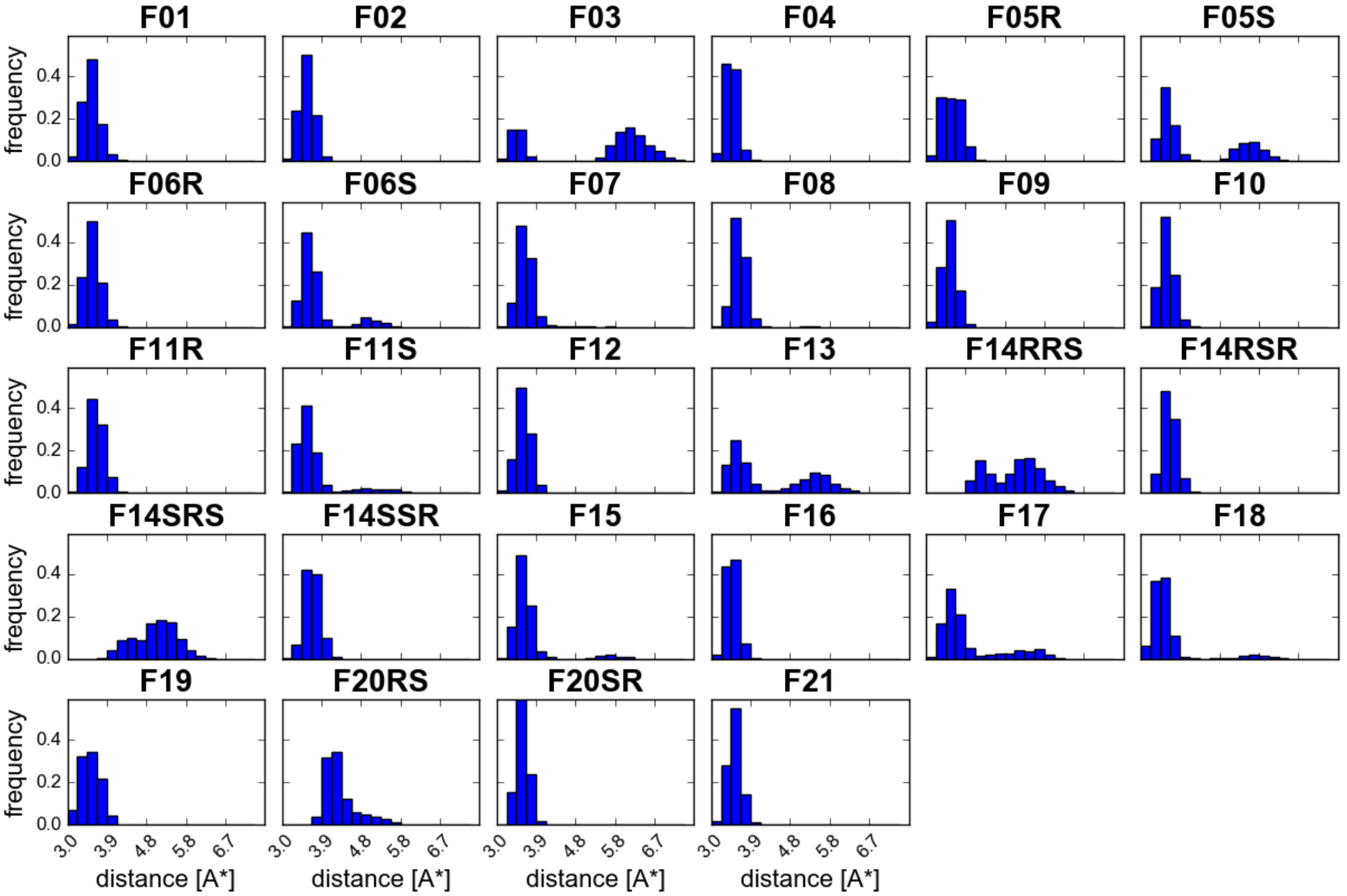

Figure SM-DIS-1. Distributions of the distance between Cgamma of D147 and ligands' piperidine nitrogen.
Data are collected from last 10ns of production in 3 replicas.

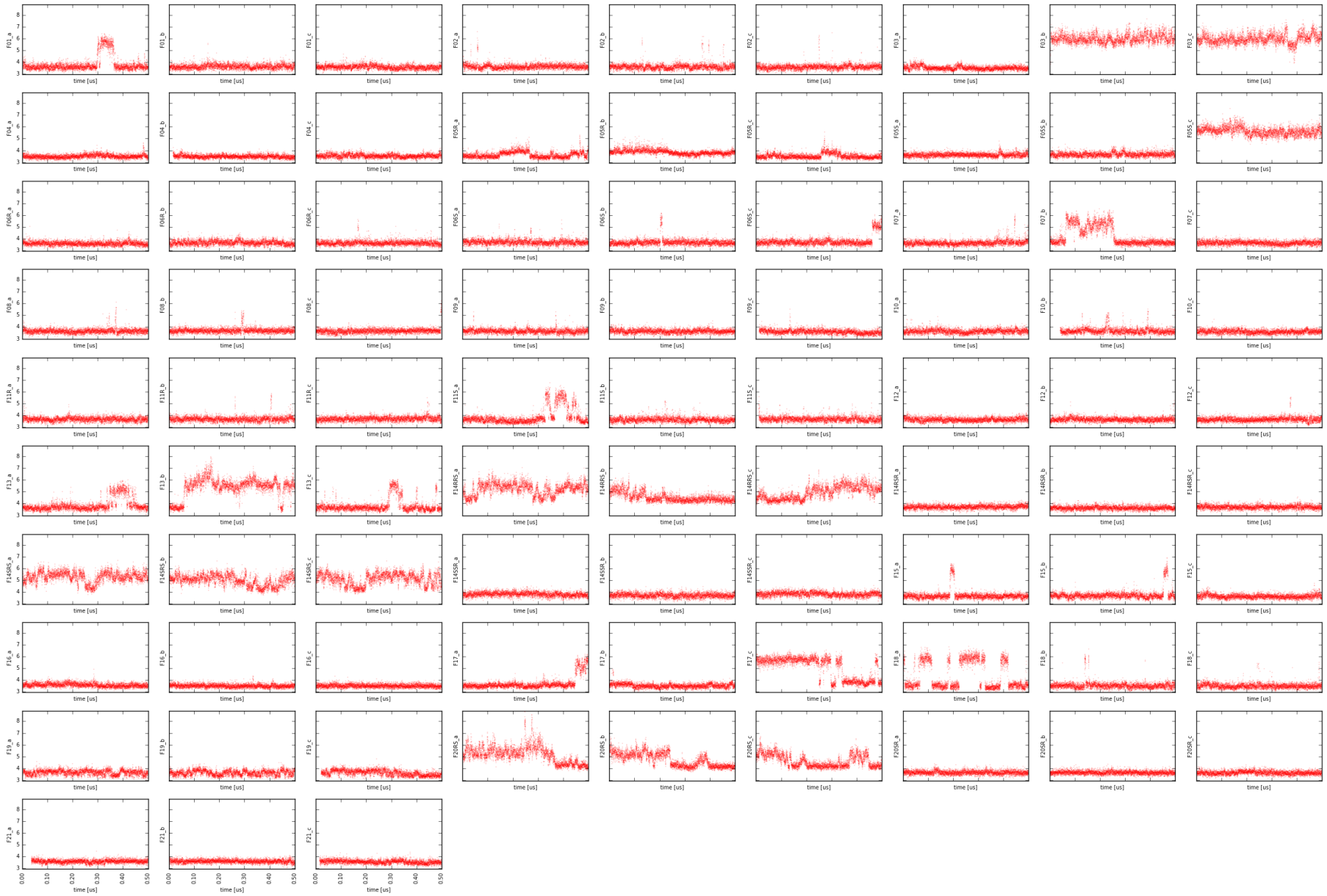

Figure SM-DIS-2. Time evolution of the distance between Cgamma of D147 and ligands' piperidine nitrogen.
Y-values are given in angstroms.

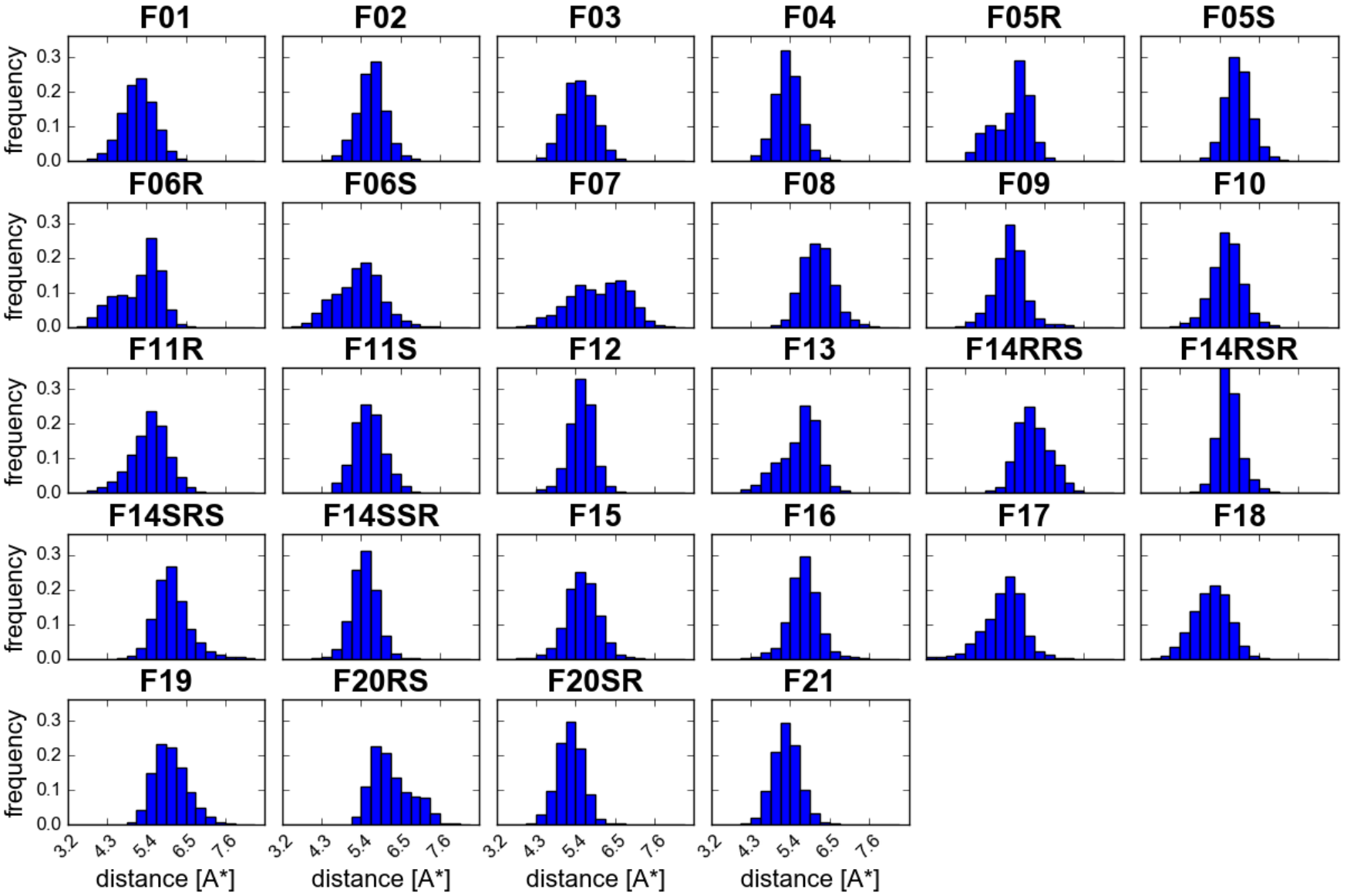

Figure SM-DIS-3. Distributions of the distance between Cgamma of D147 and phenolic O of Y326.
Data are collected from last 10ns of production in 3 replicas.

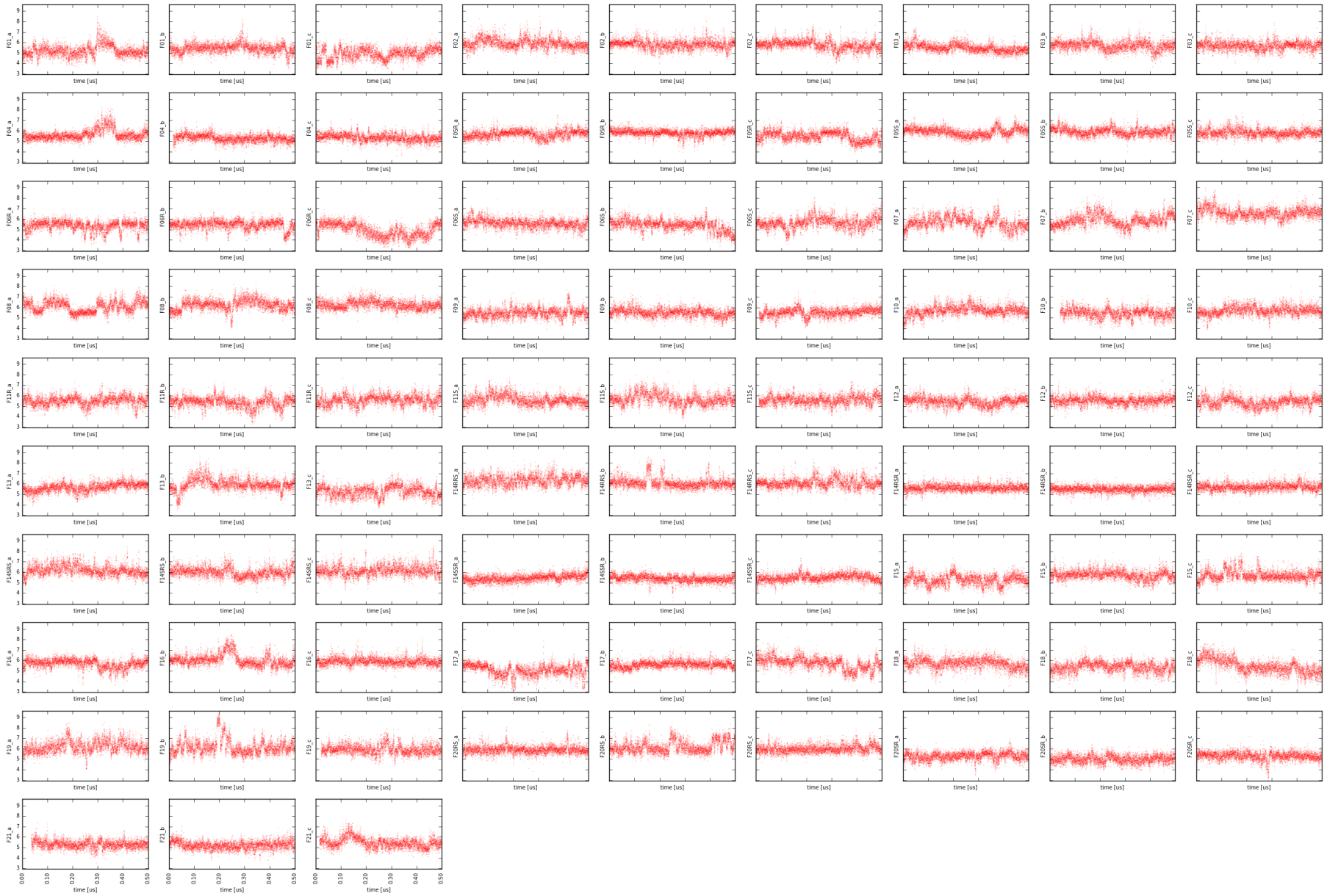

Figure SM-DIS-4. Time evolution of the distance between Cgamma of D147 and phenolic O of Y326.
Y-values are given in angstroms.

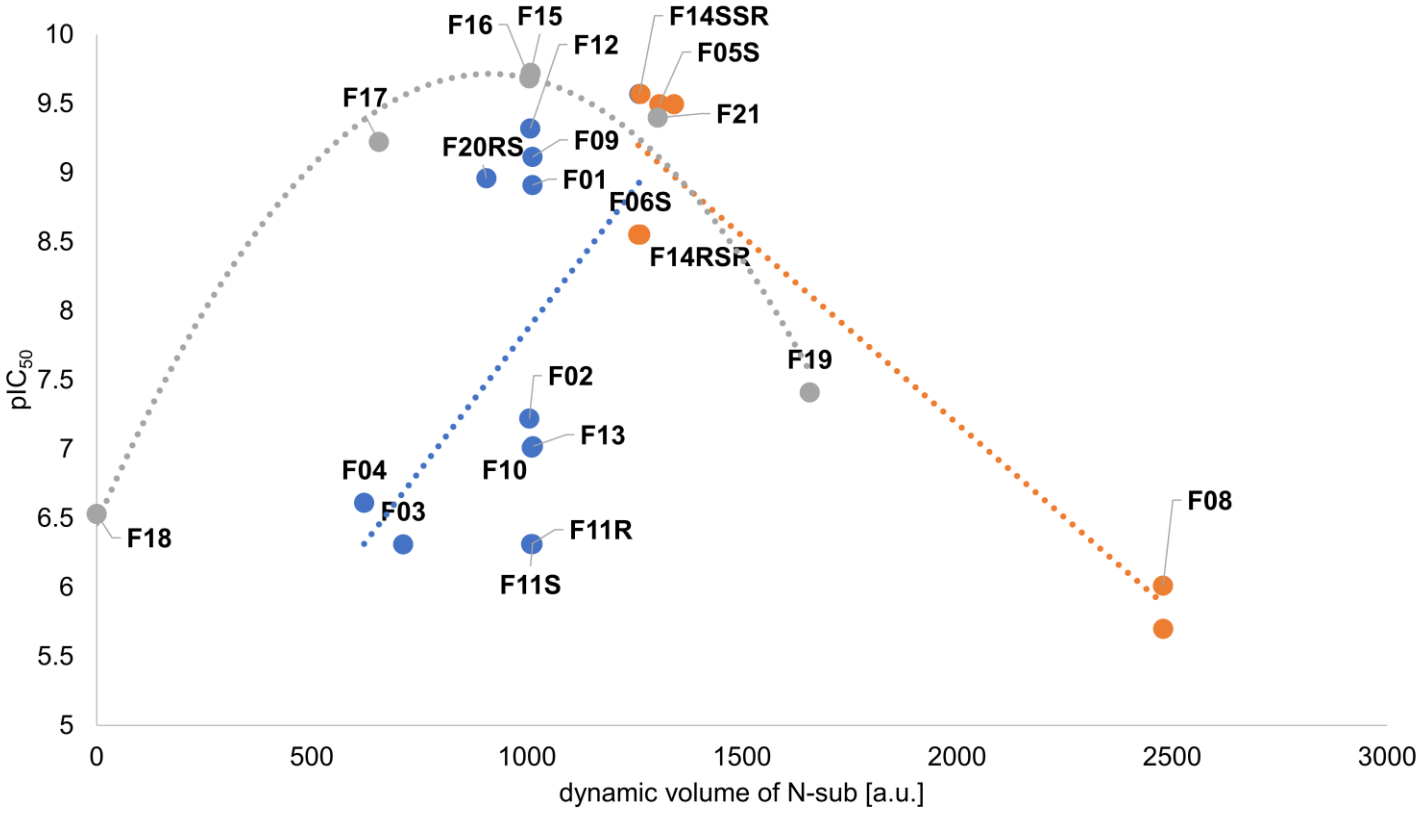

Figure SM-VOL-1. pIC50 values plotted against the dynamic volume of N-substituent for all compounds except for F14RRS, F14SRS and F20RS. *Volume data are collected from last 10ns of production in 3 replicas.*

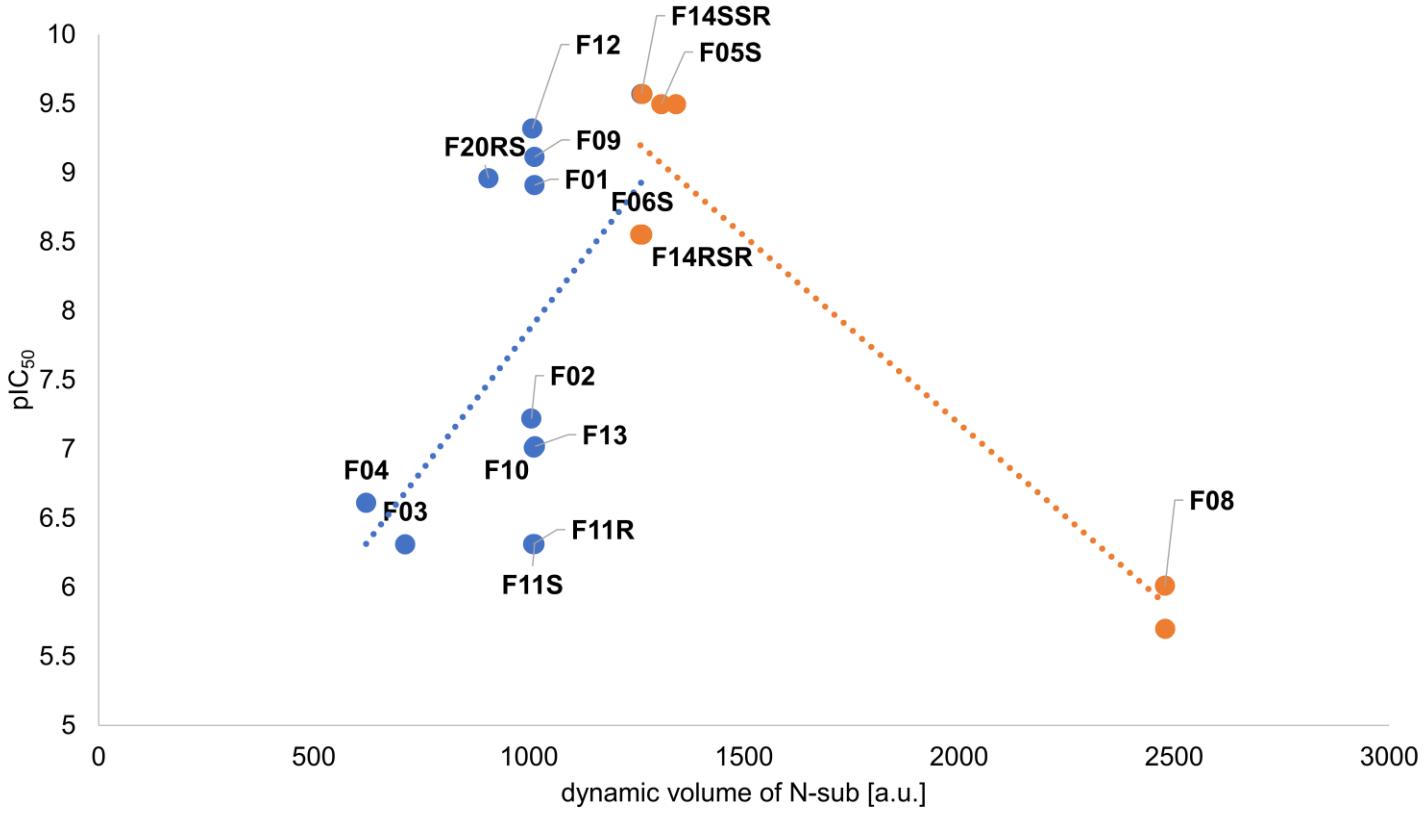

Figure SM-VOL-2. pIC50 values plotted against the dynamic volume of N-substituent.
4-axially substituted derivatives not shown. Neither F14RRS, F14SRS and F20RS. Volume data are collected from last 10ns of production in 3 replicas.

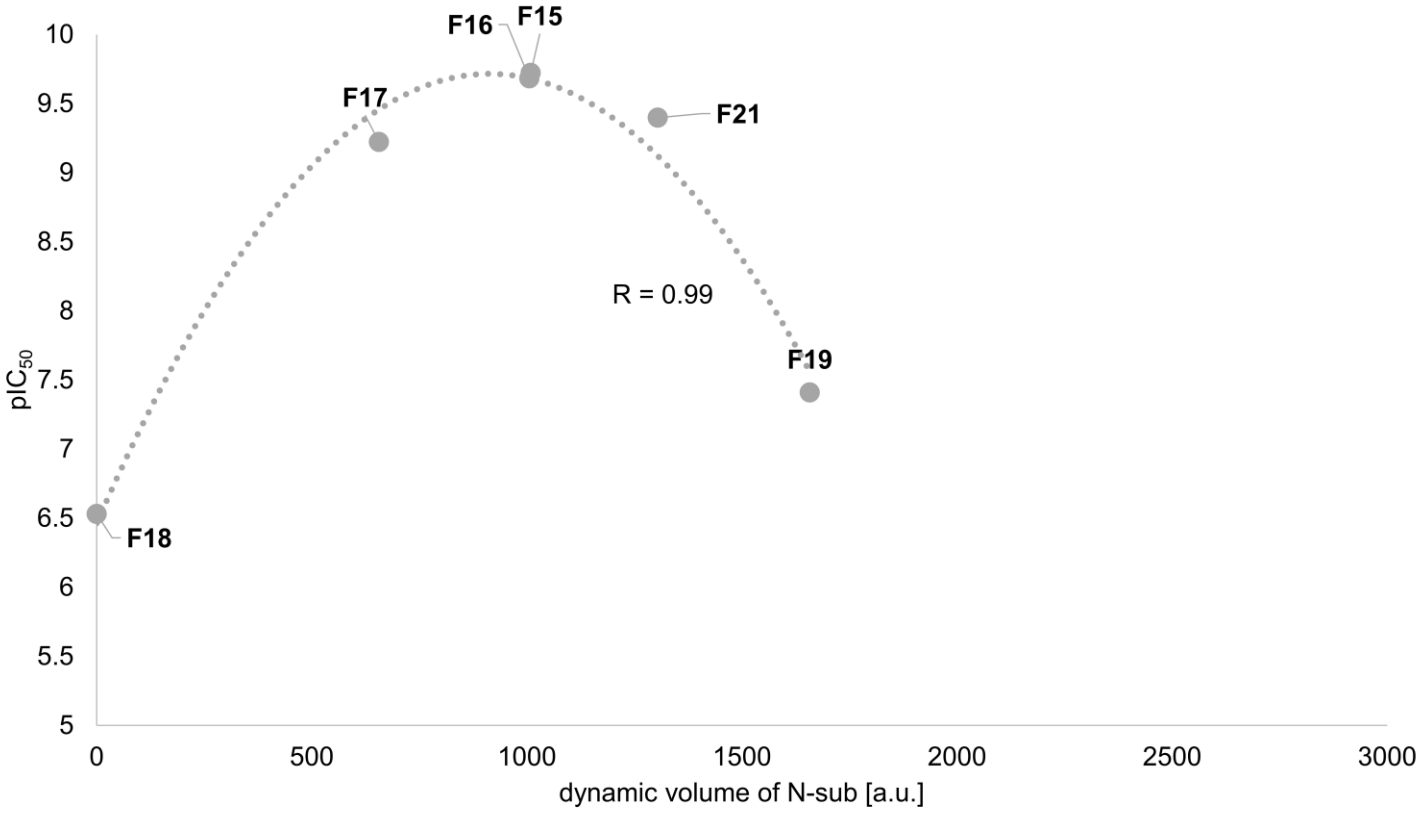

Figure SM-VOL-3. pIC50 values plotted against the dynamic volume of N-substituent for 4-axially substituted derivatives.
Volume data are collected from last 10ns of production in 3 replicas.

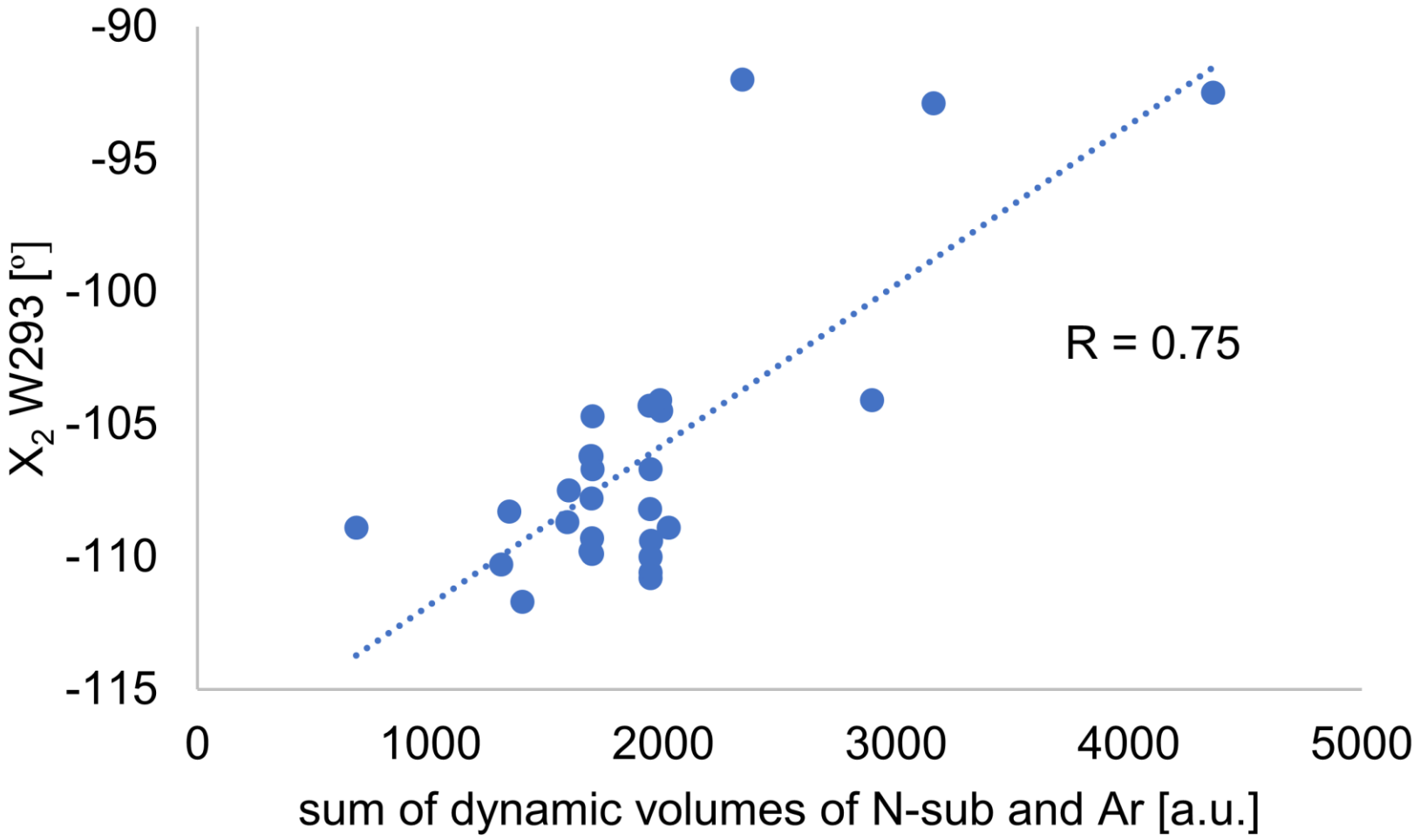

Figure SM-VOL-4. Correlation of mean X2 W293 dihedral measures with the sum of dynamic volumes of N-substituent and anilide's aromatic. *R = 0.75, n = 28. Volume data are collected from last 10ns of production in 3 replicas. Mean dihedrals are calculated from last 10ns of production in 3 replicas.*

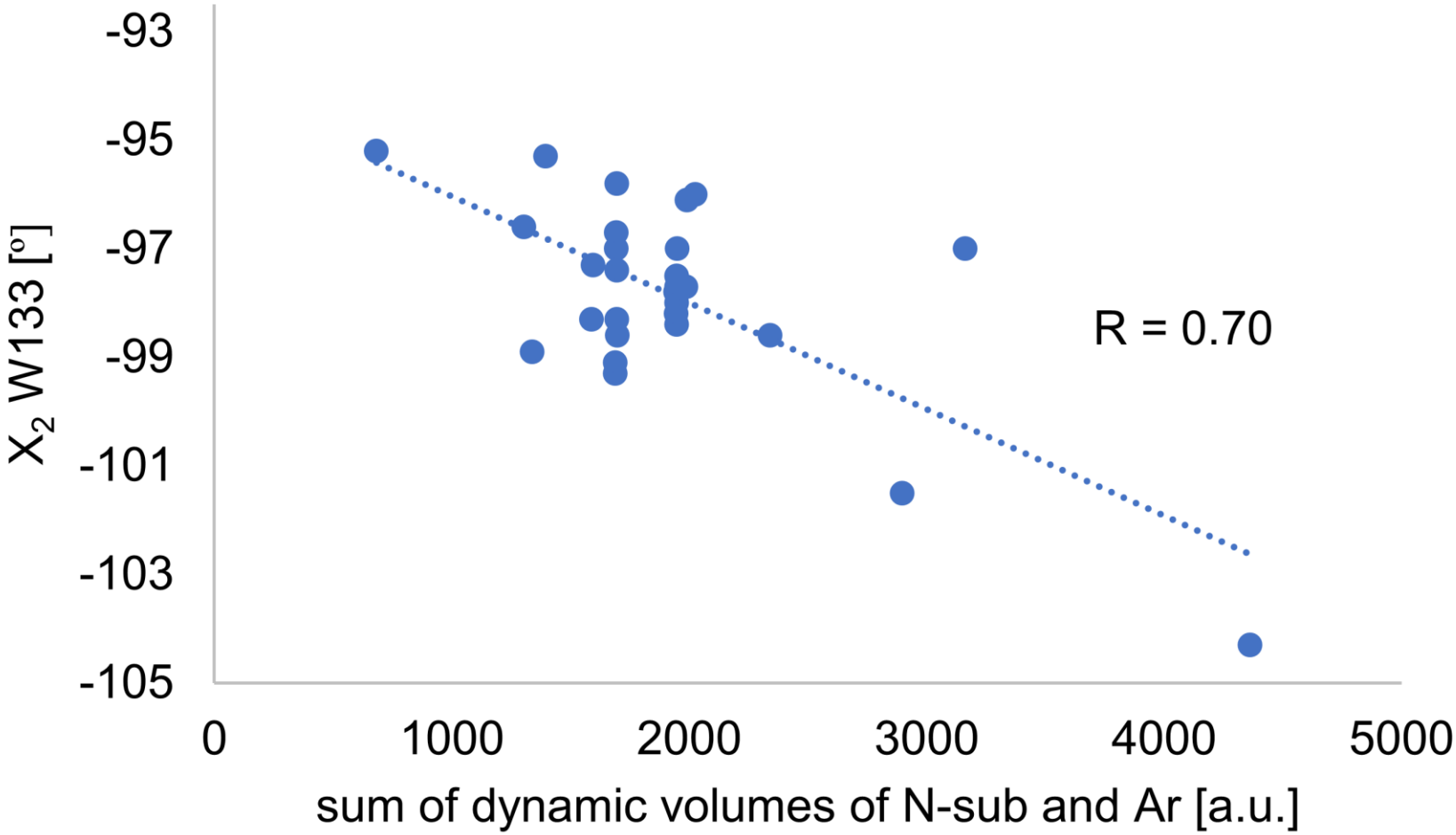

Figure SM-VOL-5. Correlation of mean X2 W133 dihedral measures with the sum of dynamic volumes of N-substituent and anilide's aromatic. *R = 0.70, n = 28. Volume data are collected from last 10ns of production in 3 replicas. Mean dihedrals are calculated from last 10ns of production in 3 replicas.*

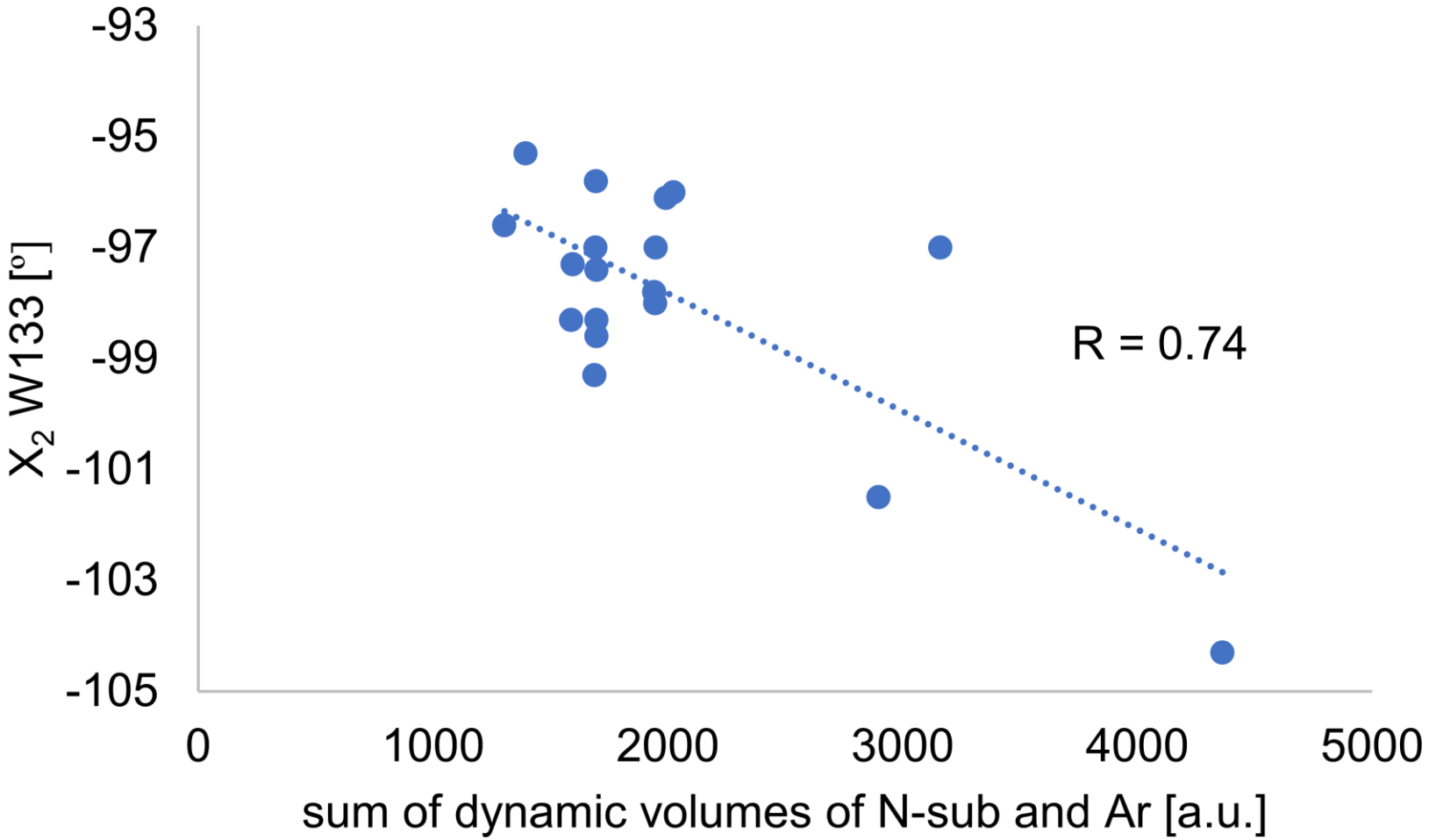

Figure SM-VOL-6. Correlation of mean X2 W133 dihedral measures with the sum of dynamic volumes of N-substituent and anilide's aromatic. *R = 0.74, n = 18. Volume data are collected from last 10ns of production in 3 replicas. Mean dihedrals are calculated from last 10ns of production in 3 replicas.*

Figure SM-RMS-1. Root mean square deviation of receptor protein backbone over time.
Y-values are given in angstroms. For RMSD calculation taken are only backbone atoms of residues 72-92 (H1), 104-128 (H2), 139-169 (H3), 185-204 (H4), 227-260 (H5), 275-304 (H6), 314-338 (H7).

Table SM-RMS-1. Root mean square fluctuations of receptor protein backbone

Calculated as a mean RMSD over last 10 ns of simulations in 3 replicas. For RMSD calculation taken are only backbone atoms of residues 72-92 (H1), 104-128 (H2), 139-169 (H3), 185-204 (H4), 227-260 (H5), 275-304 (H6), 314-338 (H7).

derivative	replica							
	a		b		c			
	mean	sem	mean	sem	mean	sem	MEAN	SEM
F01	0.95	0.04	0.87	0.01	0.93	0.04	0.92	0.02
F02	1.09	0.03	1.02	0.02	0.96	0.02	1.02	0.04
F03	1.01	0.03	0.85	0.03	0.76	0.01	0.87	0.07
F04	0.96	0.03	1.07	0.04	1.05	0.03	1.03	0.03
F05R	0.96	0.01	0.91	0.02	0.98	0.04	0.95	0.02
F05S	0.94	0.04	0.92	0.04	0.84	0.03	0.9	0.03
F06R	0.87	0.05	0.94	0.02	0.98	0.03	0.93	0.03
F06S	0.84	0.02	0.91	0.02	0.83	0.02	0.86	0.03
F07	1	0.03	0.9	0.02	0.94	0.02	0.95	0.03
F08	1.2	0.03	0.93	0.04	0.99	0.01	1.04	0.08
F09	0.88	0.03	0.82	0.03	0.91	0.02	0.87	0.03
F10	0.88	0.02	1.11	0.02	0.95	0.03	0.98	0.07
F11R	0.78	0.02	0.91	0.03	0.89	0.03	0.86	0.04
F11S	1.23	0.03	0.82	0.02	0.88	0.02	0.98	0.13
F12	0.93	0.03	0.85	0.02	0.8	0.02	0.86	0.04
F13	0.82	0.02	0.86	0.01	0.97	0.02	0.88	0.04
F14RRS	0.86	0.03	0.9	0.02	0.92	0.03	0.89	0.02
F14RSR	1.05	0.02	0.94	0.03	0.92	0.03	0.97	0.04
F14SRS	1.01	0.01	0.88	0.02	1.04	0.03	0.98	0.05
F14SSR	0.85	0.02	0.9	0.04	0.99	0.03	0.91	0.04
F15	0.89	0.02	0.77	0.03	0.91	0.02	0.86	0.04
F16	0.9	0.02	1.02	0.04	0.95	0.02	0.96	0.03
F17	0.96	0.02	0.96	0.03	0.82	0.02	0.91	0.05
F18	0.96	0.02	0.86	0.02	1.01	0.02	0.94	0.04
F19	0.83	0.02	0.81	0.03	1.11	0.05	0.92	0.1
F20RS	1.02	0.03	1.28	0.03	1.1	0.06	1.13	0.08
F20SR	0.83	0.02	1	0.02	0.89	0.02	0.91	0.05
F21	0.9	0.02	1.01	0.04	0.86	0.03	0.92	0.04

Figure SM-RMS-2. Root mean square deviation of TM1 helix backbone over time.
Y-values are given in angstroms. For RMSD calculation taken are only backbone atoms of residues 72-92 (H1).

Table SM-RMS-2. Root mean square fluctuations of TM1 helix backbone.
Calculated as a mean RMSD over last 10 ns of simulations in 3 replicas. For RMSD calculation taken are only backbone atoms of residues 72-92 (H1).

derivative	replica							
	a		b		c			
	mean	sem	mean	sem	mean	sem	MEAN	SEM
F01	0.6	0.04	0.79	0.04	0.68	0.02	0.69	0.06
F02	1.04	0.06	1	0.06	0.9	0.04	0.98	0.04
F03	1.12	0.06	1.09	0.07	0.8	0.05	1	0.1
F04	0.87	0.02	1.24	0.07	1.02	0.06	1.04	0.11
F05R	0.93	0.04	0.95	0.05	1.06	0.05	0.98	0.04
F05S	0.99	0.05	0.96	0.06	0.69	0.03	0.88	0.1
F06R	0.76	0.06	1.04	0.06	1	0.06	0.93	0.09
F06S	0.76	0.04	1.11	0.06	1.02	0.06	0.96	0.1
F07	0.77	0.05	0.95	0.05	0.97	0.04	0.9	0.06
F08	1.21	0.08	1	0.07	1.12	0.05	1.11	0.06
F09	0.89	0.03	0.85	0.04	0.82	0.04	0.85	0.02
F10	1.04	0.06	1.07	0.07	0.99	0.07	1.03	0.02
F11R	0.7	0.04	1.01	0.06	0.89	0.04	0.87	0.09
F11S	1.33	0.06	0.81	0.06	1.01	0.03	1.05	0.15
F12	0.74	0.04	0.69	0.02	0.69	0.04	0.71	0.02
F13	0.78	0.04	0.77	0.04	0.97	0.05	0.84	0.07
F14RRS	0.99	0.07	0.94	0.05	0.85	0.06	0.93	0.04
F14RSR	0.99	0.06	1.07	0.02	1.01	0.06	1.02	0.02
F14SRS	1.38	0.05	0.78	0.06	1.09	0.03	1.08	0.17
F14SSR	0.75	0.04	0.89	0.05	0.87	0.05	0.84	0.04
F15	0.93	0.04	0.79	0.05	1.03	0.05	0.92	0.07
F16	1.02	0.04	0.97	0.04	0.85	0.04	0.95	0.05
F17	1.19	0.06	0.72	0.06	0.78	0.05	0.9	0.15
F18	0.93	0.03	0.84	0.04	1.04	0.04	0.94	0.06
F19	0.94	0.06	0.75	0.04	1.1	0.06	0.93	0.1
F20RS	0.87	0.05	1.02	0.05	0.91	0.07	0.93	0.04
F20SR	0.81	0.06	1.04	0.03	0.78	0.03	0.88	0.08
F21	0.84	0.05	0.85	0.04	1.01	0.03	0.9	0.06

Figure SM-RMS-3. Root mean square deviation of TM2 helix backbone over time.
Y-values are given in angstroms. For RMSD calculation taken are only backbone atoms of residues 104-128 (H2).

Table SM-RMS-3. Root mean square fluctuations of TM2 helix backbone.
Calculated as a mean RMSD over last 10 ns of simulations in 3 replicas. For RMSD calculation taken are only backbone atoms of residues 104-128 (H2).

derivative	replica							
	a		b		c			
	mean	sem	mean	sem	mean	sem	MEAN	SEM
F01	0.74	0.04	0.82	0.04	0.92	0.05	0.83	0.05
F02	1.3	0.05	0.79	0.06	0.95	0.04	1.01	0.15
F03	0.99	0.04	0.67	0.05	0.67	0.02	0.78	0.11
F04	0.74	0.04	1.13	0.05	1.06	0.07	0.98	0.12
F05R	0.77	0.03	0.7	0.04	1.03	0.03	0.83	0.1
F05S	1	0.07	0.89	0.04	0.56	0.04	0.82	0.13
F06R	0.85	0.07	0.94	0.04	0.95	0.03	0.91	0.03
F06S	0.54	0.02	0.76	0.03	0.56	0.04	0.62	0.07
F07	0.72	0.04	0.79	0.04	0.88	0.04	0.8	0.05
F08	1.15	0.04	0.98	0.05	1.05	0.03	1.06	0.05
F09	0.71	0.04	0.66	0.04	1.03	0.03	0.8	0.12
F10	0.74	0.04	0.81	0.04	0.88	0.03	0.81	0.04
F11R	0.72	0.05	0.93	0.05	0.81	0.06	0.82	0.06
F11S	1.74	0.05	0.72	0.04	0.65	0.02	1.04	0.35
F12	0.71	0.03	0.64	0.04	0.72	0.05	0.69	0.03
F13	0.56	0.05	0.69	0.03	0.91	0.04	0.72	0.1
F14RRS	0.71	0.03	0.68	0.03	0.87	0.06	0.75	0.06
F14RSR	0.99	0.04	0.7	0.03	0.94	0.06	0.88	0.09
F14SRS	0.66	0.05	0.62	0.02	0.63	0.05	0.64	0.01
F14SSR	0.67	0.04	0.86	0.05	0.74	0.06	0.76	0.06
F15	0.83	0.03	0.65	0.06	0.89	0.06	0.79	0.07
F16	0.8	0.05	1.09	0.07	0.79	0.04	0.89	0.1
F17	1.03	0.05	0.96	0.04	0.78	0.05	0.92	0.07
F18	0.77	0.02	0.77	0.03	0.89	0.04	0.81	0.04
F19	0.68	0.02	0.64	0.04	1.05	0.08	0.79	0.13
F20RS	1.2	0.06	1.39	0.03	1.06	0.09	1.22	0.1
F20SR	0.83	0.03	0.95	0.02	0.8	0.03	0.86	0.05
F21	0.71	0.04	0.74	0.03	0.64	0.06	0.7	0.03

Figure SM-RMS-4. Root mean square deviation of TM3 helix backbone over time.
Y-values are given in angstroms. For RMSD calculation taken are only backbone atoms of residues 139-169 (H3).

Table SM-RMS-4. Root mean square fluctuations of TM3 helix backbone.
Calculated as a mean RMSD over last 10 ns of simulations in 3 replicas. For RMSD calculation taken are only backbone atoms of residues 139-169 (H3).

derivative	replica							
	a		b		c			
	mean	sem	mean	sem	mean	sem	MEAN	SEM
F01	0.92	0.03	0.89	0.03	0.78	0.04	0.86	0.04
F02	0.81	0.03	0.76	0.06	0.8	0.02	0.79	0.02
F03	0.7	0.03	0.8	0.04	0.67	0.02	0.72	0.04
F04	0.73	0.03	0.76	0.04	0.67	0.03	0.72	0.03
F05R	0.76	0.03	0.68	0.03	0.88	0.03	0.77	0.06
F05S	0.78	0.04	0.74	0.04	0.79	0.06	0.77	0.02
F06R	0.76	0.06	0.76	0.02	0.78	0.05	0.77	0.01
F06S	0.79	0.03	0.66	0.03	0.56	0.02	0.67	0.07
F07	0.76	0.02	0.65	0.02	0.74	0.03	0.72	0.03
F08	0.9	0.03	0.68	0.03	0.86	0.05	0.81	0.07
F09	0.71	0.02	0.74	0.04	0.69	0.02	0.71	0.01
F10	0.62	0.03	1	0.03	0.79	0.05	0.8	0.11
F11R	0.63	0.04	0.65	0.03	0.76	0.04	0.68	0.04
F11S	0.89	0.07	0.67	0.03	0.6	0.03	0.72	0.09
F12	0.73	0.02	0.77	0.04	0.73	0.03	0.74	0.01
F13	0.64	0.04	0.76	0.05	0.83	0.03	0.74	0.06
F14RRS	0.67	0.05	0.64	0.05	0.69	0.02	0.67	0.01
F14RSR	0.7	0.03	0.65	0.03	0.68	0.03	0.68	0.01
F14SRS	0.72	0.03	0.74	0.06	0.74	0.03	0.73	0.01
F14SSR	0.7	0.02	0.77	0.04	0.72	0.03	0.73	0.02
F15	0.69	0.04	0.69	0.06	0.84	0.04	0.74	0.05
F16	0.62	0.03	0.81	0.05	0.77	0.03	0.73	0.06
F17	0.82	0.03	0.72	0.04	0.74	0.04	0.76	0.03
F18	0.8	0.02	0.66	0.02	0.77	0.02	0.74	0.04
F19	0.64	0.03	0.72	0.04	0.78	0.05	0.71	0.04
F20RS	0.77	0.04	0.99	0.04	0.88	0.05	0.88	0.06
F20SR	0.66	0.03	0.7	0.03	0.61	0.03	0.66	0.03
F21	0.82	0.04	0.84	0.04	0.8	0.04	0.82	0.01

Figure SM-RMS-5. Root mean square deviation of TM4 helix backbone over time.
Y-values are given in angstroms. For RMSD calculation taken are only backbone atoms of residues 185-204 (H4).

Table SM-RMS-5. Root mean square fluctuations of TM4 helix backbone.
Calculated as a mean RMSD over last 10 ns of simulations in 3 replicas. For RMSD calculation taken are only backbone atoms of residues 185-204 (H4).

derivative	replica							
	a		b		c			
	mean	sem	mean	sem	mean	sem	MEAN	SEM
F01	1.59	0.08	1.07	0.04	1.01	0.09	1.22	0.18
F02	1.43	0.05	1.45	0.04	1.34	0.08	1.41	0.03
F03	1.46	0.06	1.18	0.09	0.96	0.06	1.2	0.14
F04	1.14	0.07	1.23	0.05	1.68	0.1	1.35	0.17
F05R	1.4	0.06	1.42	0.03	1.25	0.1	1.36	0.05
F05S	1.48	0.06	1.46	0.11	1.09	0.05	1.34	0.13
F06R	1.19	0.11	1.35	0.07	1.36	0.11	1.3	0.06
F06S	1.34	0.08	1.23	0.05	1.16	0.06	1.24	0.05
F07	1.53	0.09	1.11	0.05	1.24	0.04	1.29	0.12
F08	1.07	0.04	1.18	0.11	1.24	0.05	1.16	0.05
F09	1.14	0.06	1.08	0.09	1.39	0.05	1.2	0.09
F10	1.24	0.05	1.19	0.09	1.45	0.04	1.29	0.08
F11R	1.13	0.06	1.39	0.11	1.36	0.06	1.29	0.08
F11S	1.64	0.07	1.24	0.05	1.21	0.08	1.36	0.14
F12	1.55	0.11	1.44	0.07	1.19	0.08	1.39	0.11
F13	1.4	0.06	1.13	0.05	1.45	0.07	1.33	0.1
F14RRS	1.2	0.06	1.43	0.08	1.28	0.07	1.3	0.07
F14RSR	1.82	0.06	1.34	0.04	1.09	0.1	1.42	0.21
F14SRS	1.2	0.06	1.23	0.04	1.62	0.07	1.35	0.14
F14SSR	1.09	0.08	1.17	0.07	1.54	0.07	1.27	0.14
F15	1	0.04	0.93	0.05	1.15	0.06	1.03	0.06
F16	1.1	0.08	1.29	0.06	1.59	0.05	1.33	0.14
F17	1.02	0.11	1.35	0.09	1.1	0.06	1.16	0.1
F18	1.38	0.09	1.13	0.06	1.25	0.09	1.25	0.07
F19	1.05	0.05	1.11	0.06	1.67	0.12	1.28	0.2
F20RS	1.33	0.08	1.84	0.07	1.45	0.09	1.54	0.15
F20SR	1.14	0.08	1.46	0.06	1.4	0.04	1.33	0.1
F21	1.31	0.06	1.25	0.07	1.14	0.1	1.23	0.05

Figure SM-RMS-6. Root mean square deviation of TM5 helix backbone over time.
Y-values are given in angstroms. For RMSD calculation taken are only backbone atoms of residues 227-260 (H5).

Table SM-RMS-6. Root mean square fluctuations of TM5 helix backbone.
Calculated as a mean RMSD over last 10 ns of simulations in 3 replicas. For RMSD calculation taken are only backbone atoms of residues 227-260 (H5).

derivative	replica							
	a		b		c			
	mean	sem	mean	sem	mean	sem	MEAN	SEM
F01	**1.11**	**0.06**	**1.08**	**0.04**	**0.97**	**0.06**	**1.05**	**0.04**
F02	1.05	0.05	1.11	0.04	0.99	0.04	1.05	0.03
F03	0.9	0.04	0.71	0.04	0.7	0.03	0.77	0.07
F04	1.04	0.06	1.09	0.09	0.97	0.04	1.03	0.03
F05R	0.97	0.05	1.05	0.03	0.98	0.04	1	0.03
F05S	0.75	0.03	0.8	0.04	0.99	0.07	0.85	0.07
F06R	0.87	0.06	0.79	0.02	0.91	0.04	0.86	0.04
F06S	0.79	0.04	0.76	0.04	0.69	0.03	0.75	0.03
F07	0.98	0.06	0.93	0.04	0.87	0.06	0.93	0.03
F08	1.57	0.04	0.89	0.07	0.89	0.04	1.12	0.23
F09	0.92	0.06	0.78	0.05	0.81	0.04	0.84	0.04
F10	0.81	0.04	1.58	0.05	0.8	0.07	1.06	0.26
F11R	0.75	0.03	0.78	0.04	0.71	0.04	0.75	0.02
F11S	1.06	0.05	0.86	0.05	0.85	0.04	0.92	0.07
F12	1.02	0.04	0.82	0.05	0.72	0.04	0.85	0.09
F13	0.66	0.03	0.87	0.02	0.92	0.05	0.82	0.08
F14RRS	0.69	0.03	0.81	0.03	0.91	0.07	0.8	0.06
F14RSR	1.04	0.07	0.88	0.05	0.9	0.04	0.94	0.05
F14SRS	1.01	0.04	0.89	0.04	1.23	0.04	1.04	0.1
F14SSR	0.91	0.05	0.94	0.06	1.19	0.03	1.01	0.09
F15	0.92	0.03	0.73	0.04	0.84	0.04	0.83	0.06
F16	0.85	0.06	0.96	0.06	0.98	0.04	0.93	0.04
F17	0.84	0.05	1.05	0.03	0.77	0.03	0.89	0.08
F18	0.98	0.04	0.82	0.04	1.05	0.04	0.95	0.07
F19	0.78	0.05	0.9	0.05	1.17	0.09	0.95	0.12
F20RS	1.06	0.07	1.48	0.06	1.12	0.07	1.22	0.13
F20SR	0.76	0.05	0.92	0.04	0.87	0.05	0.85	0.05
F21	0.79	0.03	1.19	0.08	0.85	0.04	0.94	0.12

Figure SM-RMS-7. Root mean square deviation of TM6 helix backbone over time.
Y-values are given in angstroms. For RMSD calculation taken are only backbone atoms of residues 275-304 (H6).

Table SM-RMS-7. Root mean square fluctuations of TM6 helix backbone.
Calculated as a mean RMSD over last 10 ns of simulations in 3 replicas. For RMSD calculation taken are only backbone atoms of residues 275-304 (H6).

derivative	replica							
	a		b		c			
	mean	sem	mean	sem	mean	sem	MEAN	SEM
F01	0.67	0.05	0.65	0.02	1.06	0.02	0.79	0.13
F02	0.97	0.06	0.82	0.08	0.81	0.02	0.87	0.05
F03	1.1	0.05	0.75	0.03	0.76	0.03	0.87	0.12
F04	1.14	0.04	1.05	0.07	1	0.05	1.06	0.04
F05R	0.94	0.03	0.75	0.06	0.78	0.03	0.82	0.06
F05S	0.78	0.04	0.92	0.03	0.78	0.03	0.83	0.05
F06R	0.84	0.05	0.95	0.03	0.94	0.05	0.91	0.04
F06S	0.75	0.03	0.96	0.03	1.02	0.05	0.91	0.08
F07	1.19	0.06	0.99	0.06	0.83	0.03	1	0.1
F08	1.36	0.03	0.95	0.04	0.96	0.04	1.09	0.14
F09	0.92	0.05	0.85	0.04	0.85	0.03	0.87	0.02
F10	0.91	0.06	0.96	0.03	0.89	0.07	0.92	0.02
F11R	0.68	0.03	0.78	0.03	0.92	0.05	0.79	0.07
F11S	0.9	0.05	0.71	0.03	0.96	0.06	0.86	0.08
F12	0.78	0.03	0.72	0.04	0.83	0.04	0.78	0.03
F13	0.84	0.08	0.98	0.03	0.75	0.03	0.86	0.07
F14RRS	0.95	0.05	0.82	0.05	0.84	0.04	0.87	0.04
F14RSR	0.79	0.04	1.07	0.07	1	0.04	0.95	0.08
F14SRS	0.86	0.05	1	0.03	0.94	0.04	0.93	0.04
F14SSR	0.91	0.04	0.85	0.07	0.9	0.04	0.89	0.02
F15	0.96	0.02	0.81	0.03	0.79	0.03	0.85	0.05
F16	1.08	0.04	1.11	0.08	0.76	0.03	0.98	0.11
F17	0.92	0.03	0.93	0.03	0.78	0.03	0.88	0.05
F18	0.9	0.04	0.96	0.03	1.18	0.05	1.01	0.09
F19	0.88	0.03	0.72	0.04	1.03	0.06	0.88	0.09
F20RS	0.96	0.06	1.04	0.05	1.26	0.05	1.09	0.09
F20SR	0.82	0.02	1.07	0.05	0.88	0.05	0.92	0.08
F21	0.85	0.03	1.09	0.04	0.73	0.04	0.89	0.11

Figure SM-RMS-8. Root mean square deviation of TM7 helix backbone over time.
Y-values are given in angstroms. For RMSD calculation taken are only backbone atoms of residues 314-338 (H7).

Table SM-RMS-8. Root mean square fluctuations of TM7 helix backbone.
Calculated as a mean RMSD over last 10 ns of simulations in 3 replicas. For RMSD calculation taken are only backbone atoms of residues 314-338 (H7).

derivative	replica							
	a		b		c			
	mean	sem	mean	sem	mean	sem	MEAN	SEM
F01	0.78	0.05	0.66	0.03	0.96	0.08	0.8	0.09
F02	1.02	0.04	1.08	0.02	0.94	0.03	1.01	0.04
F03	0.82	0.03	0.76	0.03	0.75	0.03	0.78	0.02
F04	0.97	0.03	0.99	0.02	0.91	0.04	0.96	0.02
F05R	0.95	0.02	0.7	0.03	0.96	0.06	0.87	0.09
F05S	0.85	0.05	0.69	0.02	0.81	0.02	0.78	0.05
F06R	0.83	0.03	0.76	0.03	0.89	0.03	0.83	0.04
F06S	0.79	0.02	0.89	0.04	0.71	0.03	0.8	0.05
F07	0.88	0.02	0.87	0.03	1.09	0.05	0.95	0.07
F08	0.78	0.02	0.78	0.06	0.85	0.02	0.8	0.02
F09	0.8	0.02	0.8	0.03	0.8	0.04	0.8	0
F10	0.83	0.05	0.71	0.02	0.86	0.04	0.8	0.05
F11R	0.8	0.04	0.86	0.02	0.78	0.04	0.81	0.02
F11S	0.96	0.03	0.73	0.04	0.85	0.03	0.85	0.07
F12	0.83	0.03	0.76	0.03	0.69	0.02	0.76	0.04
F13	0.8	0.03	0.71	0.02	0.94	0.02	0.82	0.07
F14RRS	0.85	0.05	0.95	0.03	0.97	0.03	0.92	0.04
F14RSR	0.94	0.05	0.85	0.04	0.8	0.05	0.86	0.04
F14SRS	1.19	0.03	0.77	0.03	0.88	0.05	0.95	0.13
F14SSR	0.86	0.02	0.78	0.04	0.79	0.06	0.81	0.03
F15	0.85	0.03	0.76	0.03	0.86	0.05	0.82	0.03
F16	0.75	0.03	0.92	0.05	0.79	0.02	0.82	0.05
F17	0.91	0.04	0.86	0.03	0.78	0.02	0.85	0.04
F18	0.93	0.03	0.79	0.04	0.79	0.03	0.84	0.05
F19	0.82	0.02	0.74	0.03	0.88	0.03	0.81	0.04
F20RS	0.88	0.03	1.11	0.03	0.95	0.08	0.98	0.07
F20SR	0.79	0.03	0.89	0.02	0.82	0.04	0.83	0.03
F21	0.94	0.02	0.94	0.05	0.85	0.02	0.91	0.03

	H1	H2	H3	H4	H5	H6	H7	prot
F01	0.69	0.83	0.86	1.22	1.05	0.79	0.80	0.92
F02	0.98	1.01	0.79	1.41	1.05	0.87	1.01	1.02
F03	1.00	0.78	0.72	1.20	0.77	0.87	0.78	0.87
F04	1.04	0.98	0.72	1.35	1.03	1.06	0.96	1.03
F05R	0.98	0.83	0.77	1.36	1.00	0.82	0.87	0.95
F05S	0.88	0.82	0.77	1.34	0.85	0.83	0.78	0.90
F06R	0.93	0.91	0.77	1.30	0.86	0.91	0.83	0.93
F06S	0.96	0.62	0.67	1.24	0.75	0.91	0.80	0.86
F07	0.90	0.80	0.72	1.29	0.93	1.00	0.95	0.95
F08	1.11	1.06	0.81	1.16	1.12	1.09	0.80	1.04
F09	0.85	0.80	0.71	1.20	0.84	0.87	0.80	0.87
F10	1.03	0.81	0.80	1.29	1.06	0.92	0.80	0.98
F11R	0.87	0.82	0.68	1.29	0.75	0.79	0.81	0.86
F11S	1.05	1.04	0.72	1.36	0.92	0.86	0.85	0.98
F12	0.71	0.69	0.74	1.39	0.85	0.78	0.76	0.86
F13	0.84	0.72	0.74	1.33	0.82	0.86	0.82	0.88
F14RSR	1.02	0.88	0.68	1.42	0.94	0.95	0.86	0.97
F14SSR	0.84	0.76	0.73	1.27	1.01	0.89	0.81	0.91
F15	0.92	0.79	0.74	1.03	0.83	0.85	0.82	0.86
F16	0.95	0.89	0.73	1.33	0.93	0.98	0.82	0.96
F17	0.90	0.92	0.76	1.16	0.89	0.88	0.85	0.91
F18	0.94	0.81	0.74	1.25	0.95	1.01	0.84	0.94
F19	0.93	0.79	0.71	1.28	0.95	0.88	0.81	0.92
F20SR	0.88	0.86	0.66	1.33	0.85	0.92	0.83	0.91
F21	0.90	0.70	0.82	1.23	0.94	0.89	0.91	0.92
MEAN	0.92	0.84	0.74	1.28	0.92	0.90	0.84	0.93
STD	0.10	0.11	0.05	0.09	0.10	0.08	0.06	0.05

Figure SM-RMS-9. RMSF mean values.

Given are means from 3 simulations. H1-H7: backbone RMSF of helices. Prot: backbone RMSF of the protein. Colouring according to the order in a given category: from red (low values) to green (high values).

Table SM-DIH-1. Summary of monitored dihedral angles.

Residue	Dihedral	Value	Figures	Comment
Interacting with (or close to) piperidine				
D147	X_1	*dominant cluster*: -166.9; *minor cluster* (**F01**, **F03**, **F04**, **F09**, **F11S**, **F17**): -92.2	SM-DIH-1 and SM-DIH-2	stable, transient switches to the minor cluster in several derivatives
	X_2	several clusters	SM-DIH-3 and SM-DIH-4	no clear preference among the derivatives
Y148	X_1	-72.5	SM-DIH-5 and SM-DIH-6	stable in all derivatives
	X_2	several clusters	SM-DIH-7 and SM-DIH-8	symmetrical rotamer exchanges
Close to 4-axial substituent ("under" piperidine)				
W318	X_1	175.9	SM-DIH-9 and SM-DIH-10	stable
	X_2	-104.7	SM-DIH-11 and SM-DIH-12	stable, but differentiated with respect to derivatives, to the left given is the global mean value, however for separate sets of simulations the mean varies between -93.2 and -116.0
H319	X_1	-67.8	SM-DIH-13 and SM-DIH-14	stable
	X_2	159.6	SM-DIH-15 and SM-DIH-16	in some derivatives also minor clusters
Close to N-substituent				
M151	X_1	*dominant cluster*: 172.6 *minor cluster:* 78.7	SM-DIH-17 and SM-DIH-18	transient rotamer exchanges, without clear pattern with respect to derivatives
	X_2	*dominant cluster*: -86.1 *minor clusters:* -177.2 and 85.9	SM-DIH-19 and SM-DIH-20	transient rotamer exchanges, without clear pattern with respect to derivatives
W293	X_1	-165.2	SM-DIH-21 and SM-DIH-22	stable
	X_2	-106.3 (global mean)	10, 11, SM-VOL-4, SM-DIH-23 and SM-DIH-24	stable, but differentiated with respect to derivatives, a relationship between dihedral value and the volume sum of fentanyl's N-chain and anilide's aromatic
H297	X_1	-68.4	SM-DIH-25 and SM-DIH-26	stable

Residue	Dihedral	Value	Figures	Comment
	X_2	103.8	SM-DIH-27 and SM-DIH-28	stable
Y326	X_1	-67.6	SM-DIH-29 and SM-DIH-30	stable
	X_2	-62.3 in **F03** and **F20RS** another cluster: 92.6	SM-DIH-31 and SM-DIH-32	stable
Close to anilide's aromatic				
W133	X_1	179.1	SM-DIH-33 and SM-DIH-34	stable
	X_2	-97.8 (global mean)	SM-VOL-5, SM-VOL-6, SM-DIH-35 and SM-DIH-36	stable, but differentiated with respect to derivatives, a relationship between dihedral value and the volume sum of fentanyl's N-chain and anilide's aromatic
Outside the binding pocket				
Y336	X_1	-68.3	SM-DIH-41 and SM-DIH-42	stable
	X_2	-76.6; in **F01** and **F13** another cluster: 111.4	SM-DIH-43 and SM-DIH-44	stable

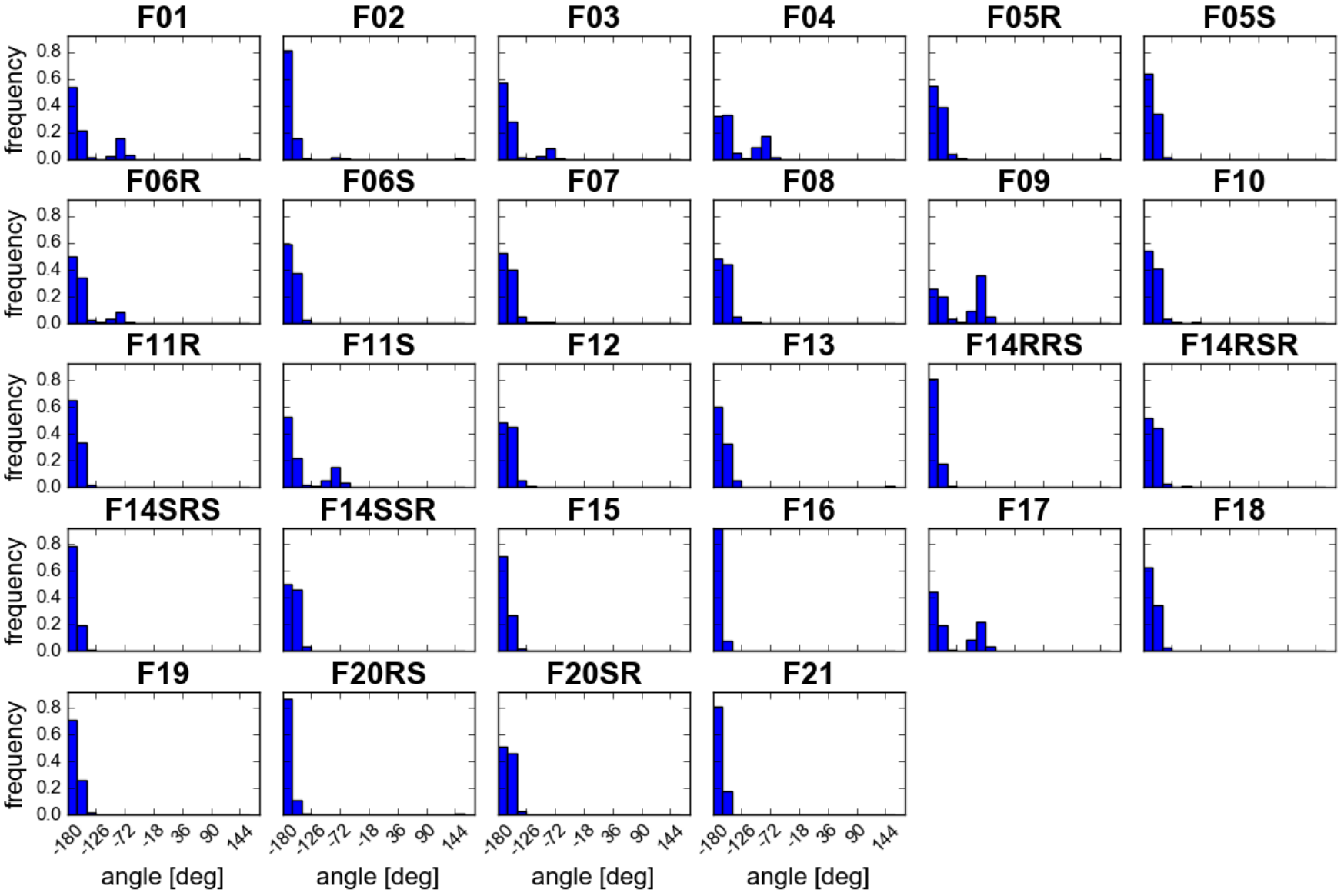

Figure SM-DIH-1. Distributions of X1 dihedral angle values of D147.
Data are collected from last 10ns of production in 3 replicas.

Figure SM-DIH-2. Time evolution of X1 dihedral angle of D147.
Y-values are given in degrees.

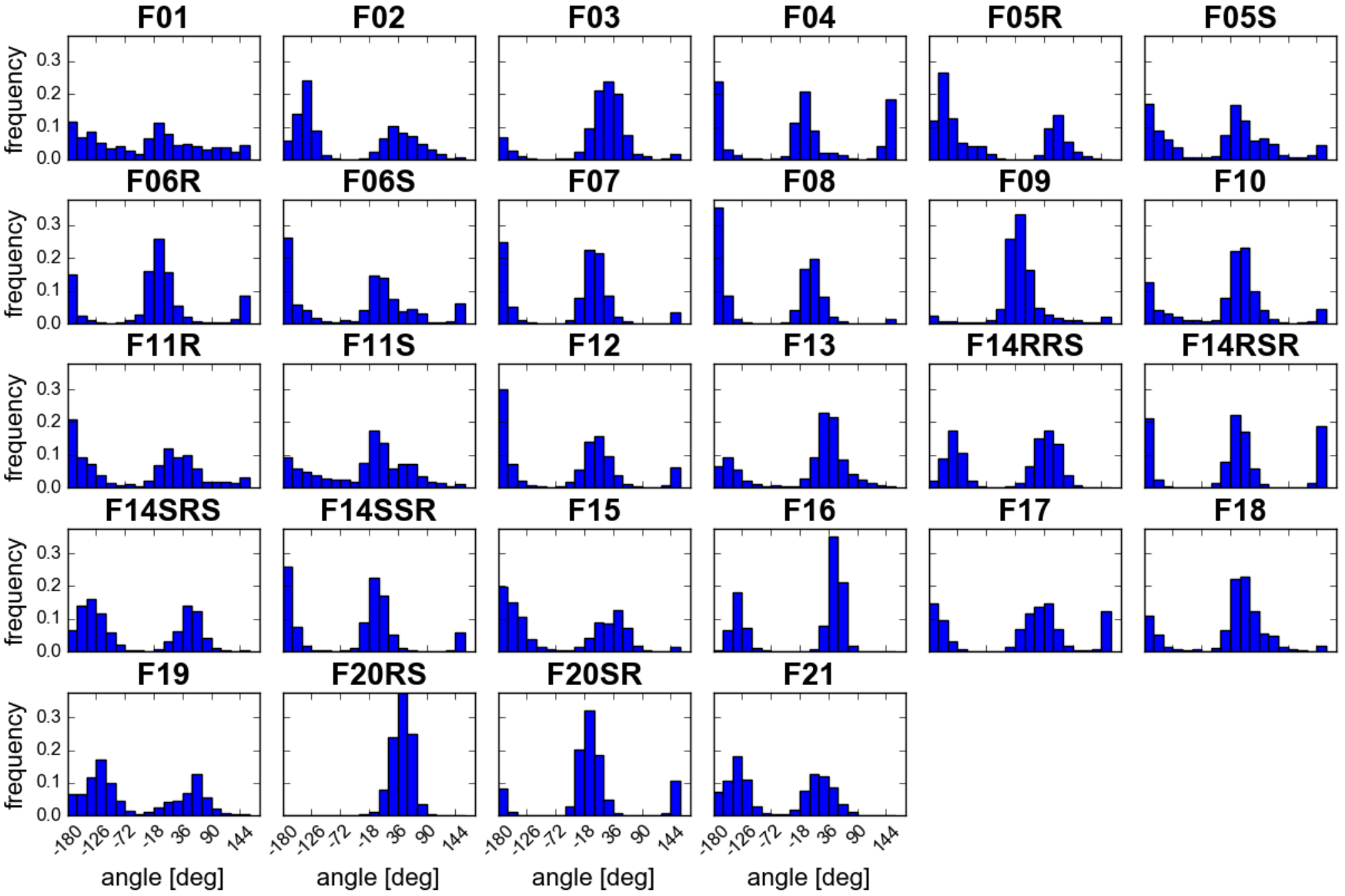

Figure SM-DIH-3. Distributions of X2 dihedral angle values of D147.
Data are collected from last 10ns of production in 3 replicas.

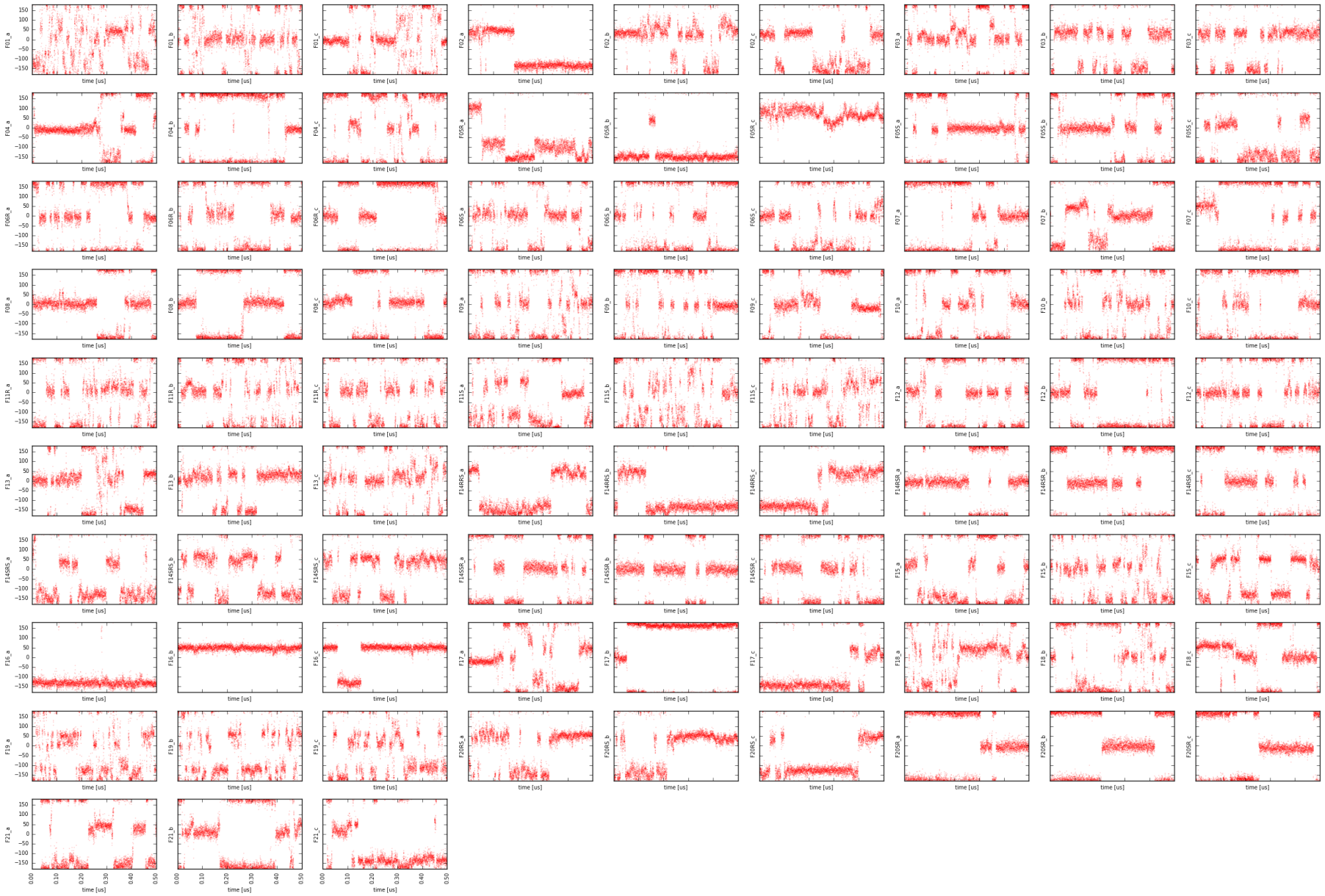

Figure SM-DIH-4. Time evolution of X2 dihedral angle of D147.
Y-values are given in degrees.

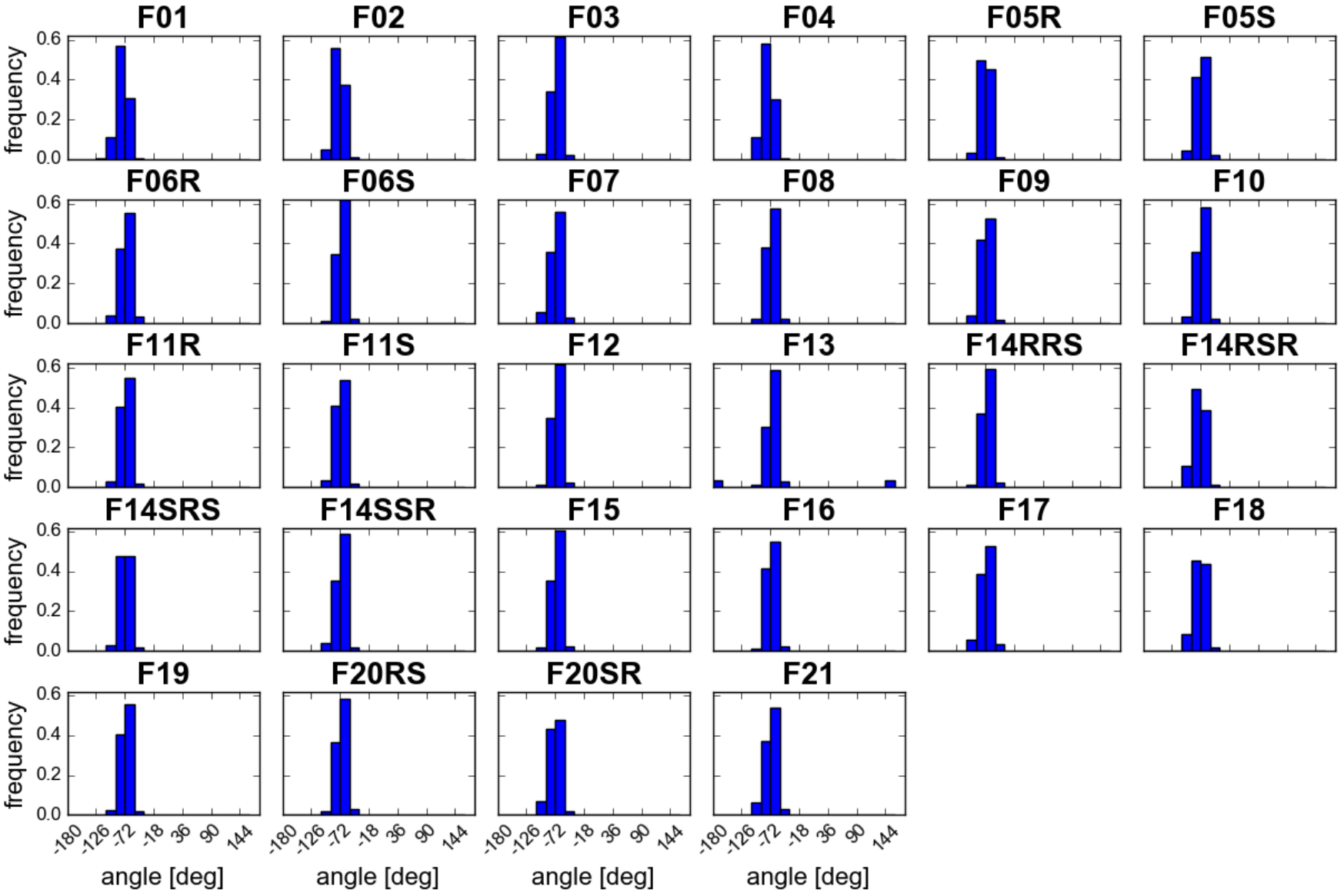

Figure SM-DIH-5. Distributions of X1 dihedral angle values of Y148.
Data are collected from last 10ns of production in 3 replicas.

Figure SM-DIH-6. Time evolution of X1 dihedral angle of Y148.
Y-values are given in degrees.

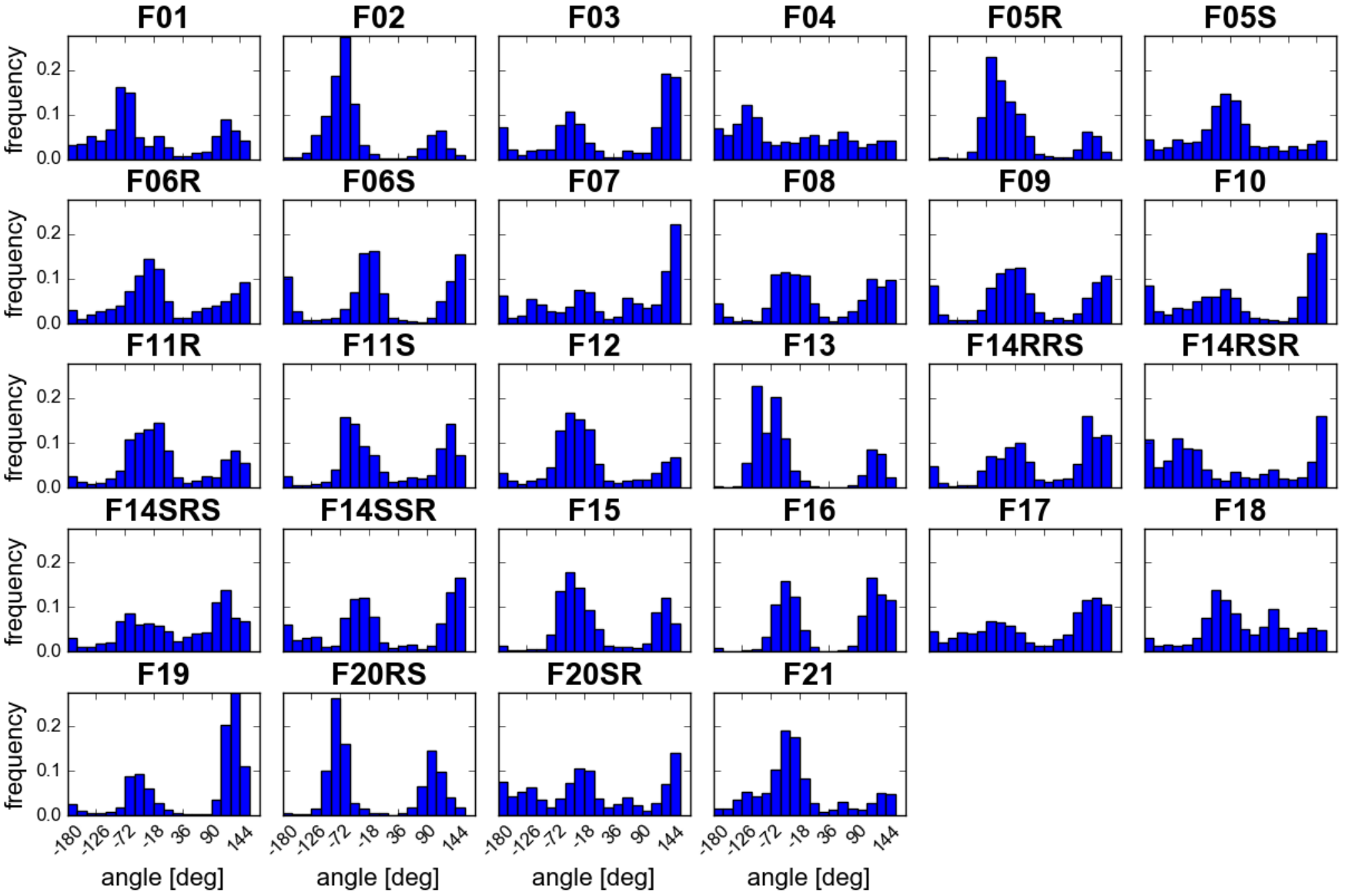

Figure SM-DIH-7. Distributions of X2 dihedral angle values of Y148.
Data are collected from last 10ns of production in 3 replicas.

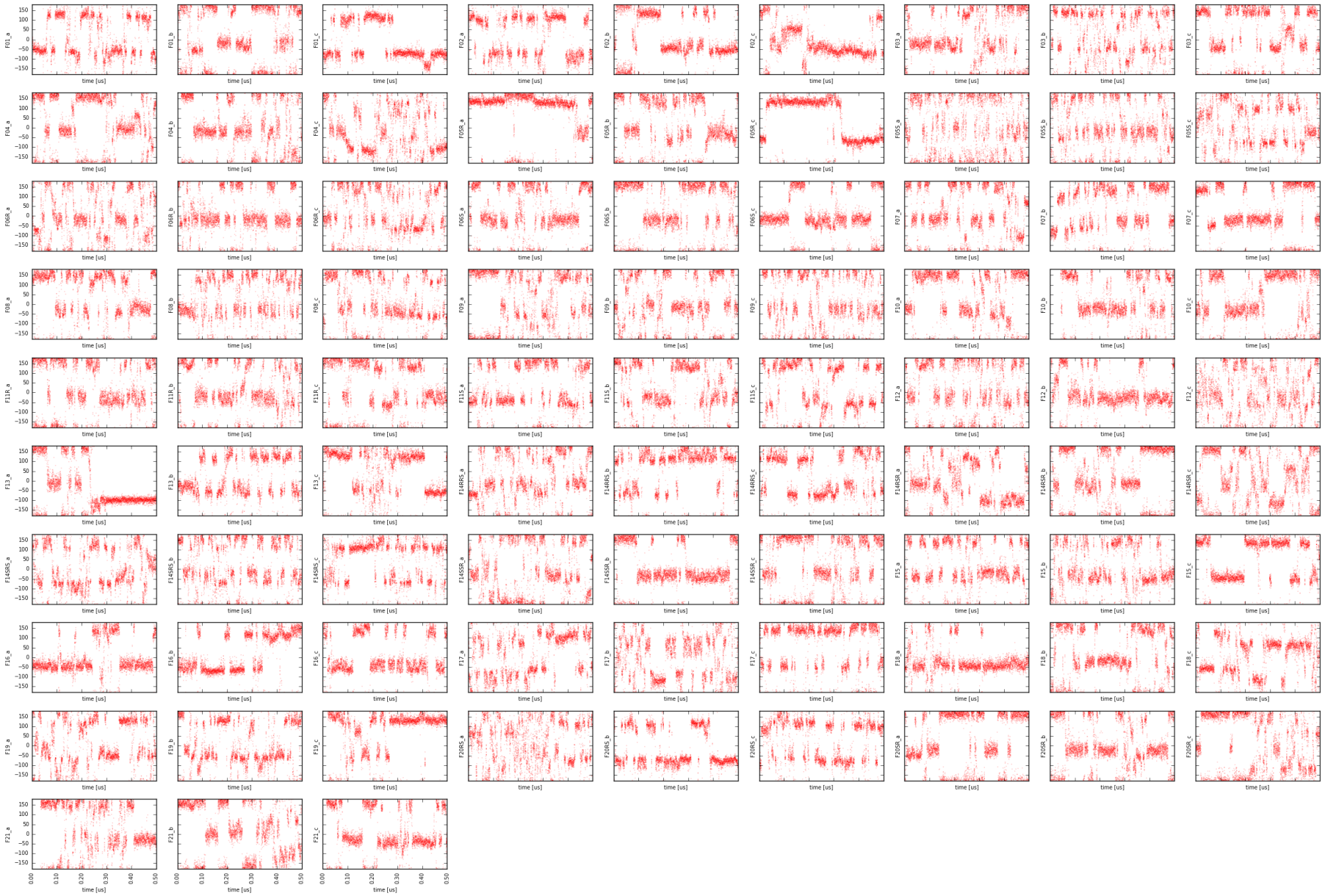

Figure SM-DIH-8. Time evolution of X2 dihedral angle of Y148.
Y-values are given in degrees.

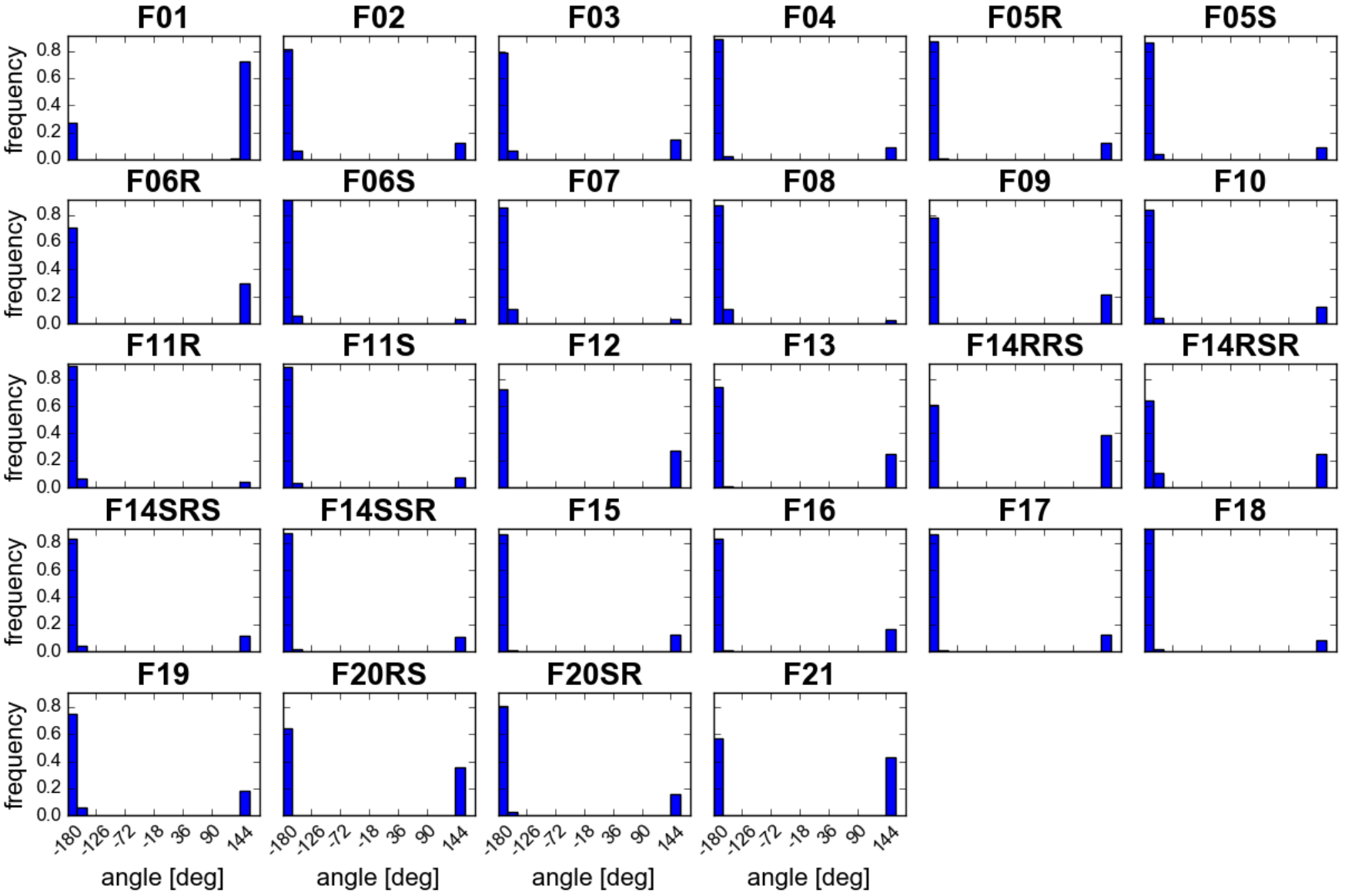

Figure SM-DIH-9. Distributions of X1 dihedral angle values of W318.
Data are collected from last 10ns of production in 3 replicas.

Figure SM-DIH-10. Time evolution of X1 dihedral angle of W318.
Y-values are given in degrees.

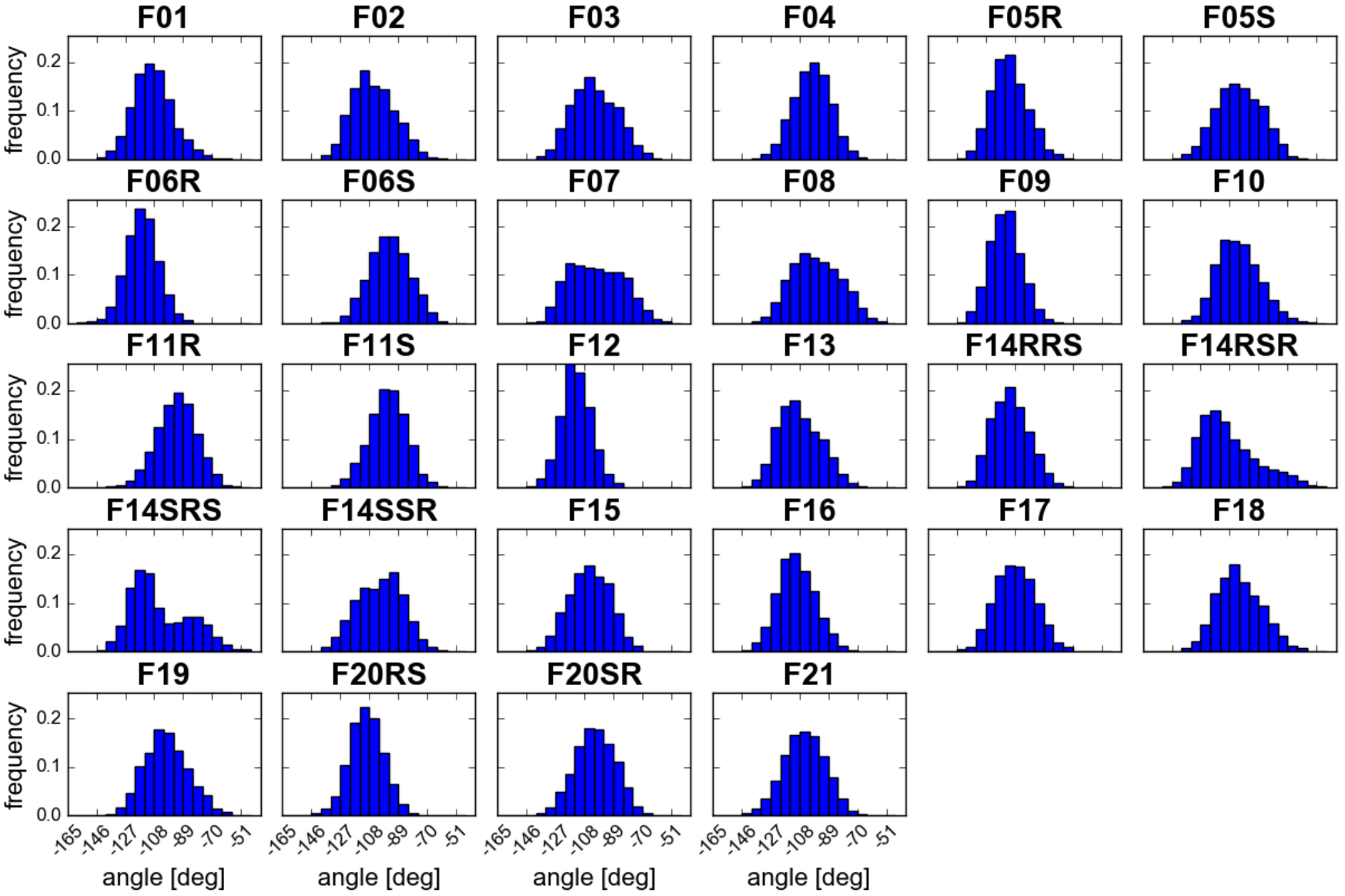

Figure SM-DIH-11. Distributions of X2 dihedral angle values of W318.
Data are collected from last 10ns of production in 3 replicas.

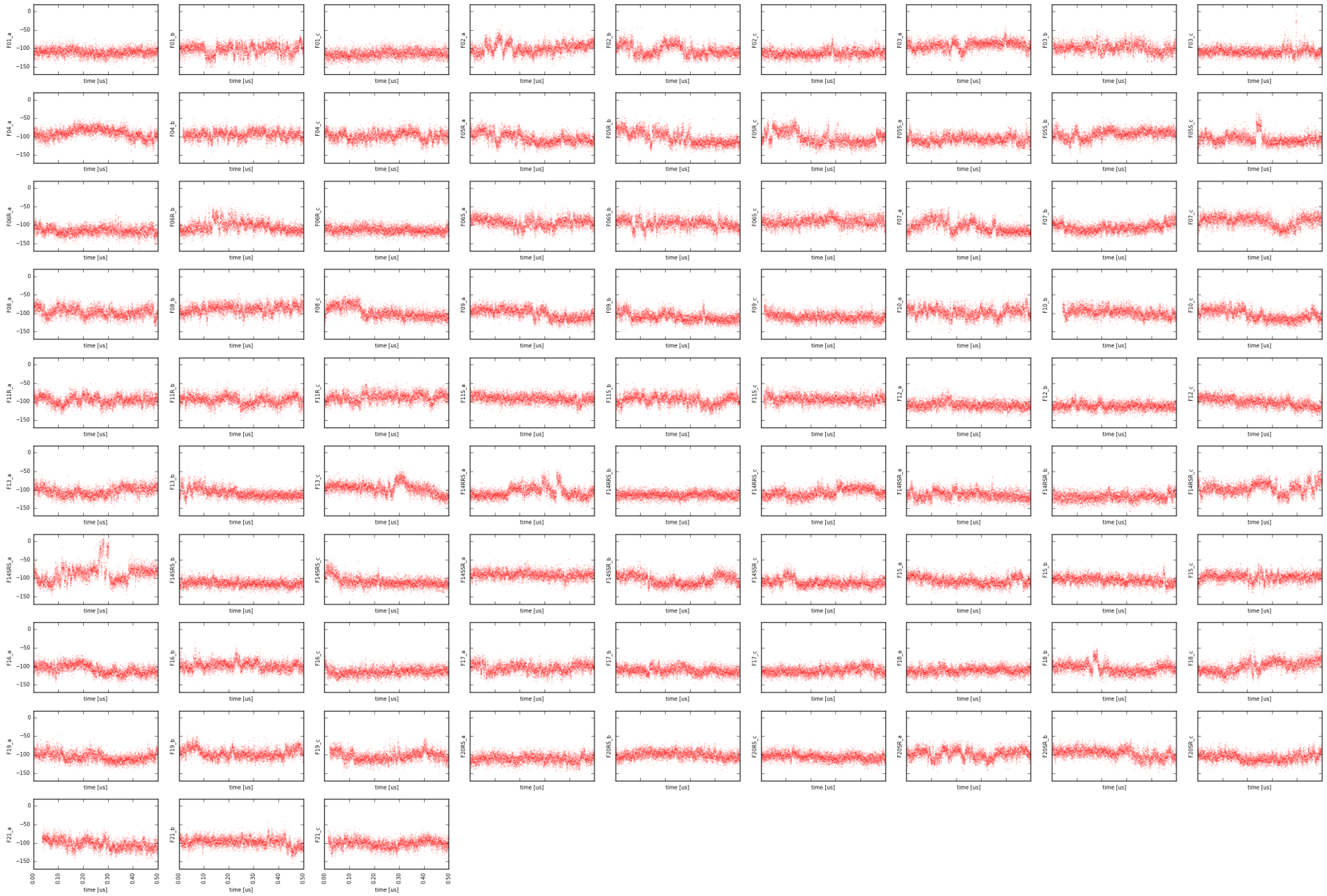

Figure SM-DIH-12. Time evolution of X2 dihedral angle of W318.
Y-values are given in degrees.

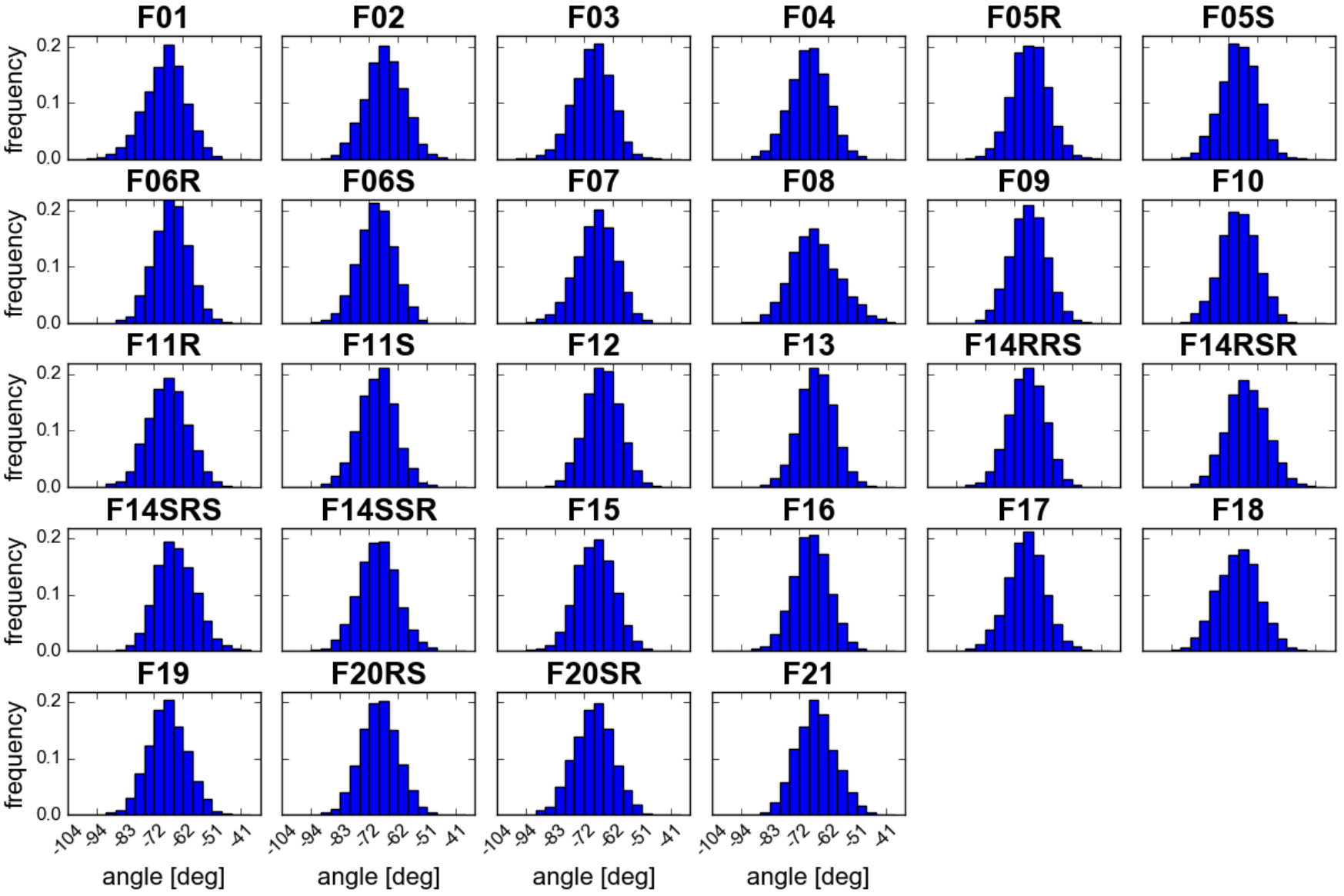

Figure SM-DIH-13. Distributions of X1 dihedral angle values of H319.
Data are collected from last 10ns of production in 3 replicas.

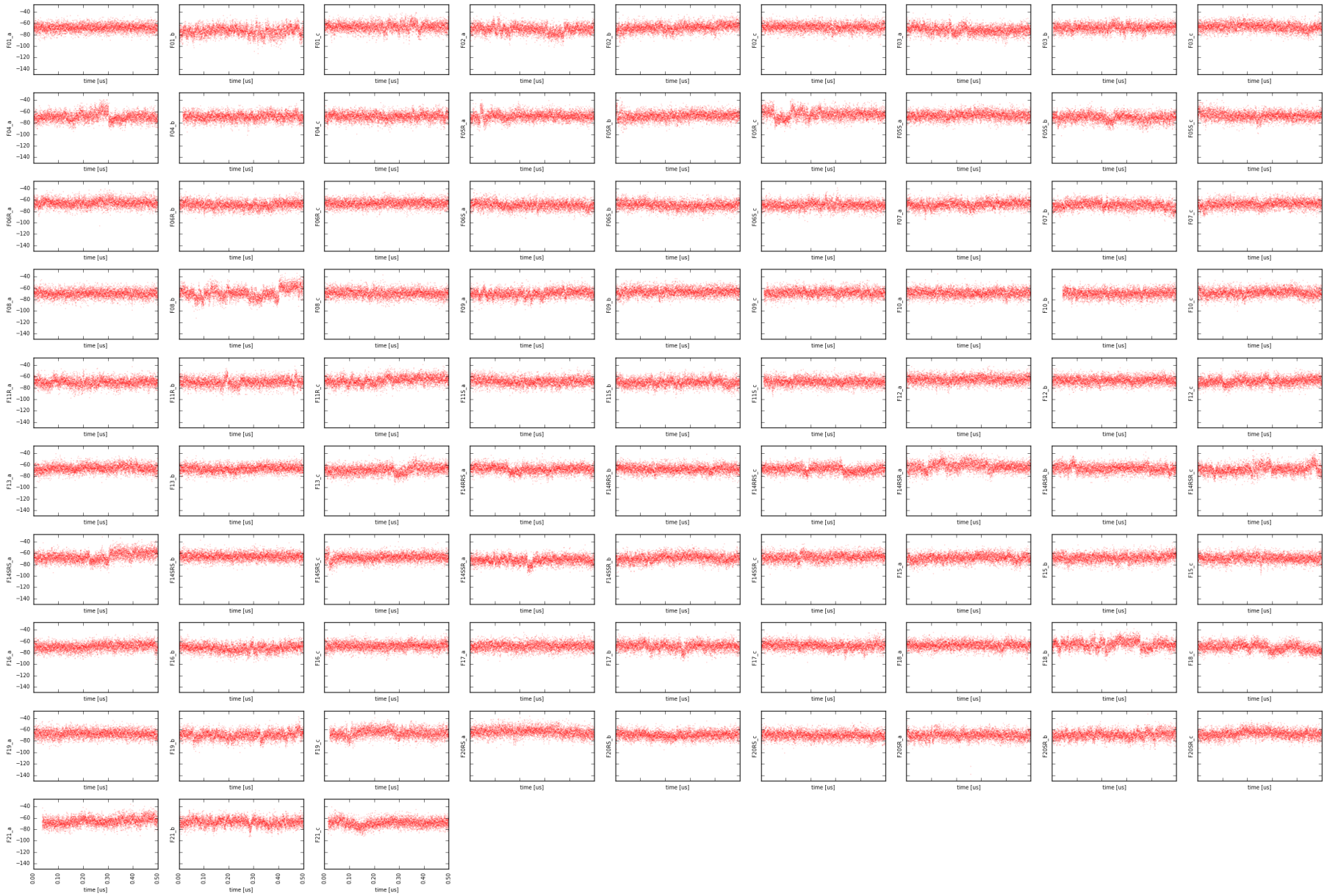

Figure SM-DIH-14. Time evolution of X1 dihedral angle of H319.
Y-values are given in degrees.

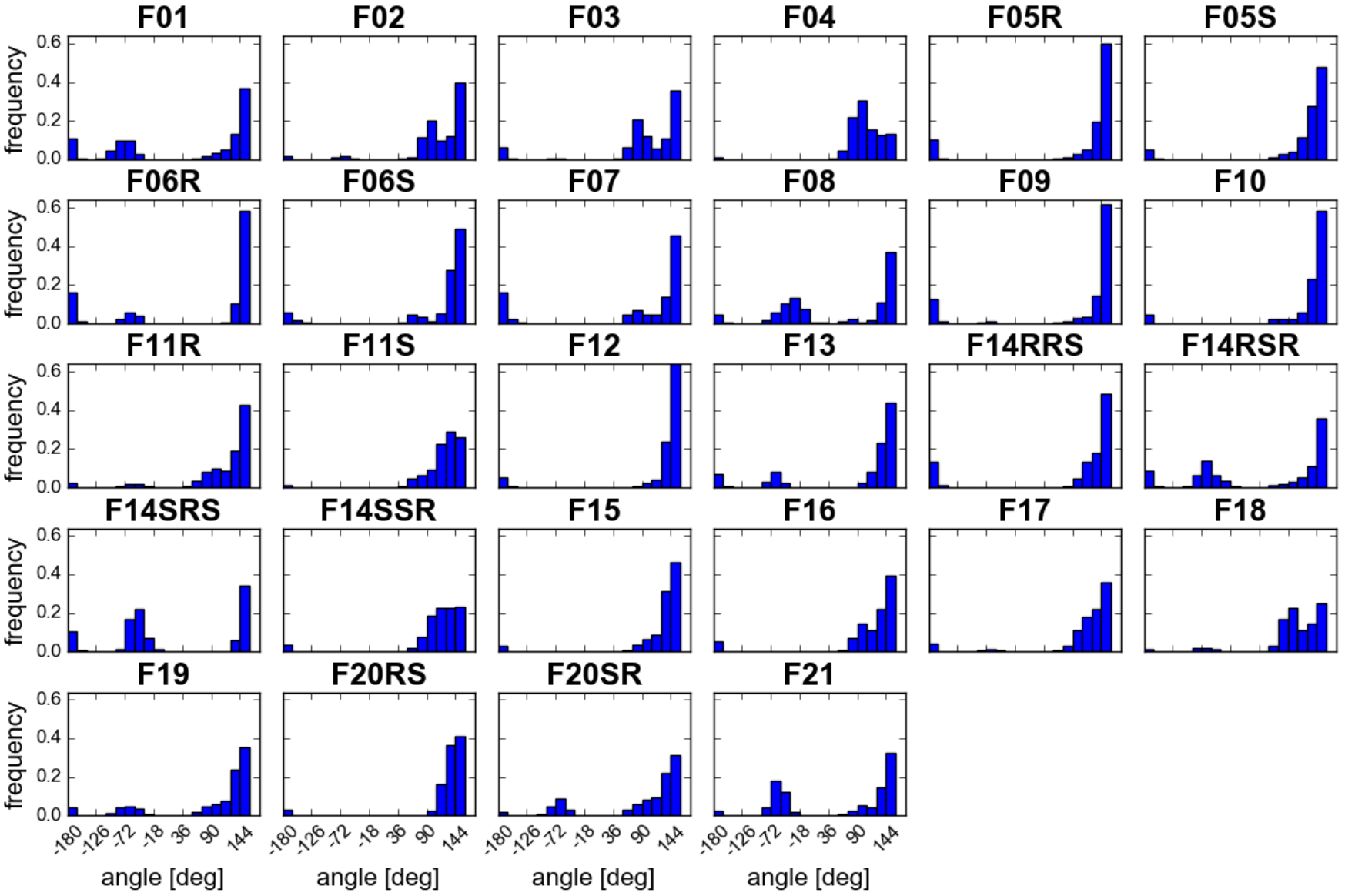

Figure SM-DIH-15. Distributions of X2 dihedral angle values of H319.
Data are collected from last 10ns of production in 3 replicas.

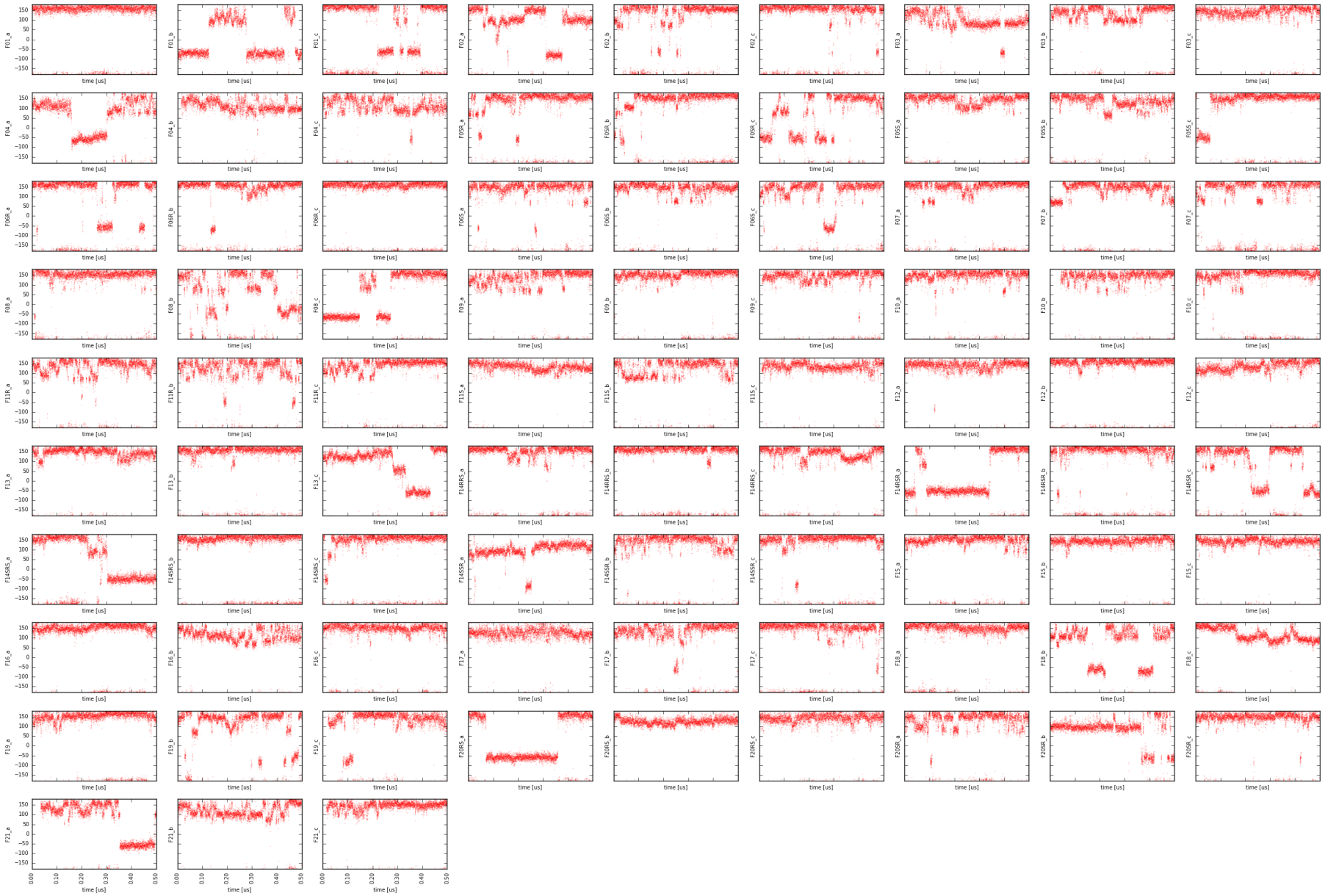

Figure SM-DIH-16. Time evolution of X2 dihedral angle of H319.
Y-values are given in degrees.

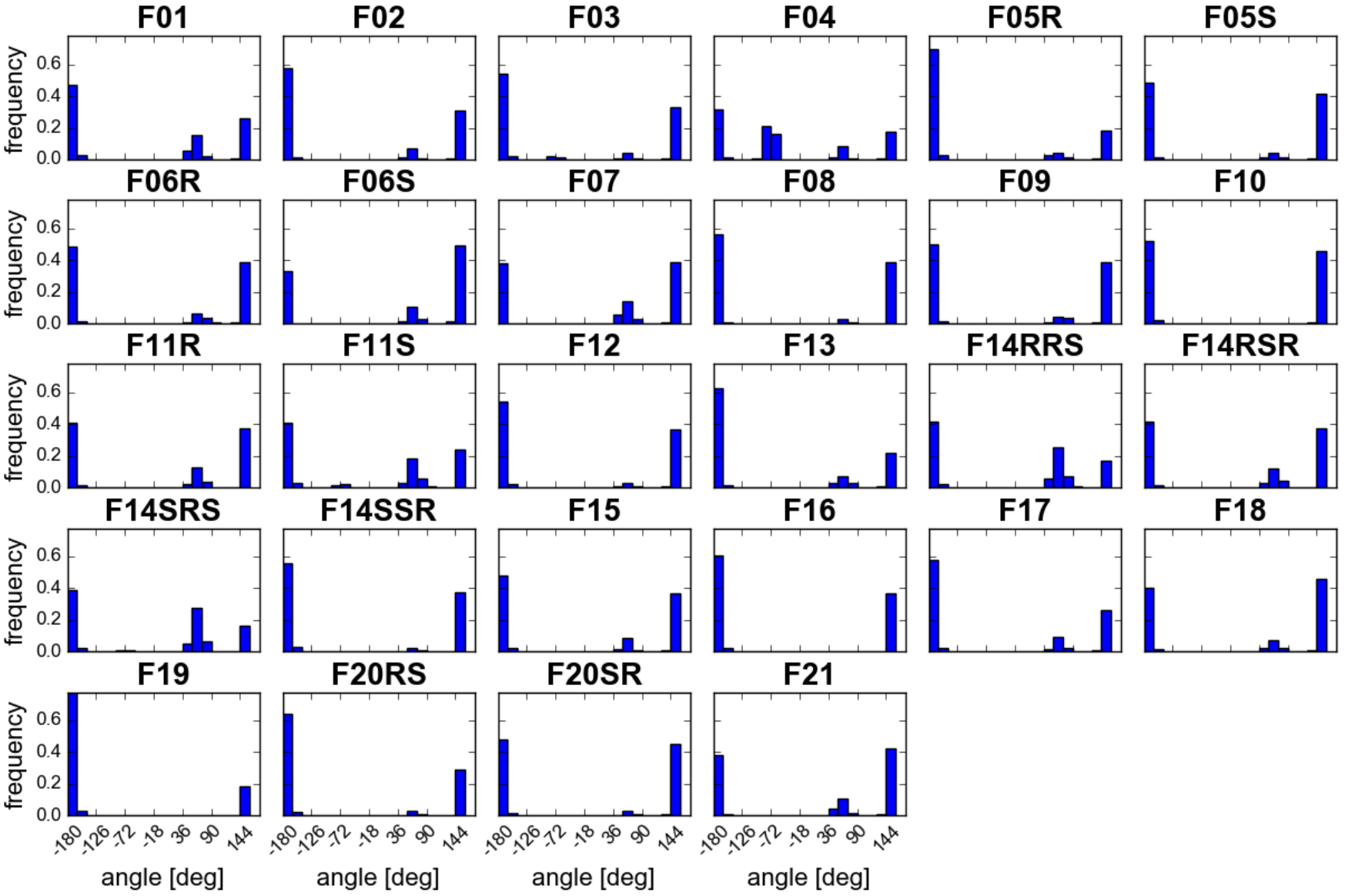

Figure SM-DIH-17. Distributions of X1 dihedral angle values of M151.
Data are collected from last 10ns of production in 3 replicas.

Figure SM-DIH-18. Time evolution of X1 dihedral angle of M151.
Y-values are given in degrees.

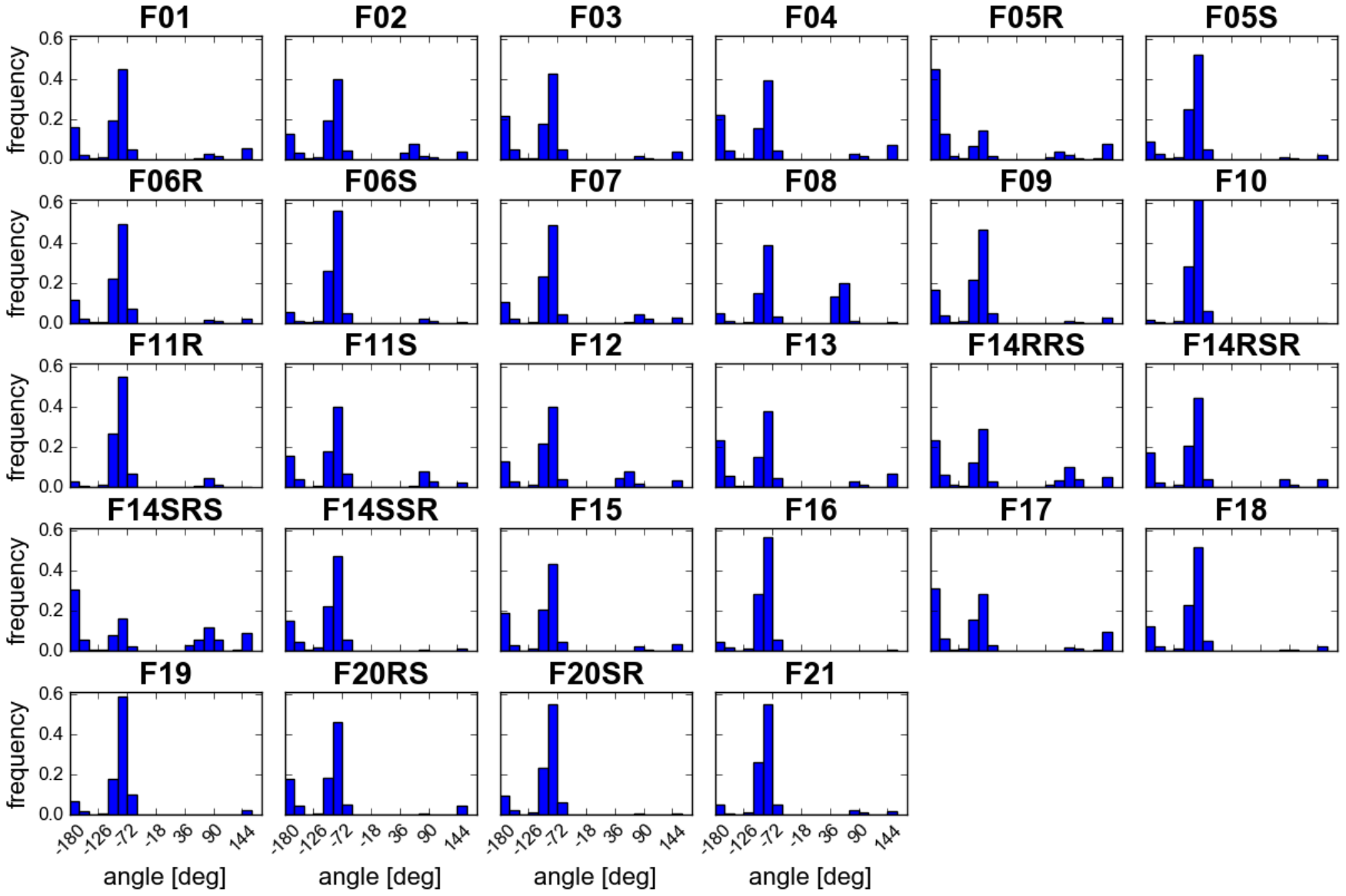

Figure SM-DIH-19. Distributions of X2 dihedral angle values of M151.
Data are collected from last 10ns of production in 3 replicas.

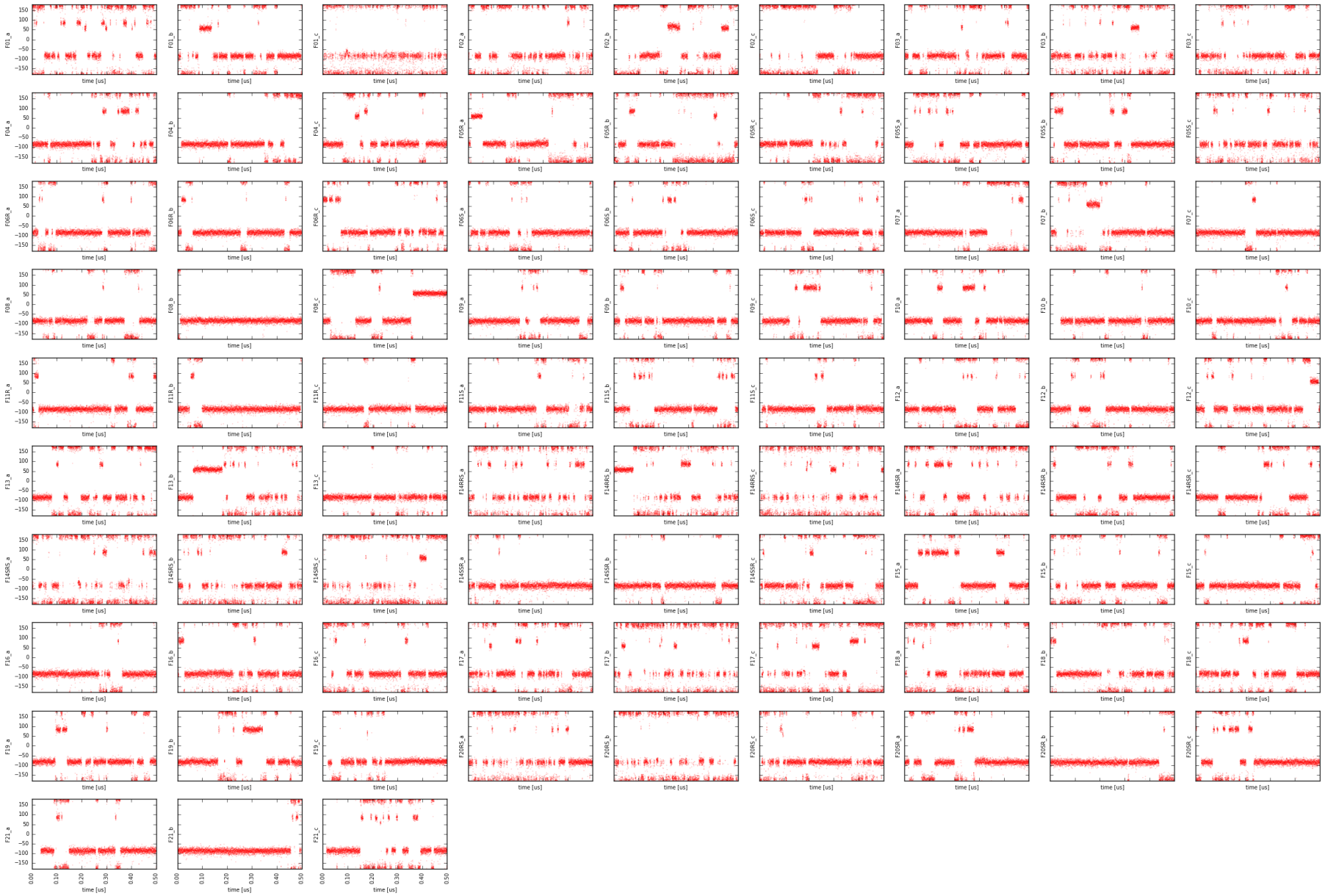

Figure SM-DIH-20. Time evolution of X2 dihedral angle of M151.
Y-values are given in degrees.

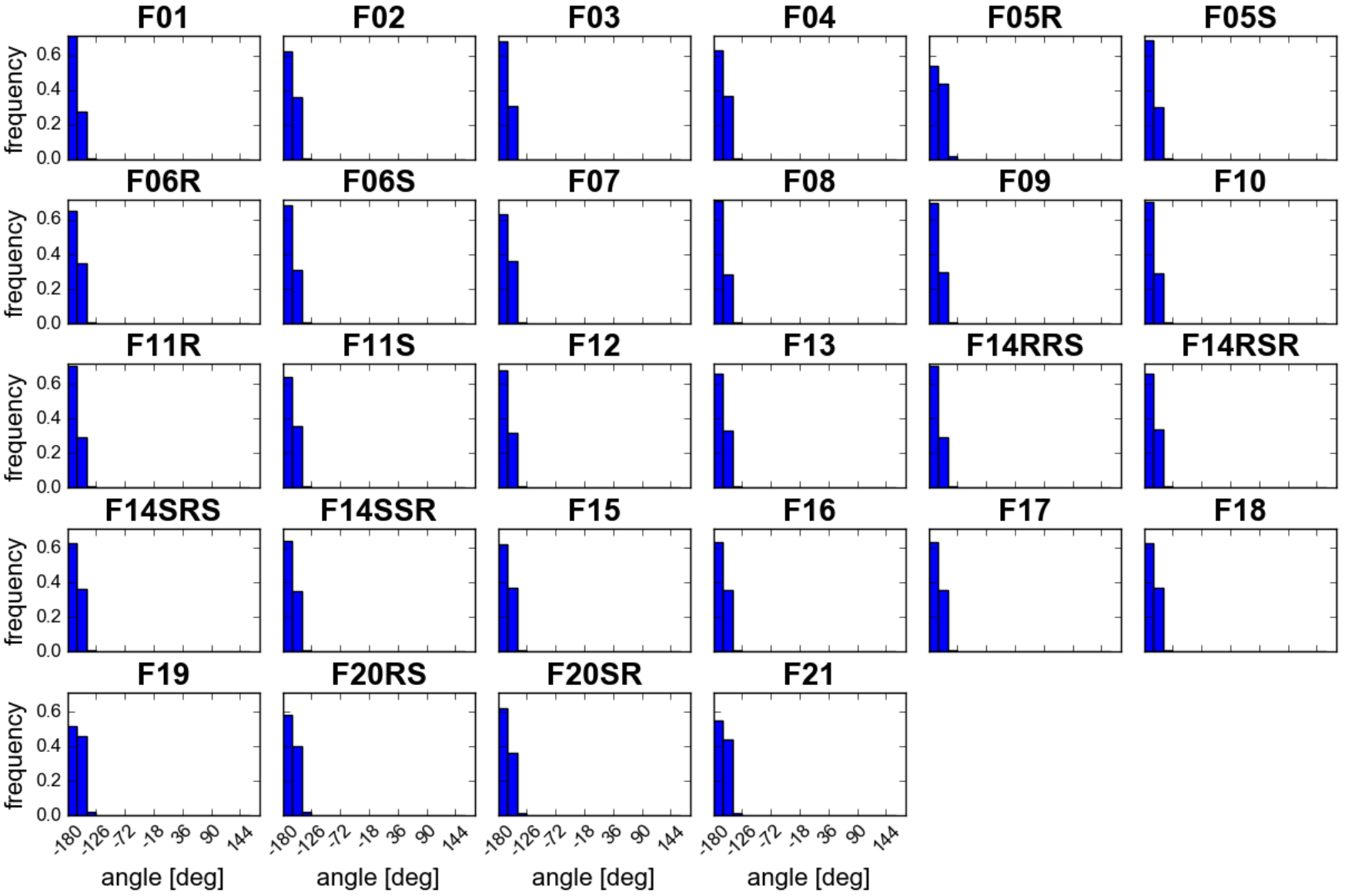

Figure SM-DIH-21. Distributions of X1 dihedral angle values of W293.
Data are collected from last 10ns of production in 3 replicas.

Figure SM-DIH-22. Time evolution of X1 dihedral angle of W293.
Y-values are given in degrees.

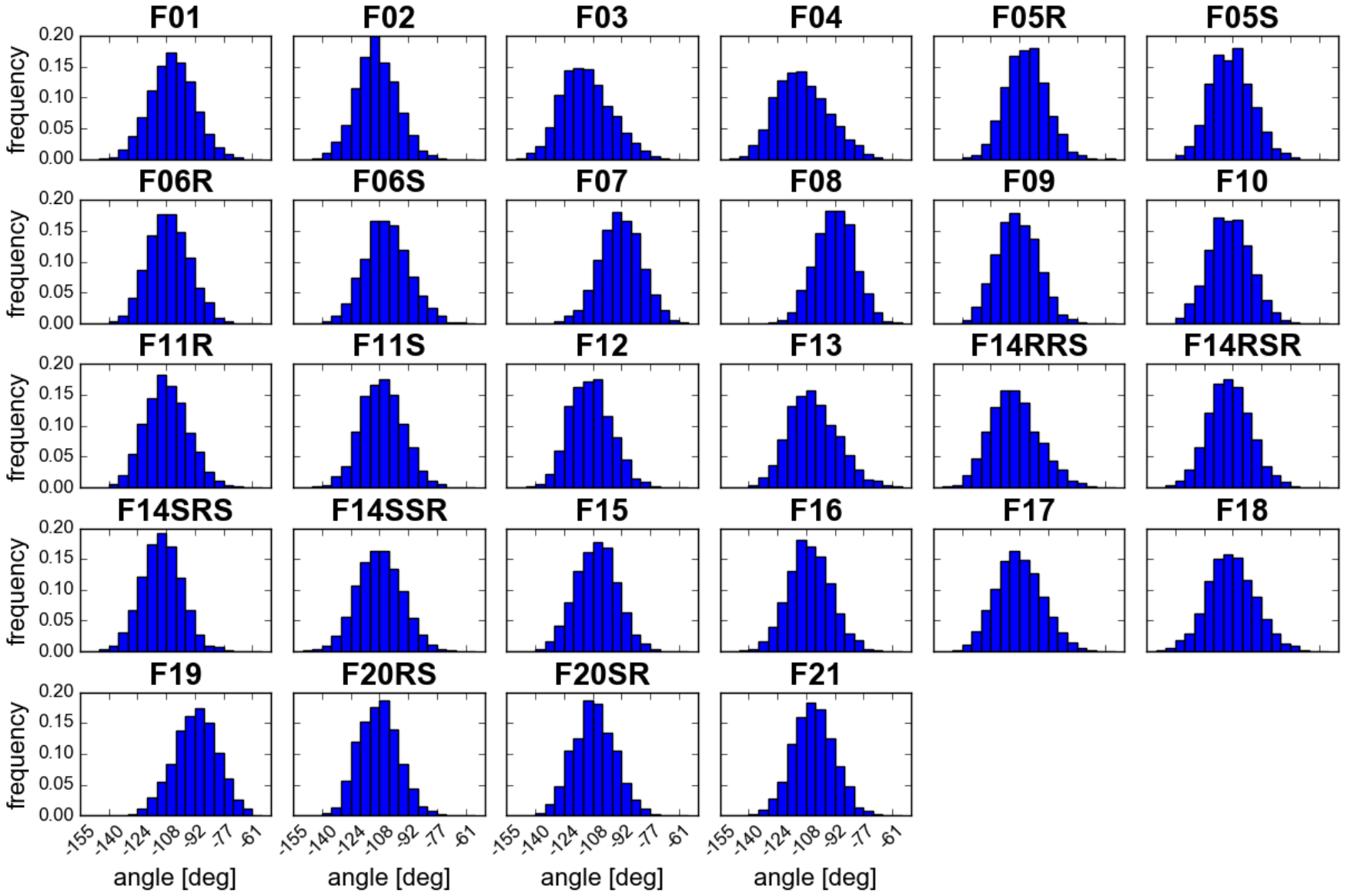

Figure SM-DIH-23. Distributions of X2 dihedral angle values of W293.
Data are collected from last 10ns of production in 3 replicas.

Figure SM-DIH-24. Time evolution of X2 dihedral angle of W293.
Y-values are given in degrees.

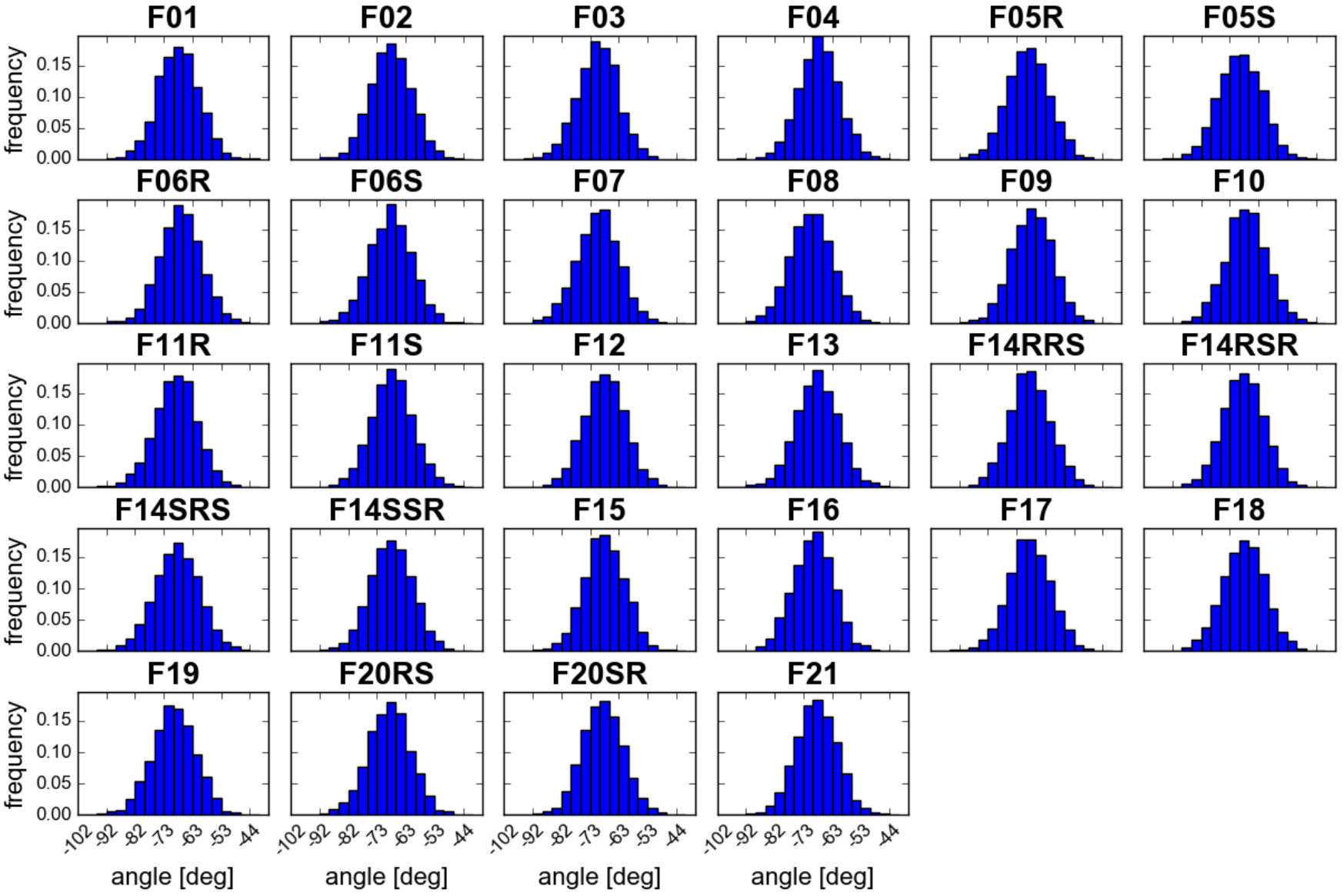

Figure SM-DIH-25. Distributions of X1 dihedral angle values of H297.
Data are collected from last 10ns of production in 3 replicas.

Figure SM-DIH-26. Time evolution of X1 dihedral angle of H297.
Y-values are given in degrees.

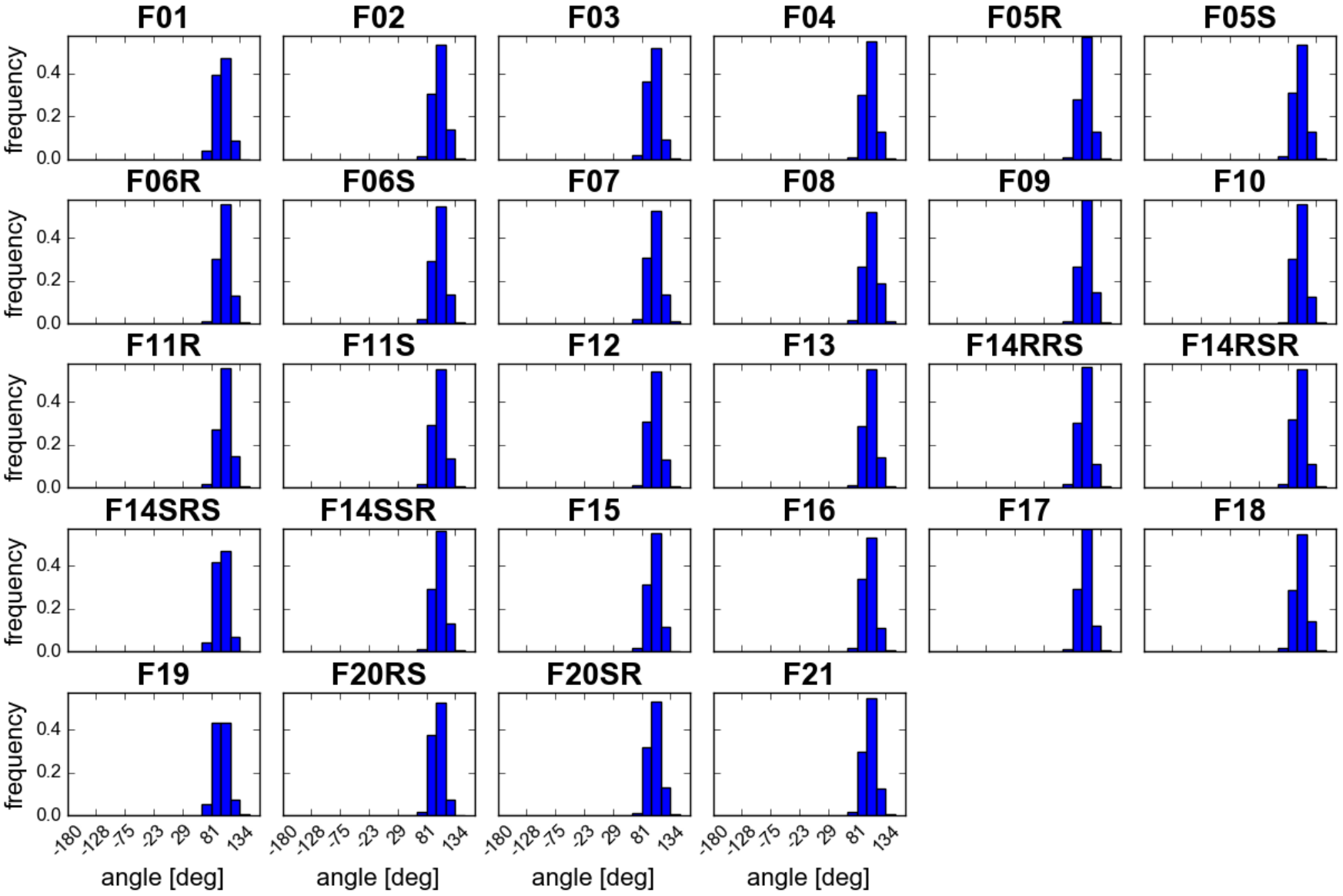

Figure SM-DIH-27. Distributions of X2 dihedral angle values of H297.
Data are collected from last 10ns of production in 3 replicas.

Figure SM-DIH-28. Time evolution of X2 dihedral angle of H297.
Y-values are given in degrees.

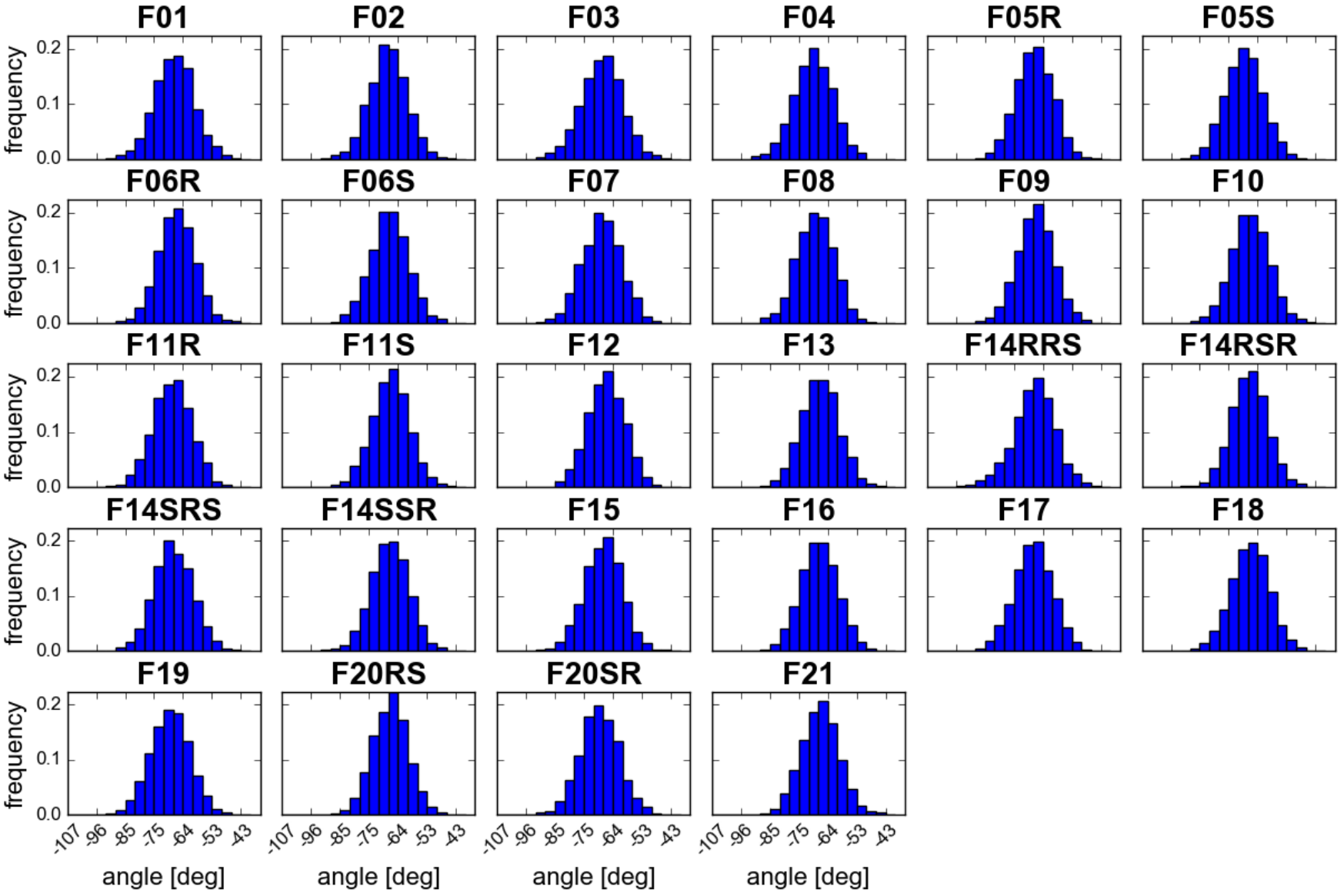

Figure SM-DIH-29. Distributions of X1 dihedral angle values of Y326.
Data are collected from last 10ns of production in 3 replicas.

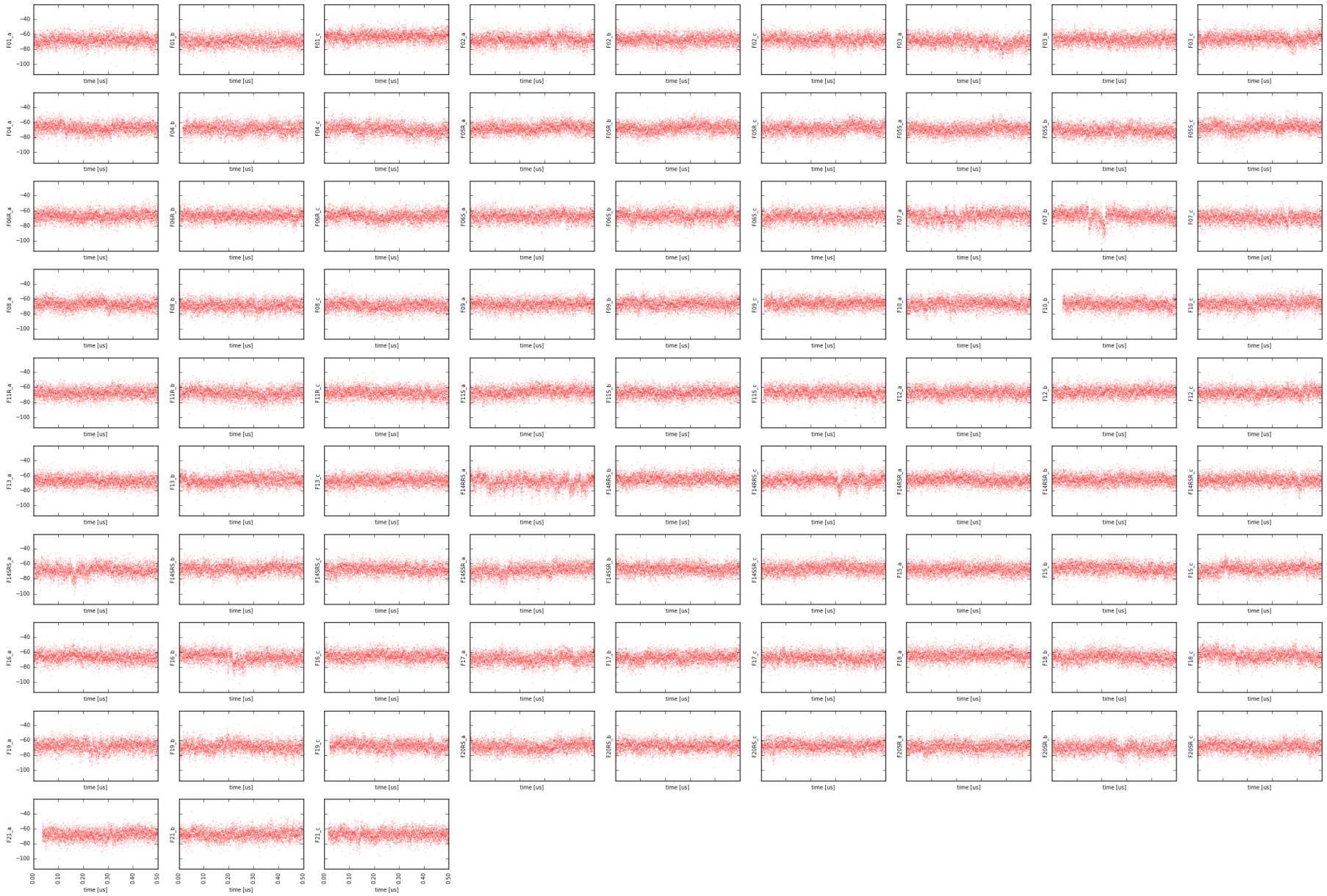

Figure SM-DIH-30. Time evolution of X1 dihedral angle of Y326.
Y-values are given in degrees.

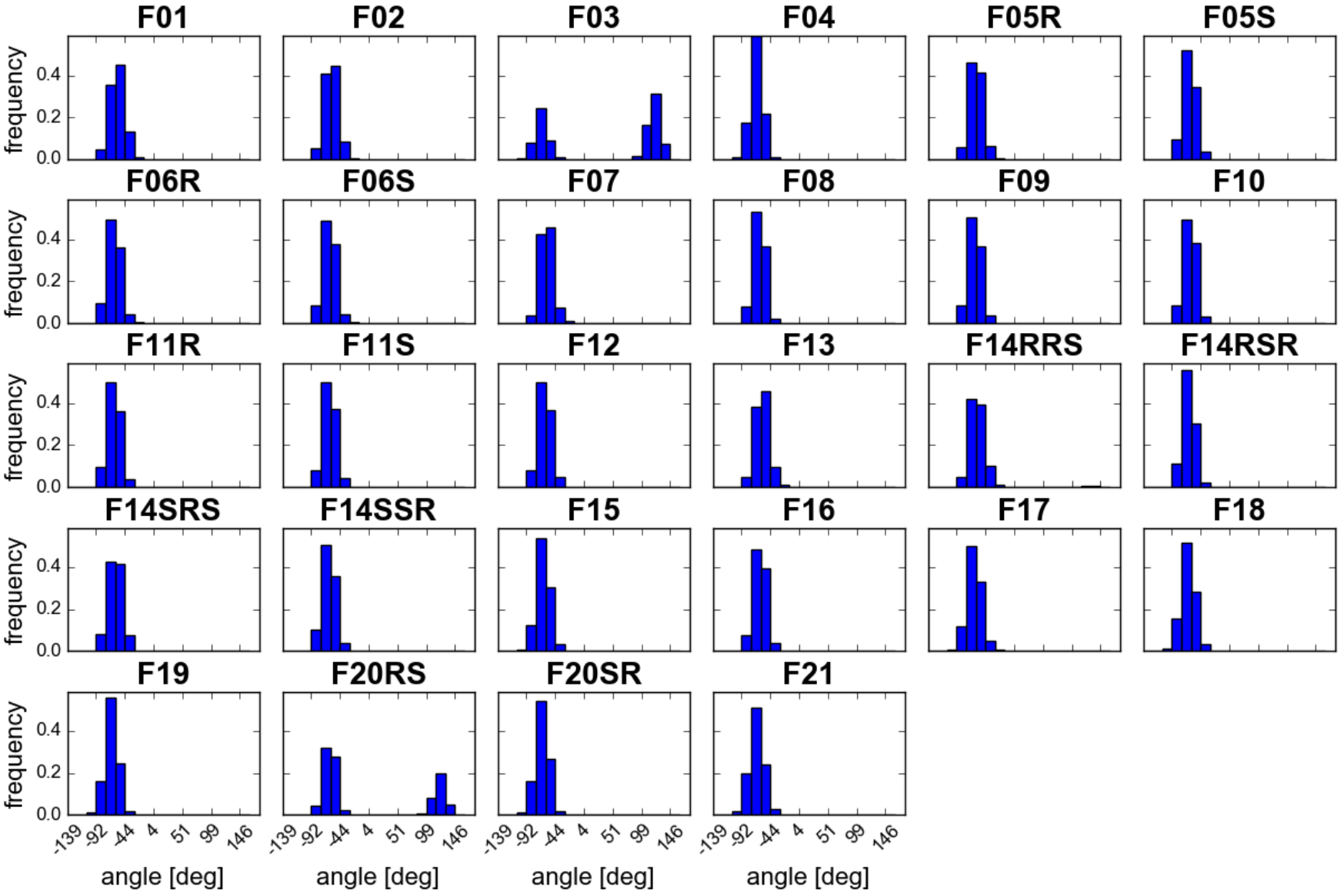

Figure SM-DIH-31. Distributions of X2 dihedral angle values of Y326.
Data are collected from last 10ns of production in 3 replicas.

Figure SM-DIH-32. Time evolution of X2 dihedral angle of Y326.
Y-values are given in degrees.

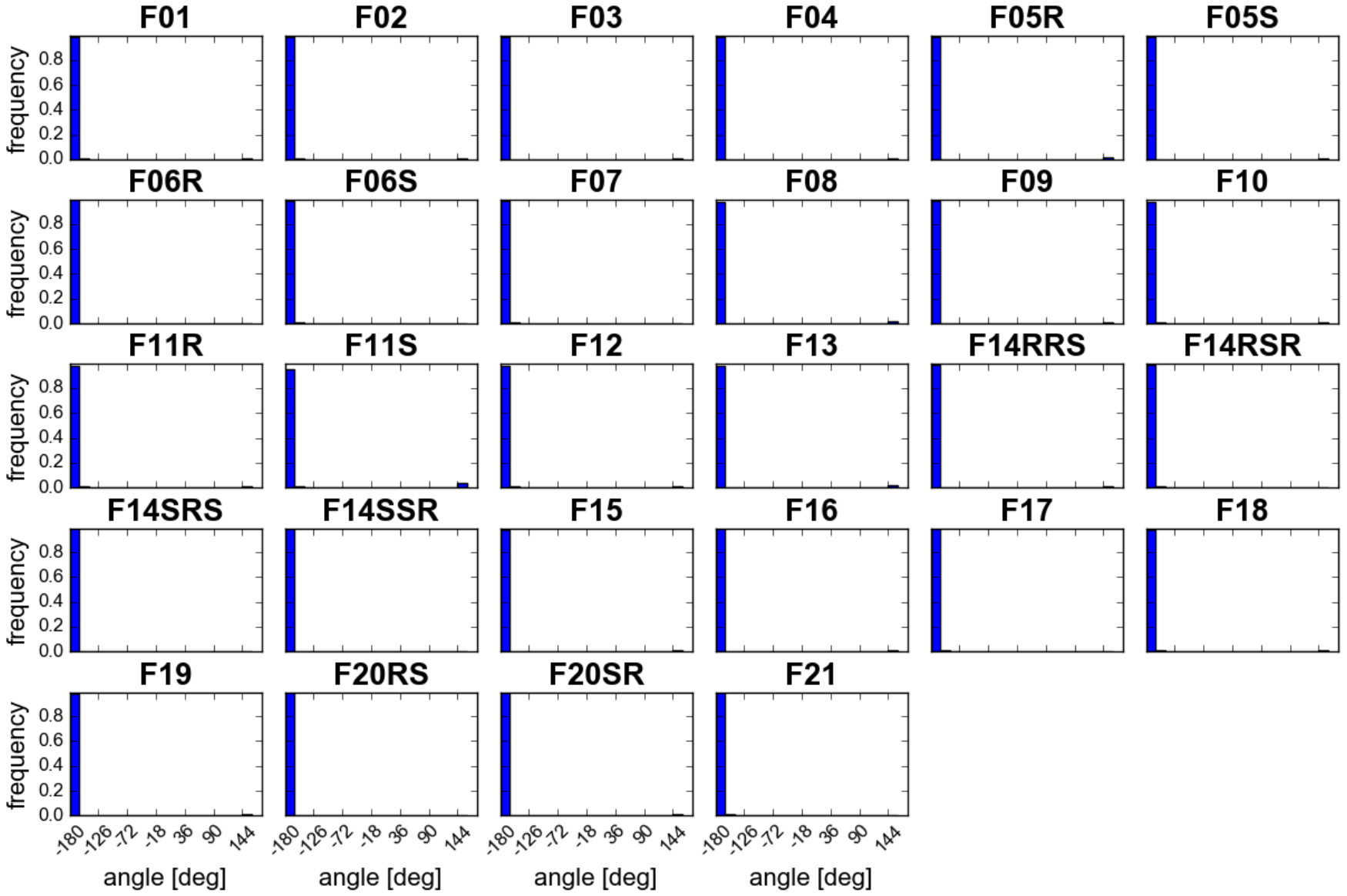

Figure SM-DIH-33. Distributions of X1 dihedral angle values of W133.
Data are collected from last 10ns of production in 3 replicas.

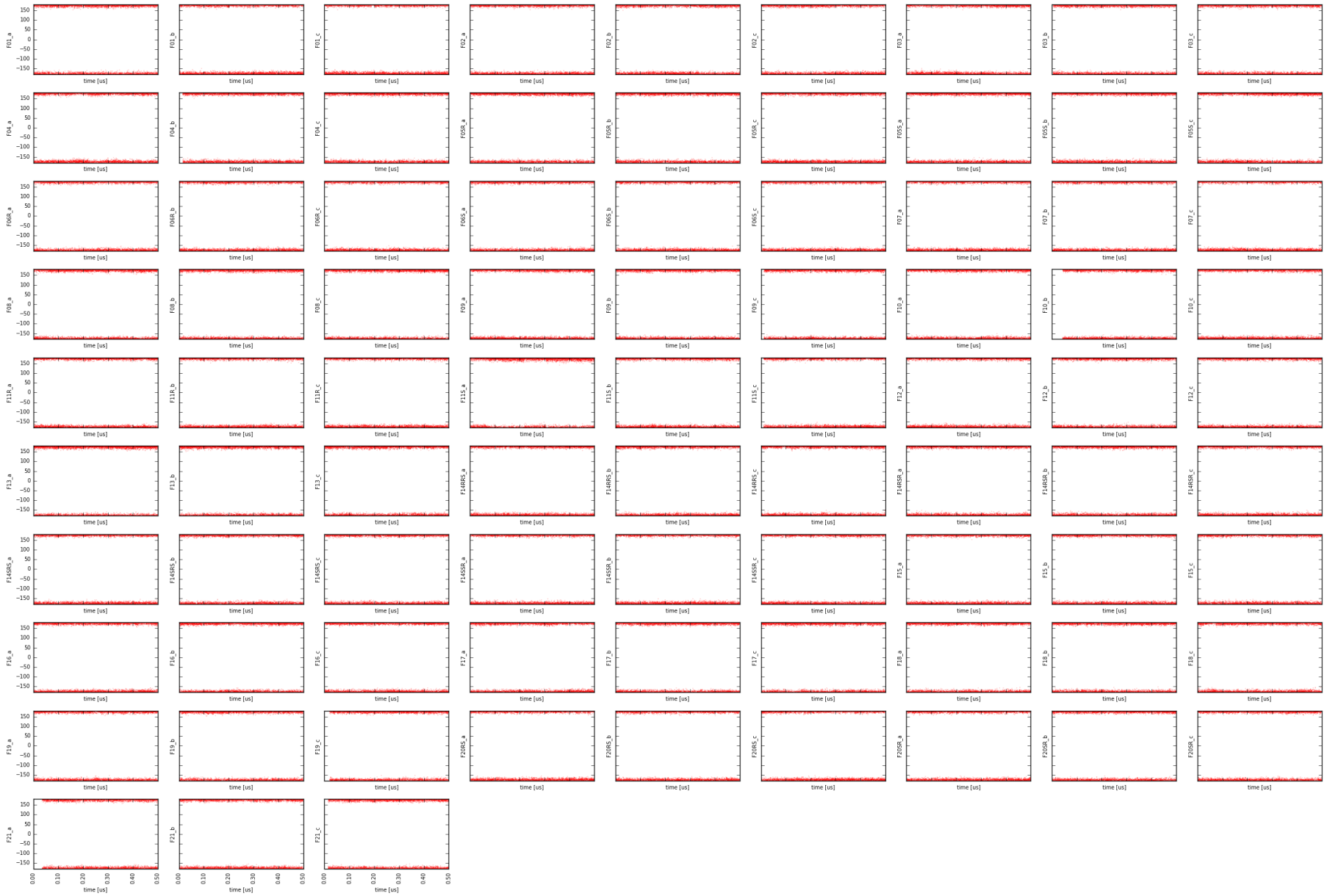

Figure SM-DIH-34. Time evolution of X1 dihedral angle of W133.
Y-values are given in degrees.

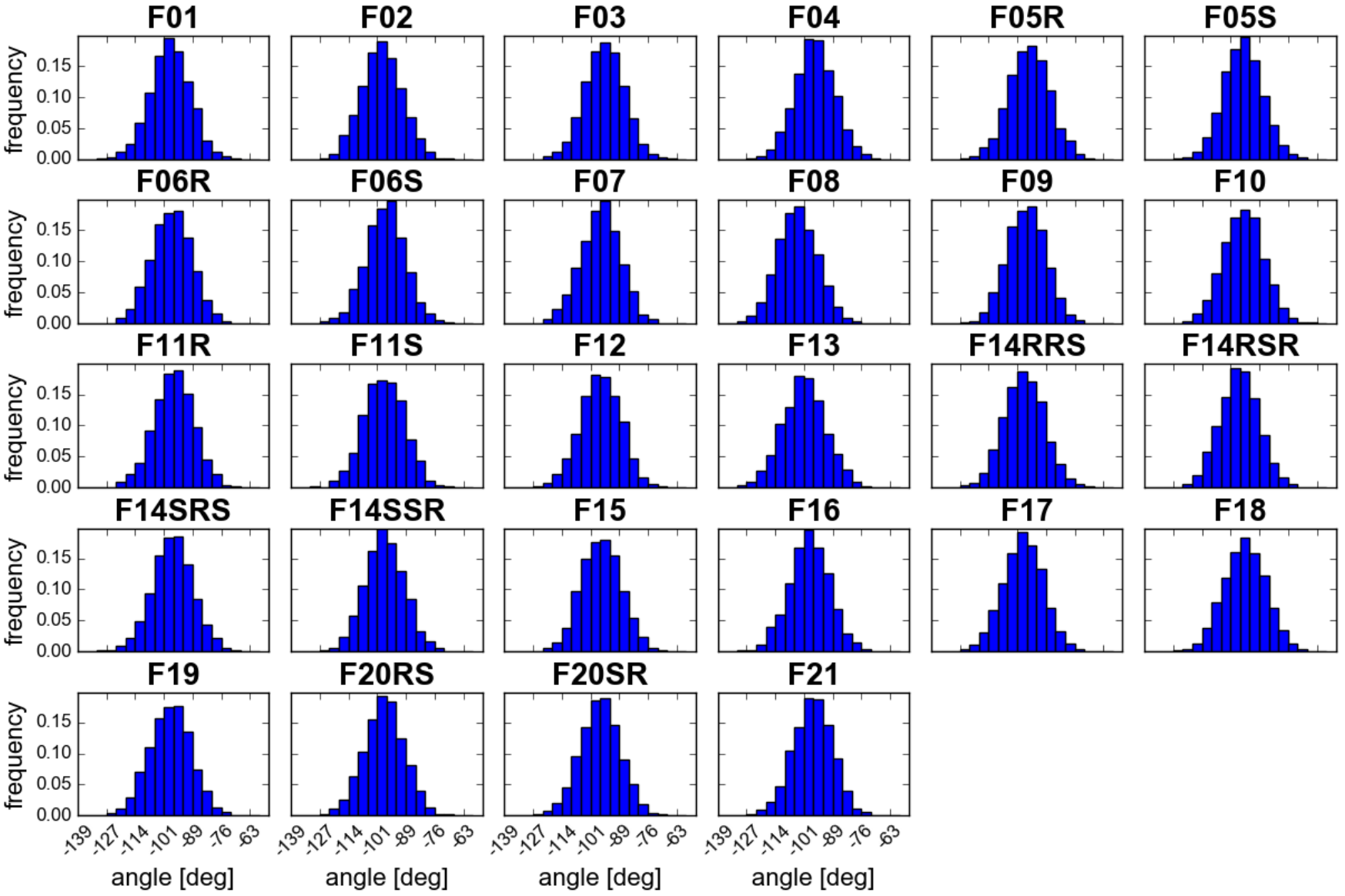

Figure SM-DIH-35. Distributions of X2 dihedral angle values of W133.
Data are collected from last 10ns of production in 3 replicas.

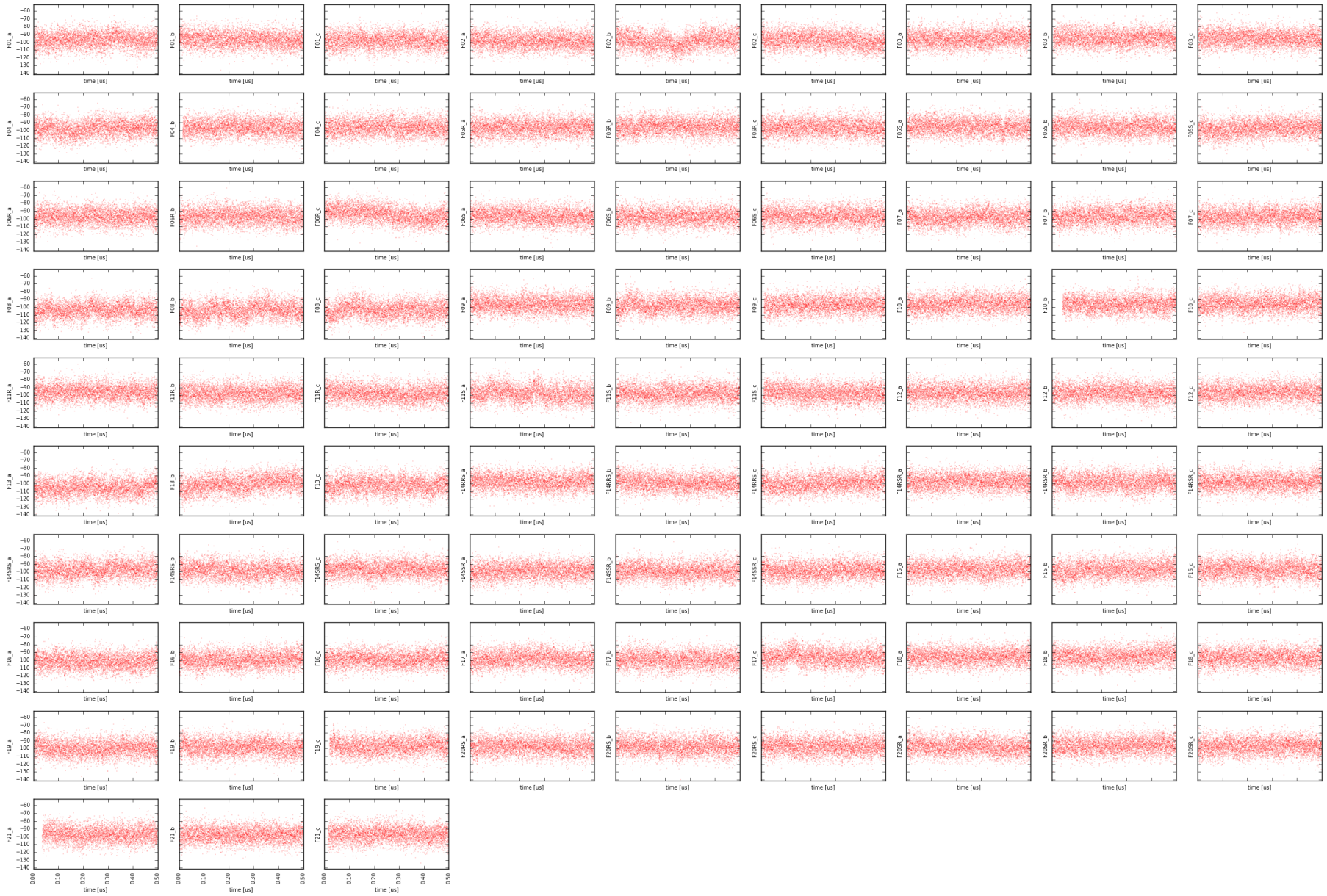

Figure SM-DIH-36. Time evolution of X2 dihedral angle of W133.
Y-values are given in degrees.

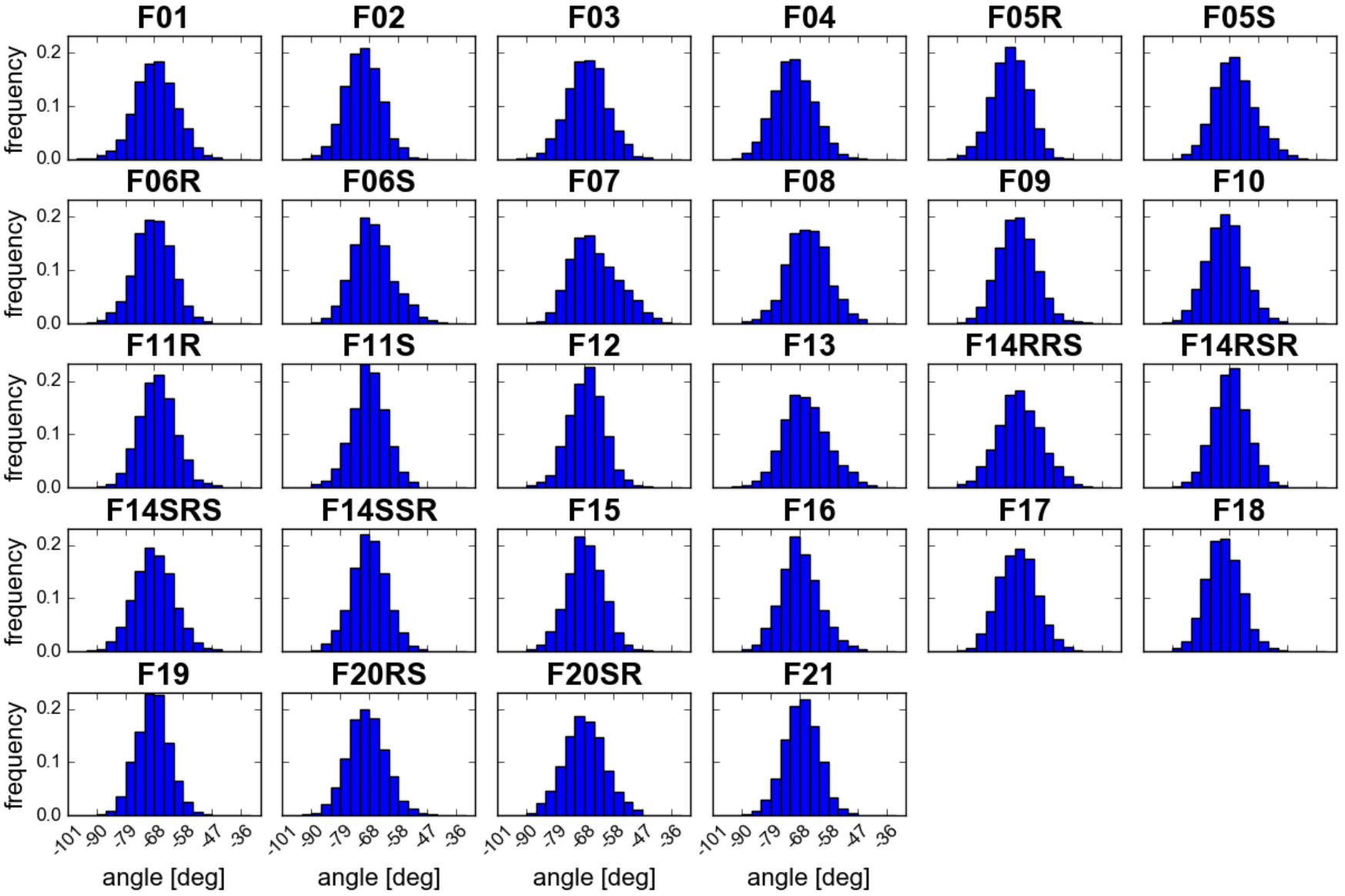

Figure SM-DIH-37. Distributions of X1 dihedral angle values of Y336.
Data are collected from last 10ns of production in 3 replicas.

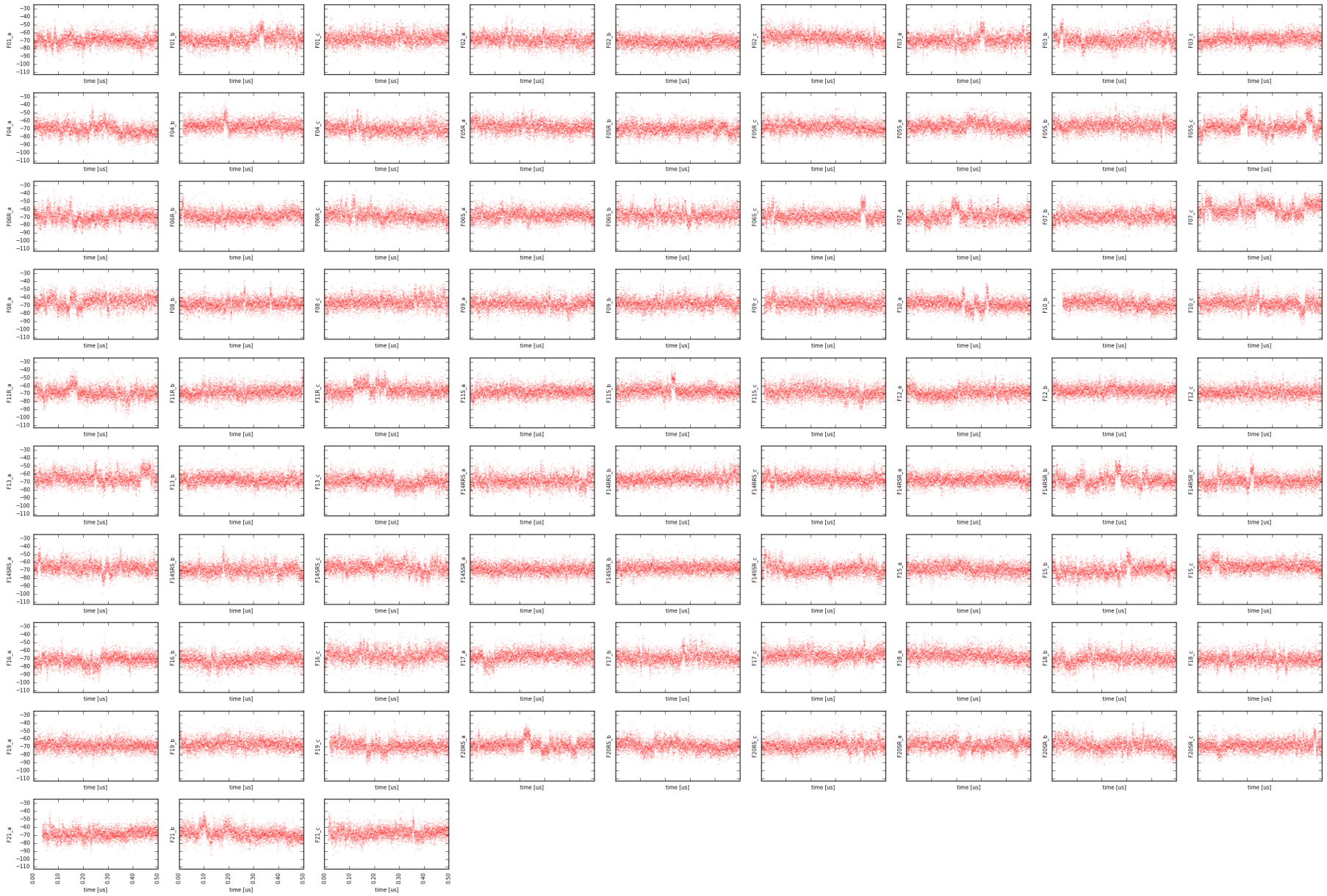

Figure SM-DIH-38. Time evolution of X1 dihedral angle of Y336.
Y-values are given in degrees.

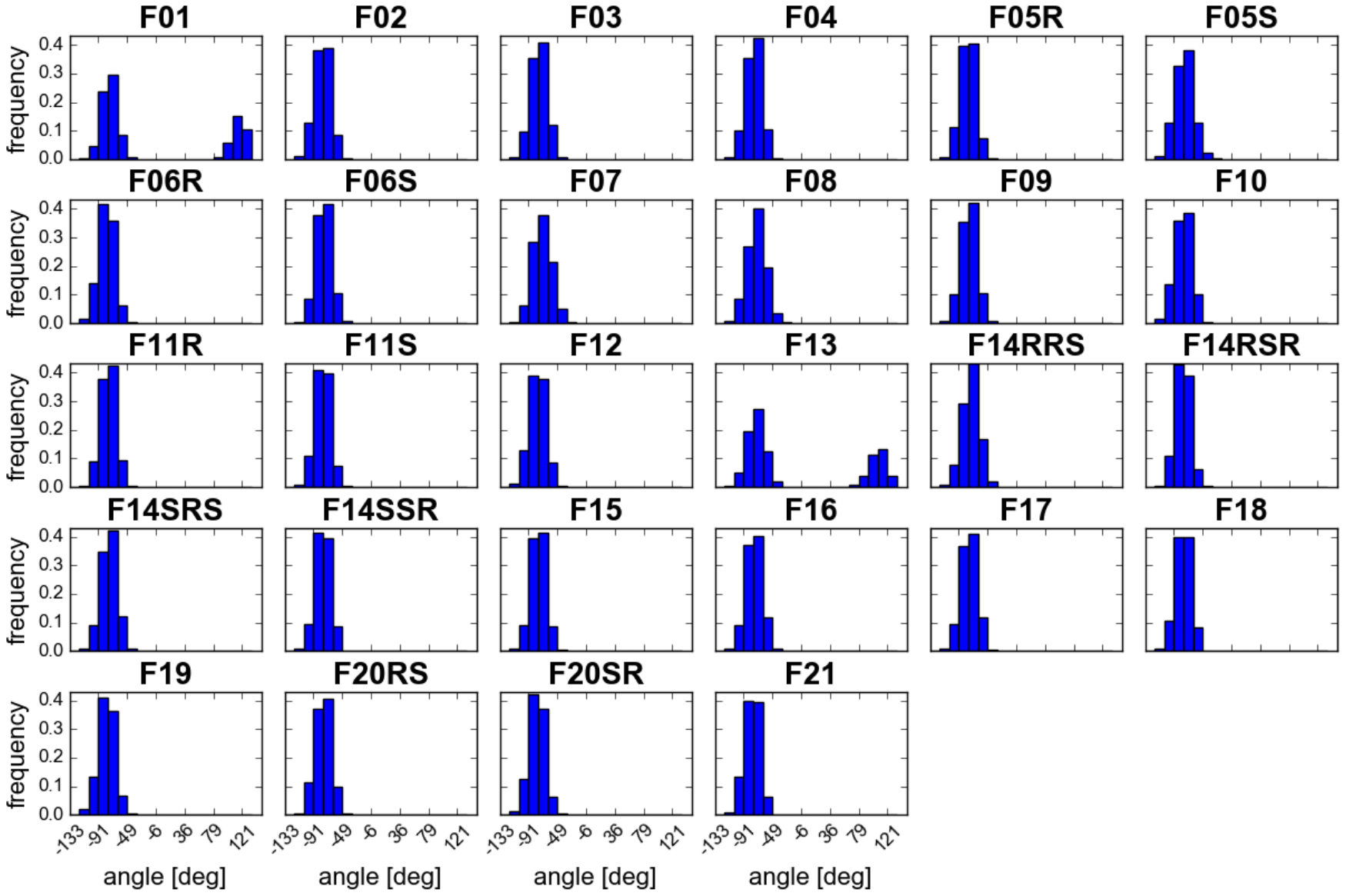

Figure SM-DIH-39. Distributions of X2 dihedral angle values of Y336.
Data are collected from last 10ns of production in 3 replicas.

Figure SM-DIH-40. Time evolution of X2 dihedral angle of Y336.
Y-values are given in degrees.

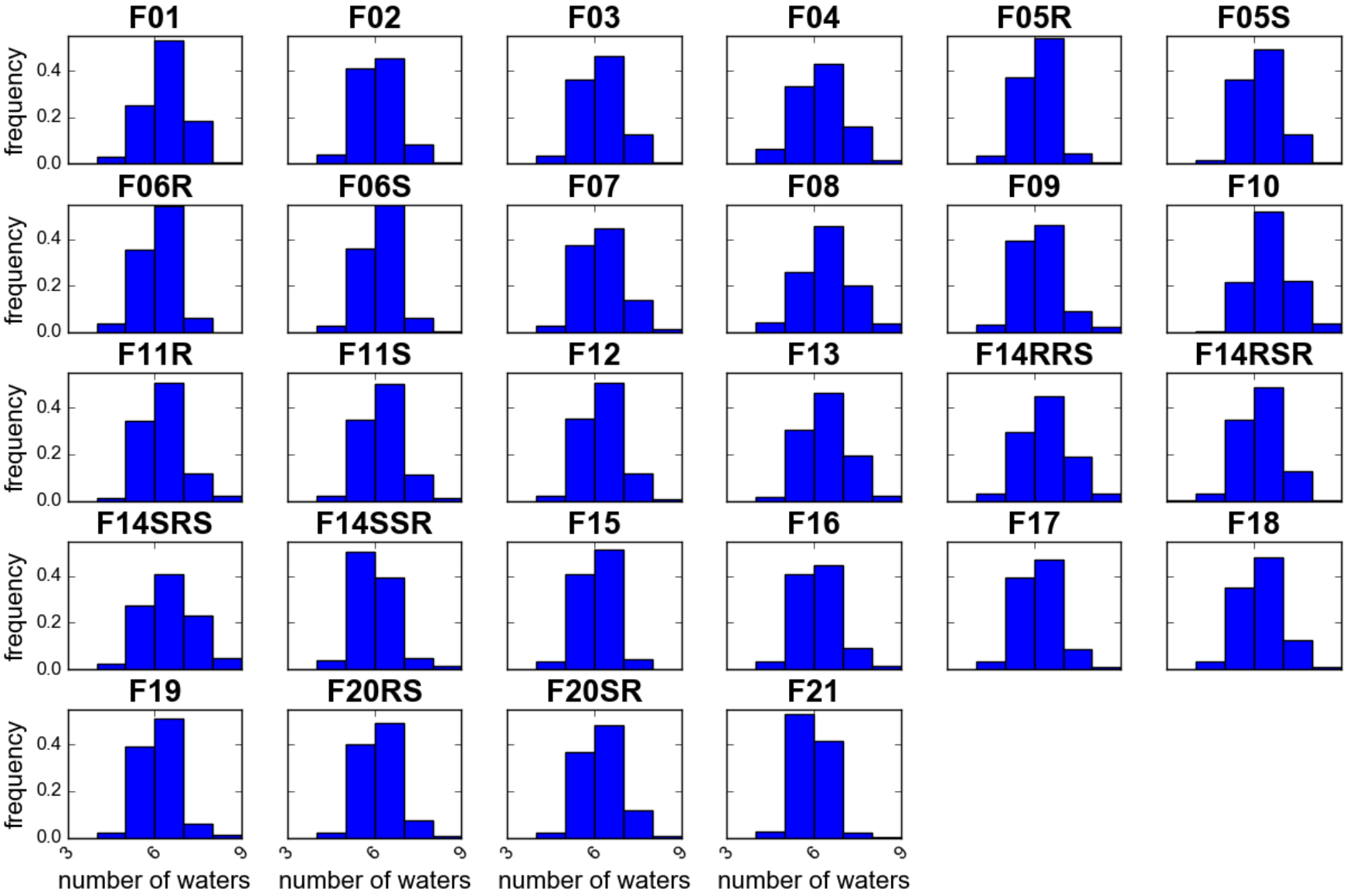

Figure SM-WAT-1. Distributions of the number of water molecules within 5.0 angstroms from Y336
Data are collected from last 10ns of production in 3 replicas.

Table SM-WAT-1. Mean number of water molecules within 5.0 angstroms from D114.
Calculated on last 10 ns of simulations in 3 replicas.

derivative	replica							
	a		b		c			
	mean	sem	mean	sem	mean	sem	MEAN	SEM
F01	5.99	0.07	6.01	0.07	5.65	0.08	5.88	0.12
F02	5.29	0.07	5.63	0.06	5.85	0.07	5.59	0.16
F03	5.97	0.06	5.68	0.06	5.49	0.04	5.71	0.14
F04	5.99	0.06	5.62	0.05	5.58	0.06	5.73	0.13
F05R	5.59	0.07	5.62	0.07	5.66	0.07	5.62	0.02
F05S	5.71	0.07	5.87	0.08	5.68	0.07	5.75	0.06
F06R	5.64	0.06	5.69	0.07	5.57	0.07	5.63	0.03
F06S	5.59	0.07	5.59	0.06	5.82	0.07	5.67	0.08
F07	5.47	0.07	5.85	0.08	5.91	0.07	5.74	0.14
F08	6.00	0.10	5.82	0.07	5.94	0.09	5.92	0.05
F09	5.52	0.06	5.59	0.05	5.96	0.06	5.69	0.14
F10	5.78	0.05	6.26	0.06	6.13	0.05	6.06	0.14
F11R	5.86	0.09	5.79	0.07	5.73	0.07	5.79	0.04
F11S	5.63	0.06	5.44	0.06	6.16	0.08	5.74	0.22
F12	5.77	0.07	5.60	0.06	5.85	0.08	5.74	0.07
F13	5.72	0.07	6.39	0.08	5.60	0.06	5.90	0.25
F14RRS	6.36	0.09	5.75	0.08	5.59	0.07	5.90	0.23
F14RSR	5.79	0.08	5.69	0.09	5.69	0.06	5.72	0.03
F14SRS	5.78	0.09	5.99	0.08	6.33	0.10	6.03	0.16
F14SSR	5.42	0.06	5.34	0.07	5.72	0.08	5.49	0.12
F15	5.43	0.07	5.63	0.05	5.62	0.06	5.56	0.07
F16	5.36	0.06	5.53	0.07	6.08	0.08	5.66	0.22
F17	5.51	0.07	5.61	0.07	5.83	0.09	5.65	0.09
F18	5.75	0.07	5.90	0.08	5.55	0.08	5.73	0.10
F19	5.65	0.04	5.72	0.06	5.61	0.05	5.66	0.03
F20RS	5.48	0.05	5.54	0.06	5.94	0.08	5.65	0.14
F20SR	5.73	0.07	5.68	0.07	5.74	0.07	5.72	0.02
F21	5.17	0.03	5.49	0.04	5.69	0.04	5.45	0.15
						MEAN	5.73	

Figure SM-WAT-2. Number of waters in proximity (5.0 angstroms) of D114 over time.
Y-values are unitless.

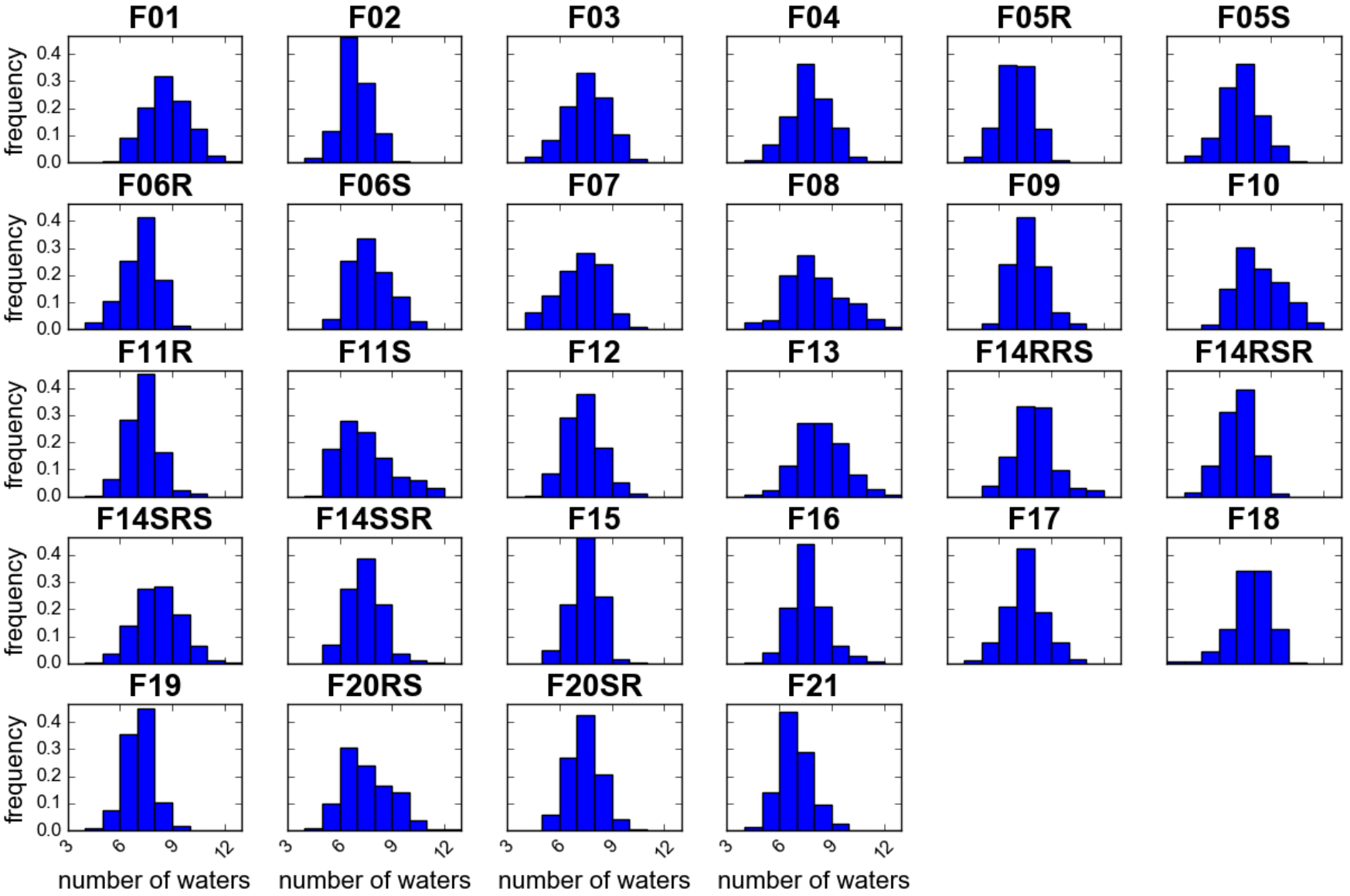

Figure SM-WAT-3. Distributions of the number of water molecules within 5.0 angstroms from Y336
Data are collected from last 10ns of production in 3 replicas.

Table SM-WAT-2. Mean number of water molecules within 5.0 angstroms from Y336.
Calculated on last 10 ns of simulations in 3 replicas.

derivative	replica							
	a		b		c			
	mean	sem	mean	sem	mean	sem	MEAN	SEM
F01	8.35	0.12	7.39	0.10	8.79	0.12	8.18	0.41
F02	6.69	0.09	6.01	0.08	6.41	0.08	6.37	0.20
F03	7.60	0.08	7.48	0.07	6.05	0.07	7.04	0.50
F04	7.09	0.07	6.87	0.08	7.79	0.10	7.25	0.28
F05R	6.89	0.08	5.93	0.09	6.57	0.09	6.46	0.28
F05S	7.41	0.10	6.69	0.09	6.19	0.12	6.76	0.35
F06R	6.74	0.08	6.52	0.13	6.70	0.09	6.65	0.07
F06S	6.47	0.06	8.05	0.12	7.10	0.12	7.21	0.46
F07	7.13	0.09	7.40	0.12	5.61	0.12	6.71	0.56
F08	8.03	0.14	6.57	0.10	8.27	0.21	7.62	0.53
F09	7.07	0.06	7.36	0.08	6.99	0.08	7.14	0.11
F10	6.79	0.05	9.20	0.07	7.38	0.07	7.79	0.73
F11R	6.86	0.08	6.52	0.08	7.07	0.11	6.82	0.16
F11S	5.71	0.07	6.58	0.09	8.57	0.13	6.95	0.85
F12	6.57	0.10	6.57	0.09	7.41	0.11	6.85	0.28
F13	7.63	0.15	8.92	0.11	7.09	0.08	7.88	0.54
F14RRS	7.62	0.16	7.36	0.11	7.47	0.08	7.48	0.08
F14RSR	6.05	0.09	6.98	0.07	6.70	0.10	6.58	0.28
F14SRS	7.26	0.12	7.92	0.11	7.87	0.15	7.68	0.21
F14SSR	6.68	0.09	6.66	0.10	7.43	0.11	6.92	0.25
F15	7.14	0.08	6.62	0.08	7.17	0.09	6.98	0.18
F16	6.87	0.06	6.67	0.09	7.98	0.13	7.17	0.41
F17	7.42	0.10	6.48	0.09	7.09	0.12	7.00	0.28
F18	6.66	0.12	7.84	0.08	7.55	0.09	7.35	0.36
F19	6.85	0.05	6.60	0.06	6.42	0.06	6.62	0.12
F20RS	6.54	0.09	6.10	0.07	8.58	0.10	7.07	0.76
F20SR	6.82	0.10	6.79	0.07	7.11	0.10	6.91	0.10
F21	6.36	0.05	5.99	0.06	6.84	0.08	6.40	0.25
						MEAN	7.07	

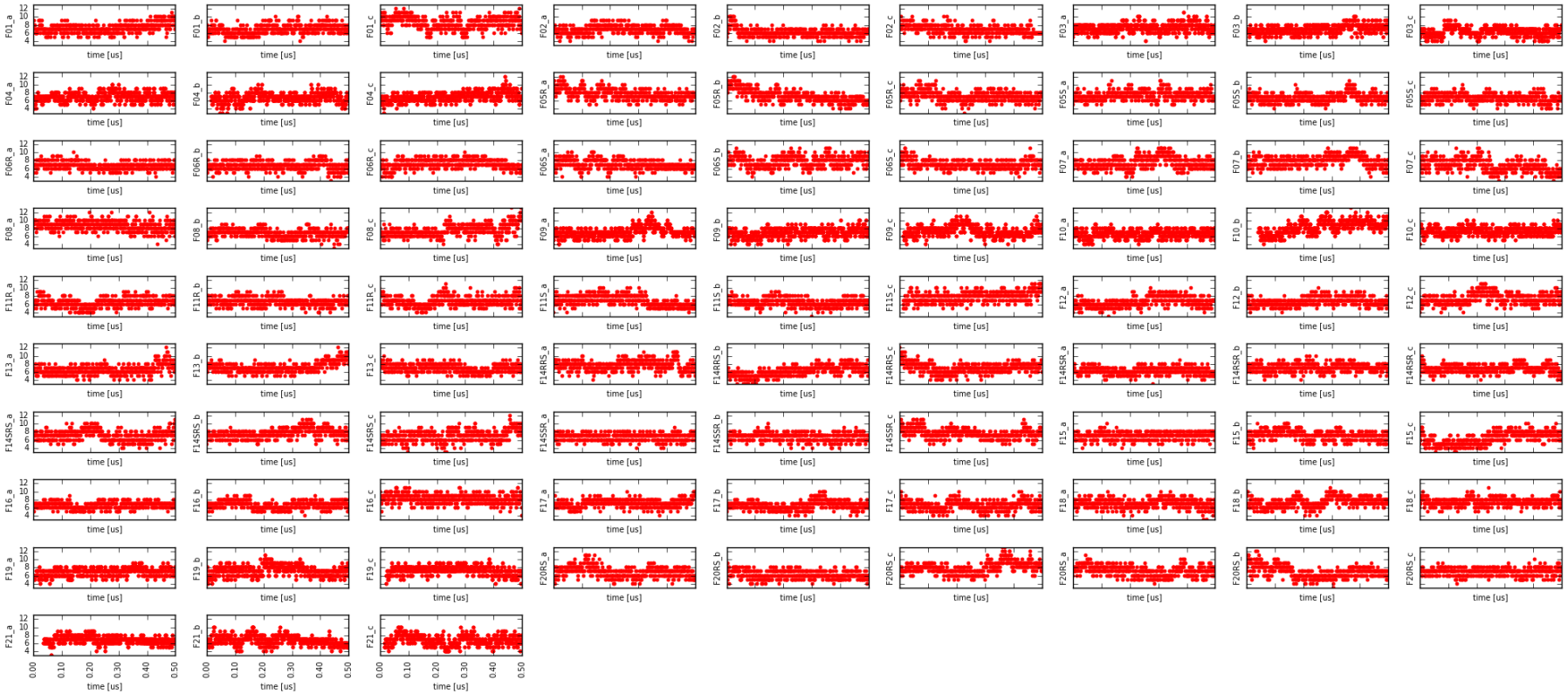

Figure SM-WAT-4. Number of waters in proximity (5.0 angstroms) of Y336 over time.
Y-values are unitless.

Table SM-SCO-1. Optimal scoring values for the tested derivatives.

By optimal is meant either minimum or maximum (depending on the scoring function) scoring made on a set of snapshots from last 10 ns of production of 3 replicas of MD simulations.

derivative	PLP1	PLP2	PMF	PMF04	DOCK_CS	DOCK_GS	Jain	LigScore1	LigScore2	Ludi1	Ludi2	Ludi3	DSX	Ludi3_LIPSCO	VINA	VINA_repulsion
F01	87.55	85.07	118.45	67.57	-55.27	-51.19	6.19	4.17	5.93	674.00	582.00	788.00	-136.70	436.00	-8.46	3.79
F02	78.59	75.72	107.63	58.75	-51.49	-48.25	5.40	3.56	5.75	630.00	553.00	707.00	-121.41	380.00	-6.71	4.04
F03	76.44	74.70	104.52	61.13	-48.45	-44.30	5.04	3.80	5.30	611.00	533.00	676.00	-106.81	380.00	-7.35	3.28
F04	70.01	72.16	100.53	61.79	-47.30	-44.49	4.72	3.51	5.30	590.00	527.00	661.00	-113.12	376.00	-6.74	4.40
F05R	85.46	83.80	123.25	71.54	-52.80	-49.76	6.36	4.31	5.87	708.00	590.00	797.00	-123.17	418.00	-8.11	4.17
F05S	86.84	82.80	113.00	65.81	-50.73	-45.35	6.25	3.96	5.65	663.00	582.00	735.00	-121.14	418.00	-7.85	3.57
F06R	87.55	87.62	119.70	65.25	-51.14	-48.81	5.48	4.10	5.80	657.00	547.00	719.00	-122.06	391.00	-7.91	4.76
F06S	88.19	85.01	118.93	69.25	-52.71	-48.58	5.90	5.25	6.28	716.00	598.00	752.00	-124.12	395.00	-8.01	3.73
F07	91.01	85.04	127.35	70.01	-56.92	-52.85	6.57	4.78	6.26	713.00	596.00	667.00	-133.66	440.00	-7.62	4.46
F08	100.67	99.32	133.51	89.36	-61.80	-58.86	6.28	5.38	6.57	678.00	594.00	698.00	-149.91	470.00	-8.75	5.51
F09	84.36	81.95	108.91	57.84	-49.85	-46.65	6.60	3.69	5.76	692.00	575.00	745.00	-119.41	409.00	-7.96	3.45
F10	85.54	83.94	118.11	63.90	-51.88	-47.97	5.95	4.81	6.12	717.00	571.00	743.00	-121.93	359.00	-7.44	3.65
F11R	84.41	85.32	127.00	73.72	-52.42	-49.84	6.76	5.30	6.19	735.00	599.00	753.00	-122.24	378.00	-7.91	3.17
F11S	77.03	76.05	119.19	64.74	-51.07	-46.34	5.05	4.35	5.90	705.00	585.00	804.00	-117.94	351.00	-7.50	4.05
F12	89.05	84.85	111.94	70.53	-51.72	-47.80	5.81	4.60	6.04	770.00	658.00	822.00	-123.73	403.00	-7.87	3.31
F13	83.58	80.32	119.59	80.36	-54.06	-50.56	5.37	4.47	5.85	676.00	594.00	693.00	-135.31	403.00	-8.06	4.22
F14RRS	81.78	78.27	117.29	58.53	-48.24	-45.50	3.05	3.04	5.41	482.00	441.00	636.00	-115.19	397.00	-7.67	2.23
F14RSR	80.19	76.44	110.32	60.92	-52.50	-49.42	5.19	3.59	5.77	595.00	523.00	739.00	-115.46	388.00	-7.89	4.11
F14SRS	82.43	79.40	106.37	60.25	-48.24	-46.17	3.28	3.25	5.65	532.00	465.00	684.00	-109.51	384.00	-7.47	3.04
F14SSR	87.65	83.99	128.24	68.24	-52.65	-47.74	6.08	4.21	5.98	670.00	554.00	727.00	-118.05	386.00	-7.62	4.67
F15	84.74	81.33	128.65	69.46	-52.18	-50.00	5.75	3.42	5.95	683.00	584.00	768.00	-122.04	422.00	-7.29	3.43
F16	86.19	81.39	117.95	64.54	-54.85	-52.03	4.28	4.03	6.00	648.00	554.00	778.00	-124.85	434.00	-7.75	3.96
F17	83.06	79.00	122.88	68.68	-52.81	-49.17	5.67	5.32	5.80	560.00	507.00	558.00	-118.92	393.00	-6.43	3.59
F18	61.11	62.12	83.26	52.10	-40.33	-38.30	4.51	3.76	5.10	557.00	481.00	485.00	-83.83	295.00	-5.74	3.06
F19	82.85	73.27	118.19	70.02	-54.73	-51.51	4.79	4.68	5.98	602.00	528.00	634.00	-112.87	393.00	-7.16	3.94
F20RS	80.05	77.46	101.51	60.38	-49.46	-46.44	3.16	2.22	5.42	491.00	462.00	544.00	-121.97	409.00	-6.89	3.00
F20SR	78.58	76.51	99.61	63.33	-49.47	-46.19	5.97	3.31	5.62	591.00	525.00	719.00	-108.94	397.00	-6.71	4.38
F21	81.37	77.56	113.83	68.62	-52.65	-49.48	5.67	4.41	6.16	678.00	590.00	737.00	-114.95	424.00	-6.73	4.12

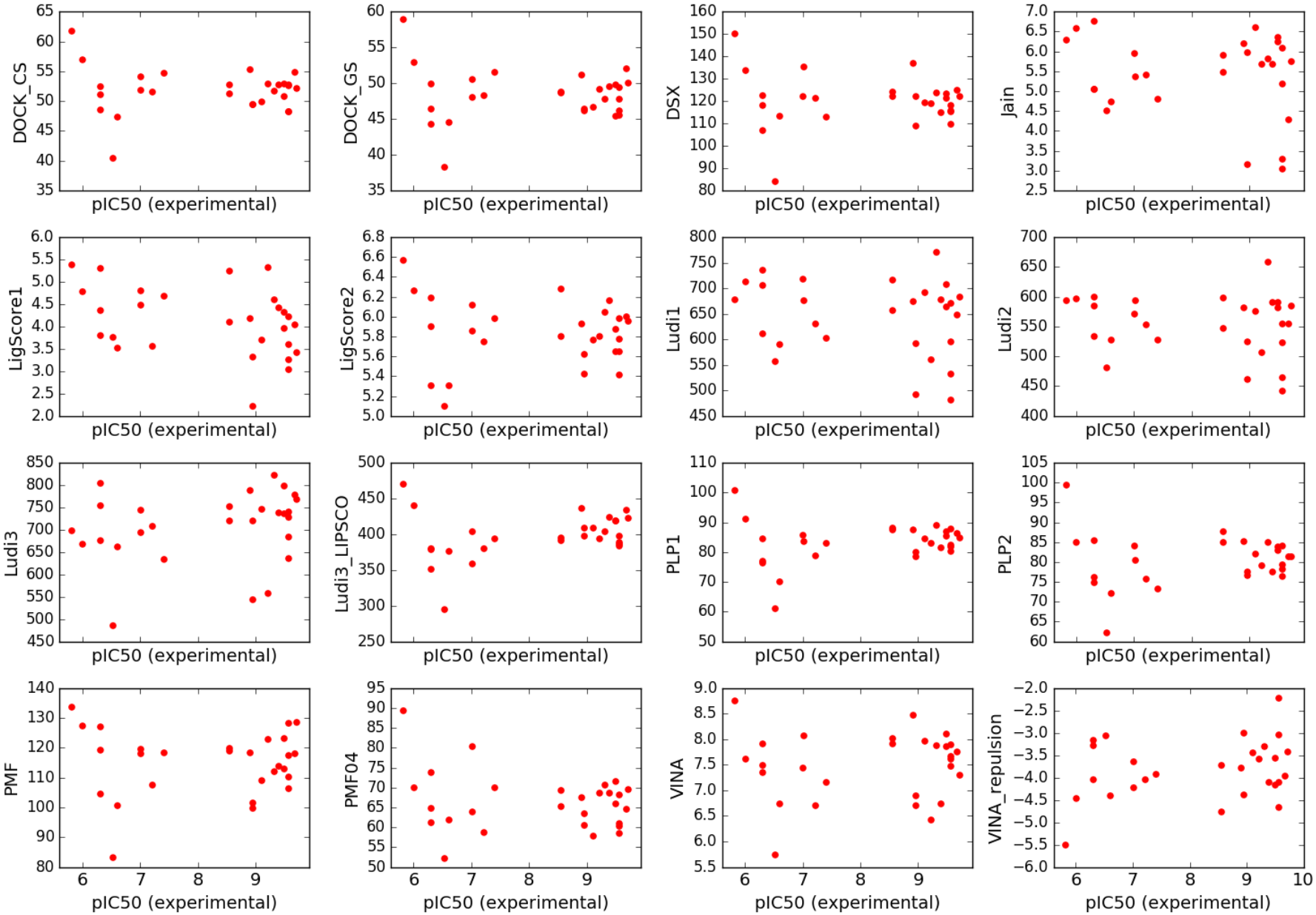

Figure SM-SCO-1. Plots of binding estimation by scoring functions (arbitrary units) against the experimental pIC50.
The plot includes all tested derivatives. See Methods section for scoring functions labels.

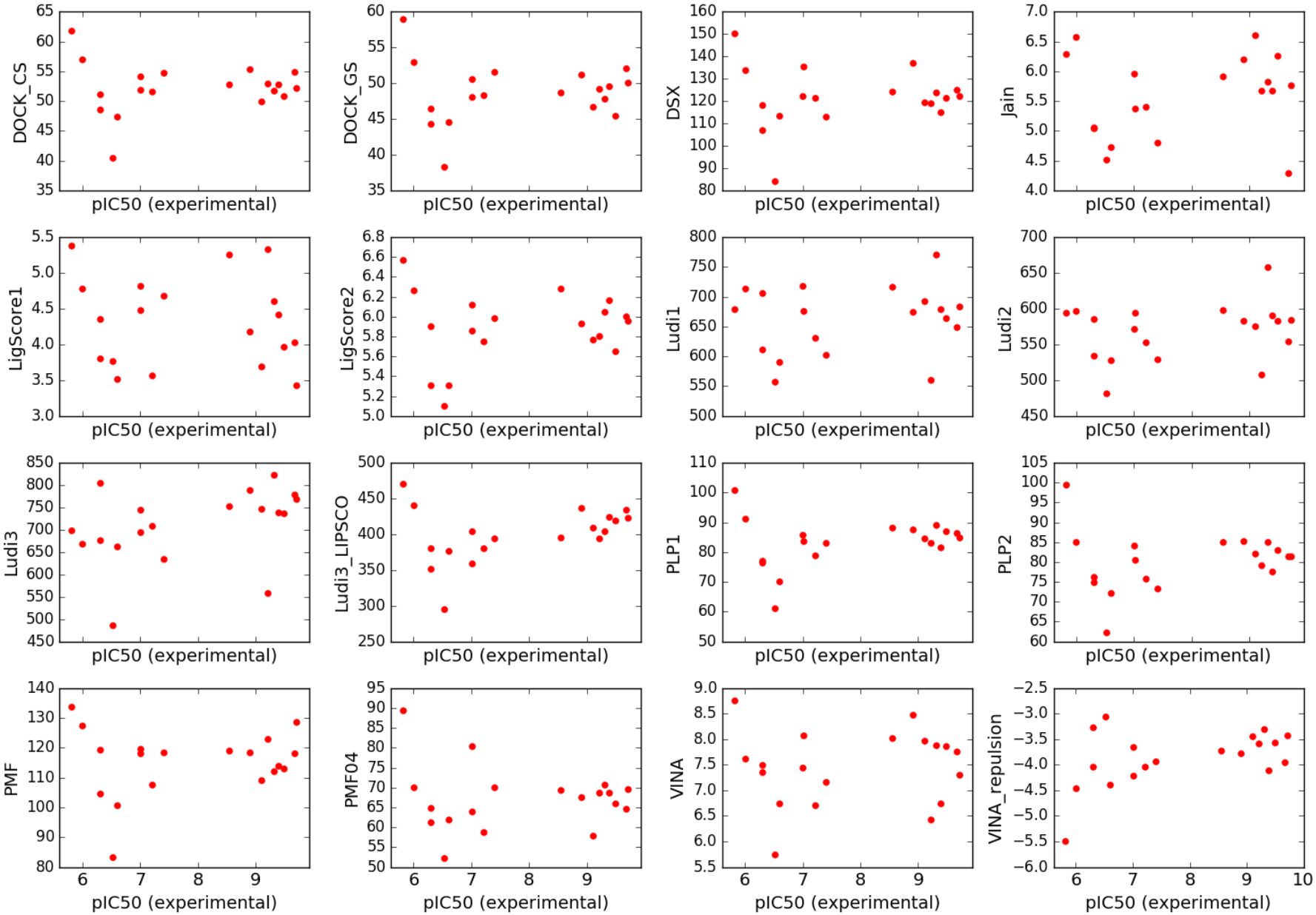

Figure SM-SCO-2. Plots of binding estimation by scoring functions (arbitrary units) against the experimental pIC50.
The plot includes all tested derivatives except for the chiral compounds. See Methods section for scoring functions labels.

pIC_{50} = -5.5527

\+ 0.00063 * AROSCO (score for aromatic interactions)

\+ 0.00389 * HBONDSCO (score for H-bonds)

\- 0.02543 * IONSCO (score for ionic interactions)

\+ 0 04235 * LIPSCO (score for lipophilic interactions)

\- 0.01135 * ROTSCO (score for rotational freedom loss)

Figure SM-SCO-3. Expression for reweighted LUDI3 scoring function.
This is internal validation on the set used for training the coefficients of the equation's elements.

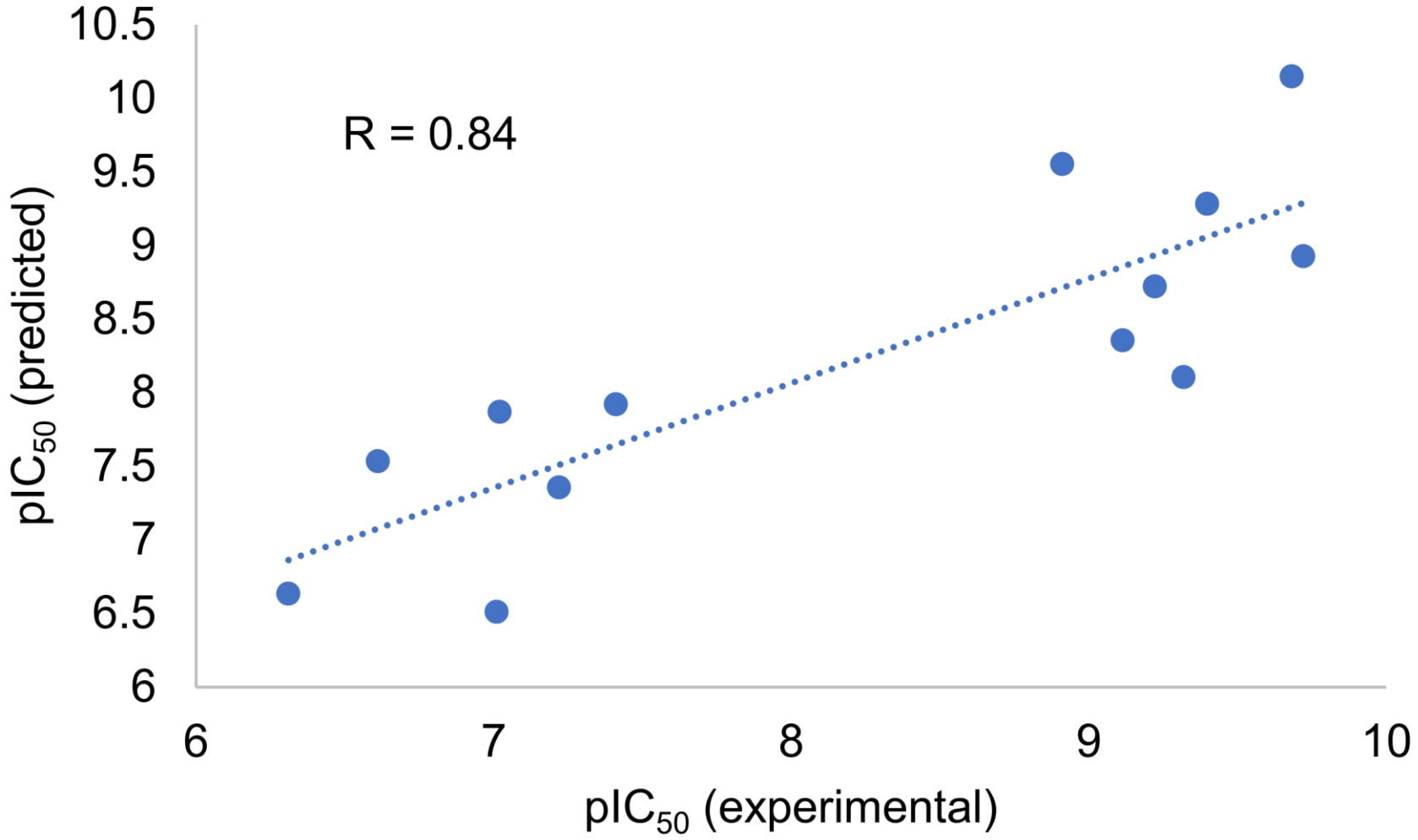

Figure SM-SCO-4. Plots of binding estimation by reweighted LUDI3 scoring function against the experimental pIC50. Internal validation. *Excluded are chiral compounds, F07, F08 and F18.*

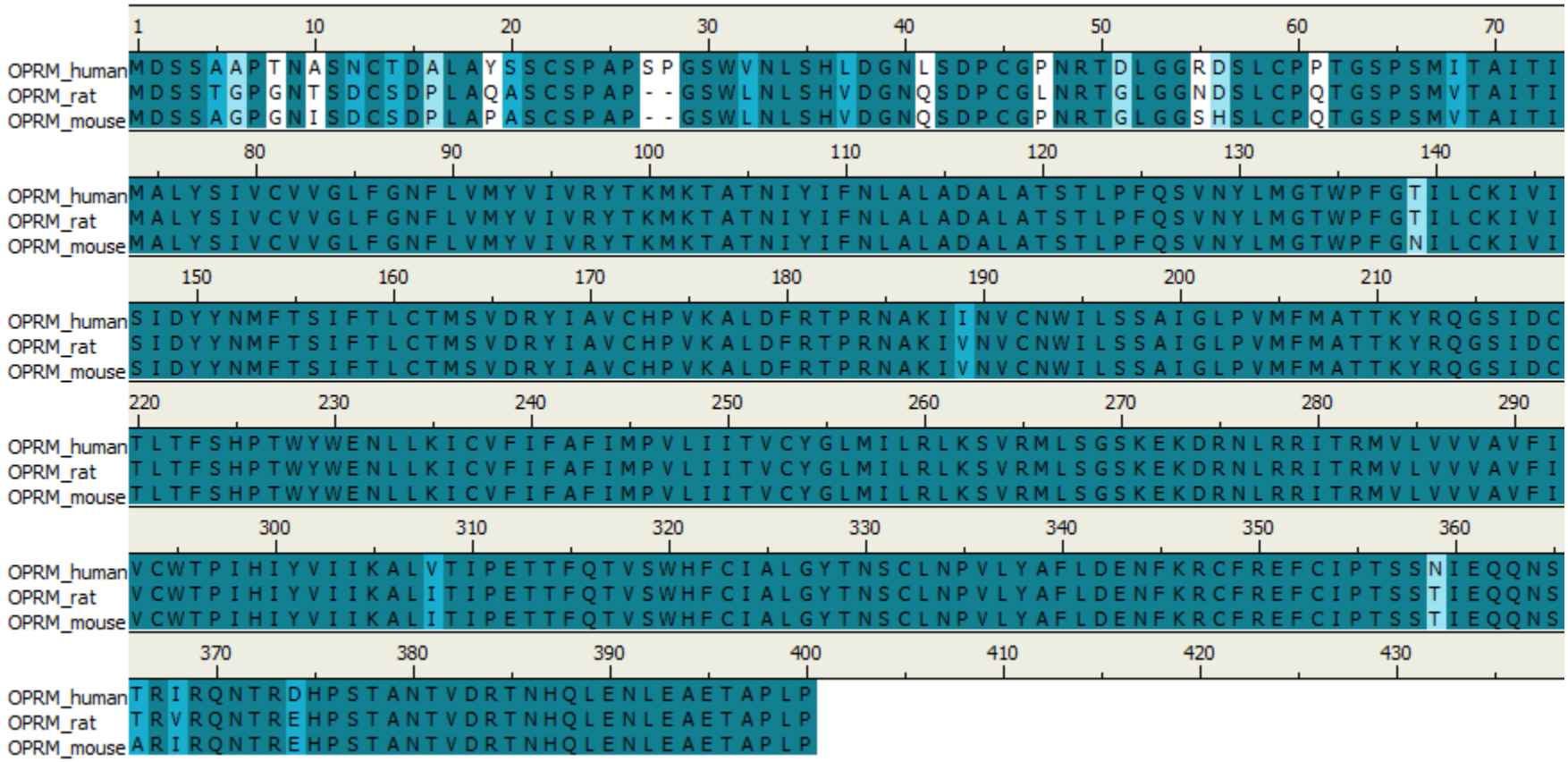

Sequence SM-SEQ-1. Sequence alignment of human, rat and murine μOR.

The interspecies differences in the sequences of μOR are of minor character and should not impact binding or scoring to a significant extent. Most of them are located in the N-terminus which is largely absent from 5C1M crystal (used for docking). Others, including 66:V:V:I (position: murine – rat – human), 137:N:T:T, 187:V:V:I, 306:I:I:V are 1) conservative 2) remote from the binding site or at least the side chain is not directed to the binding site. Three others are in the C-terminus, also absent from crystals, also remote from the binding site.